NATIONAL CENTER FOR EARTHQUAKE ENGINEERING RESEARCH
Headquartered at the State University of New York at Buffalo

ISSN 1088-3800

PB98-153430

Seismic Evaluation of Frames with Infill Walls Using Pseudo-dynamic Experiments

by

Khalid M. Mosalam, Richard N. White and Peter Gergely
Cornell University
School of Civil and Environmental Engineering
Ithaca, New York 14853

Technical Report NCEER-97-0020

December 31, 1997

This research was conducted at Cornell University and was supported in whole or in part by the National Science Foundation under Grant No. BCS 90-25010 and other sponsors.

NOTICE

This report was prepared by Cornell University as a result of research sponsored by the National Center for Earthquake Engineering Research (NCEER) through a grant from the National Science Foundation and other sponsors. Neither NCEER, associates of NCEER, its sponsors, Cornell University, nor any person acting on their behalf:

a. makes any warranty, express or implied, with respect to the use of any information, apparatus, method, or process disclosed in this report or that such use may not infringe upon privately owned rights; or

b. assumes any liabilities of whatsoever kind with respect to the use of, or the damage resulting from the use of, any information, apparatus, method, or process disclosed in this report.

Any opinions, findings, and conclusions or recommendations expressed in this publication are those of the author(s) and do not necessarily reflect the views of NCEER, the National Science Foundation, or other sponsors.

NATIONAL CENTER FOR EARTHQUAKE ENGINEERING RESEARCH
Headquartered at the State University of New York at Buffalo

Seismic Evaluation of Frames with Infill Walls Using Pseudo-dynamic Experiments

by

K.M. Mosalam[1], R.N. White[2] and P. Gergely[3]

Publication Date: December 31, 1997
Submittal Date: July 21, 1997

Technical Report NCEER-97-0020

NCEER Task Numbers 93-3111, 94-3111, 94-3112 and 95-3111

NSF Master Contract Number BCS 90-25010

1 Assistant Professor, Department of Civil and Environmental Engineering, University of California, Berkeley; former Lecturer, School of Civil and Environmental Engineering, Cornell University
2 James A. Friend Family Professor of Engineering, School of Civil and Environmental Engineering, Cornell University
3 Professor of Structural Engineering (deceased), School of Civil and Environmental Engineering, Cornell University

NATIONAL CENTER FOR EARTHQUAKE ENGINEERING RESEARCH
State University of New York at Buffalo
Red Jacket Quadrangle, Buffalo, NY 14261

PREFACE

The National Center for Earthquake Engineering Research (NCEER) was established in 1986 to develop and disseminate new knowledge about earthquakes, earthquake-resistant design and seismic hazard mitigation procedures to minimize loss of life and property. The emphasis of the Center is on eastern and central United States *structures*, and *lifelines* throughout the country that may be exposed to any level of earthquake hazard.

NCEER's research is conducted under one of four Projects: the Building Project, the Nonstructural Components Project, and the Lifelines Project, all three of which are principally supported by the National Science Foundation, and the Highway Project which is primarily sponsored by the Federal Highway Administration.

The research and implementation plan in years six through ten (1991-1996) for the Building, Nonstructural Components, and Lifelines Projects comprises four interdependent elements, as shown in the figure below. Element I, Basic Research, is carried out to support projects in the Applied Research area. Element II, Applied Research, is the major focus of work for years six through ten for these three projects. Demonstration Projects under Element III have been planned to support the Applied Research projects and include individual case studies and regional studies. Element IV, Implementation, will result from activity in the Applied Research projects, and from Demonstration Projects.

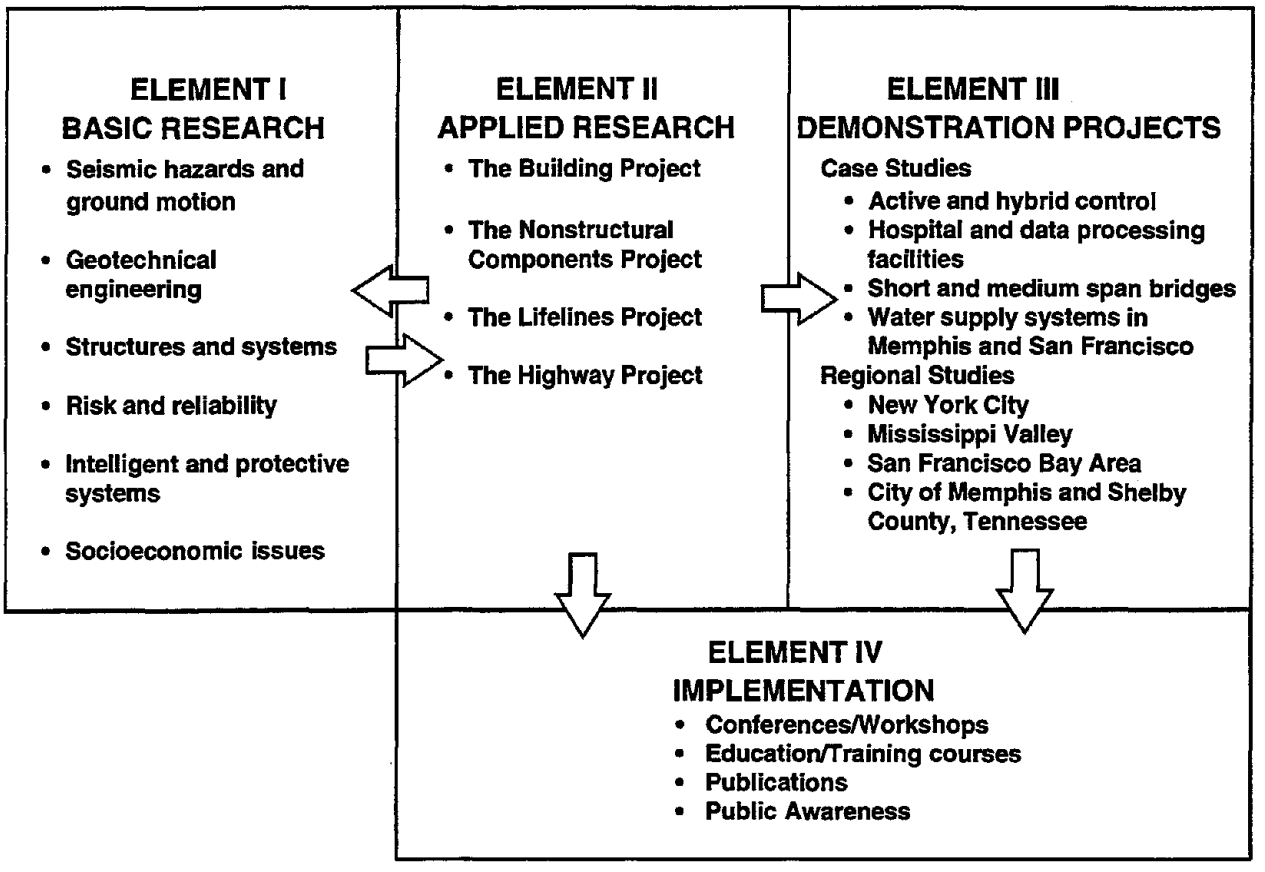

Research in the **Building Project** focuses on the evaluation and retrofit of buildings in regions of moderate seismicity. Emphasis is on lightly reinforced concrete buildings, steel semi-rigid frames, and masonry walls or infills. The research involves small- and medium-scale shake table tests and full-scale component tests at several institutions. In a parallel effort, analytical models and computer programs are being developed to aid in the prediction of the response of these buildings to various types of ground motion.

Two of the short-term products of the **Building Project** will be a monograph on the evaluation of lightly reinforced concrete buildings and a state-of-the-art report on unreinforced masonry.

The **structures and systems program** constitutes one of the important areas of research in the **Building Project**. Current tasks include the following:

1. Continued testing of lightly reinforced concrete external joints.
2. Continued development of analytical tools, such as system identification, idealization, and computer programs.
3. Perform parametric studies of building response.
4. Retrofit of lightly reinforced concrete frames, flat plates and unreinforced masonry.
5. Enhancement of the IDARC (inelastic damage analysis of reinforced concrete) computer program.
6. Research infilled frames, including the development of an experimental program, development of analytical models and response simulation.
7. Investigate the torsional response of symmetrical buildings.

This work proposes a model of behavior of mortar joints including fracture after a peak of nonlinear strength is achieved. The model is calibrated using information from rigorous testing of masonry subcomponents and materials. The model was used in a finite element analysis using a complex computational platform, DIANA, to determine the contribution of masonry infills to the behavior of framed structures. The analytical method of super-convergent path recovery is compared with a smeared crack model approach and with experiments (pseudo-dynamic and seismic simulation using the shaking table). The model was then used to generate fragility curves for infill frames with various properties resulting from variability of materials and modeling parameters. The work presents a comprehensive analytical and experimental approach which allows a complete picture of advanced analysis of masonry structures. The work integrates the efforts of NCEER in seismic loss assessment, providing reliable fragility curves for the probabilistic cost analysis. The work was part of phase one of "Loss Assessment of Memphis Buildings," and provides a strong engineering basis for the evaluation.

ABSTRACT

An accurate and practical testing technique to study the seismic performance of multi-story infilled frames is formulated. This technique is based on the pseudo-dynamic method which can provide an acceptable approximation of the dynamic performance of structures under the influence of real earthquake excitation. The pseudo-dynamic experimental technique is outlined and applied for testing a two-bay, two-story gravity load designed steel frame infilled with unreinforced concrete block masonry walls. It was shown that careful implementation of the pseudo-dynamic technique may lead to an excellent control over the experimental error propagation, even for stiff structures such as infilled frames.

Based on the obtained results of the pseudo-dynamic experiments, the structural capacity as well as the corresponding seismic demand was assessed. From this study, it is concluded that the imparted energy and the hysteretic energy correlate well with the observed damage state of the infill walls. From the observed crack patterns of the infill walls, a macro-model for the infill panels is suggested.

ACKNOWLEDGEMENTS

The financial support of the National Center for Earthquake Engineering Research, Buffalo, New York, is gratefully acknowledged. The experimental work of this study was conducted in the George Winter Structural Laboratory at Cornell University. The assistance of Timothy K. Bond, the laboratory manager, is appreciated.

TABLE OF CONTENTS

TABLE OF CONTENTS (Cont'd)

LIST OF ILLUSTRATIONS

LIST OF ILLUSTRATIONS (Cont'd)

LIST OF ILLUSTRATIONS (Cont'd)

LIST OF TABLES

SECTION 1

INTRODUCTION

A common type of construction in urban centers is low-rise and mid-rise building frames with unreinforced masonry walls filling the spaces bounded by their structural members. The walls, usually referred to as infill walls, are built after the frame is constructed as partitions or as cladding. Unreinforced masonry infill walls are usually classified as non-structural components, *i.e.* their structural contribution is neglected during the design process of the frames. Under this assumption, the bounding structural frame should be designed to withstand *all* forces: vertical due to gravity loads and lateral due to wind pressure and/or seismic ground motion.

Ignoring the contributions of infill walls during the design of the bounding frames may lead to erroneous design as the frame/wall interaction under extreme loading conditions always occurs. The effects of neglecting the infill walls are accentuated in high seismicity regions where the frame/wall interaction may cause substantial increase of stiffness resulting in possible changes in the seismic demand due to the significant reduction in the natural period of the structural system. Also, the composite action of the frame/wall system changes magnitude and distribution of straining actions in the frame members, *i.e.* critical sections in the infilled frame differ from those of the bare frame, which may lead to unconservative or poorly detailed designs. Moreover, these designs may be uneconomical since an important source of structural strength (particularly beneficial in regions of moderate seismicity) is wasted.

As a matter of fact, there is no resemblance between the responses of the infilled frame and the bare one, as the former is substantially stronger and stiffer than the latter. The performance shown by infilled frames is advantageous especially when the capacity (and ductility) of the frame itself is suspected to be inadequate. This is the case of frames mainly designed for gravity loads without or with little attention to lateral loads (usually due to wind effects) when subjected to moderate or severe lateral loads due to earthquakes.

Lessons from recent damaging earthquakes illustrate the consequence of ignoring the contribution of infill walls. In some cases, the real structure (*i.e.* the infilled frame) is subjected to demands smaller than those considered during design. Unfortunately, in other cases, the contrary occurs, *i.e.* design forces may be significantly exceeded increasing the seismic damage vulnerability of the structure. In all cases, the changes in the distribution of straining actions may render the structural detailing ineffective.

The problem of considering infill walls in the design process is partly attributed to incomplete knowledge of the behavior of *quasi-brittle* materials such as masonry and to a lack of conclusive experimental and analytical results to substantiate a reliable design procedure for this type of structure.

A series of three reports addresses the definition and investigation of experimental and computational strategies to evaluate the behavior of infilled frames subjected to earthquake loading. These reports are based on a study at Cornell University which is divided into three parts as schematically illustrated in Figure 1-1. In **Part I**, the static experiments on infilled frames are presented together with an investigation of the properties of concrete block masonry and its constituents. In **Part II**, the pseudo-dynamic experimentation and the corresponding results for a two-story infilled frame are presented. Finally, in **Part III**, different computational strategies are introduced and critically investigated.

In the first report of this series, quasi-static experimentation of single-story infilled frames was explored. The extension of the results obtained from such experiments to the case of multi-story frames, particularly under real dynamic loading, is not obvious. The present report, which is the second in the series, aims towards the formulation and application of the pseudo-dynamic testing procedure for multi-story infilled frames. The pseudo-dynamic experimentation technique is outlined in **SECTION 2**. The technique is applied for testing a two-bay, two-story Gravity Load Designed (GLD) steel frame infilled with UnReinforced concrete block Masonry (URM) walls in **SECTION 3**. Directly measured results from the pseudo-dynamic experiments are given in **SECTION 4**. On the other hand, **SECTION 5** presents results based different types of energy. From the discussion of the results, the dynamic performance of the tested structure is assessed. Finally, concluding remarks are given in **SECTION 6**.

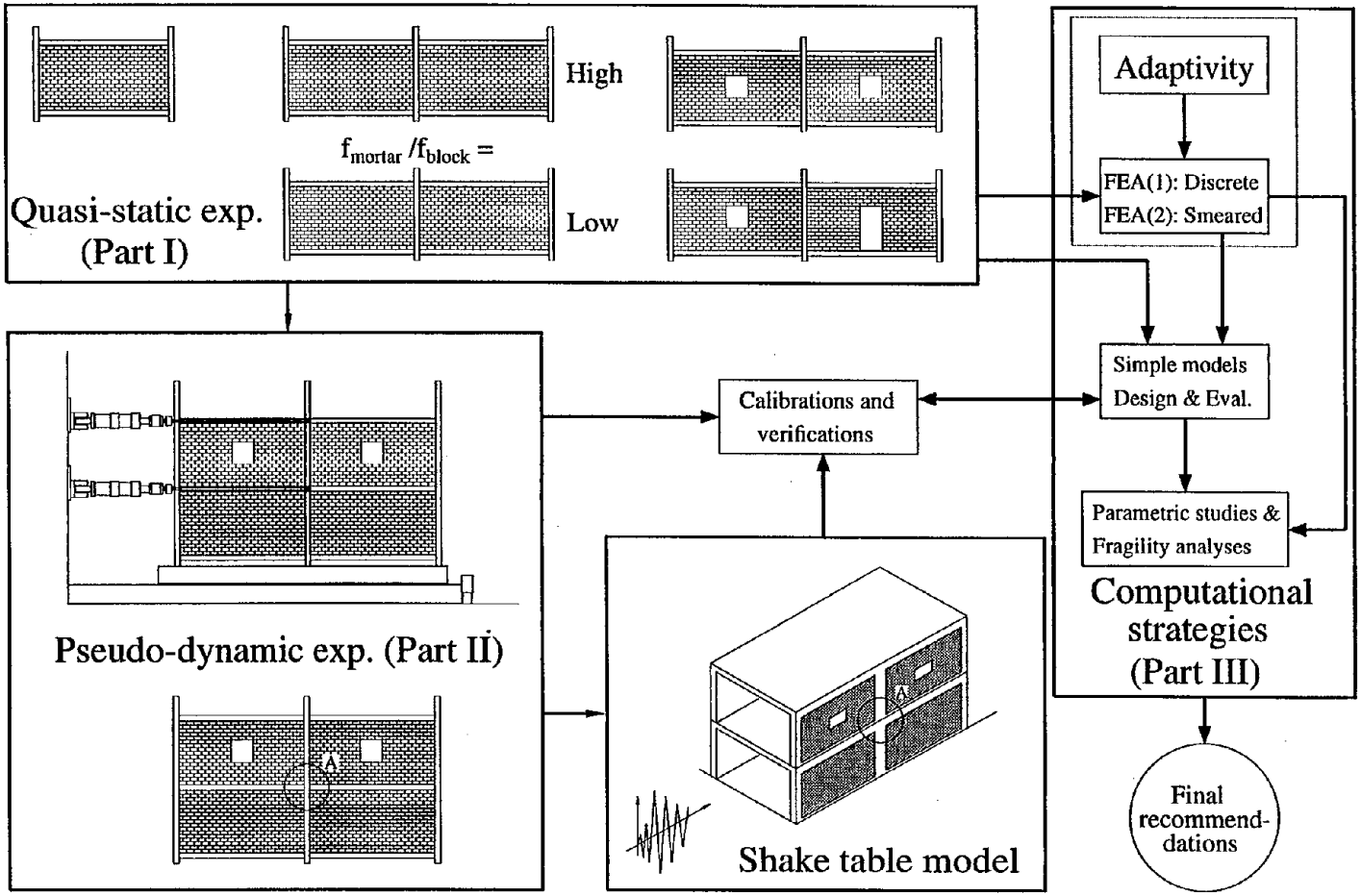

A: Typical lightly reinforced concrete joint detail, f: Compressive strength, FEA: Finite Element Analysis

FIGURE 1-1 Study program of infilled frames.

SECTION 2

PSEUDO-DYNAMIC EXPERIMENTATION

Pseudo-dynamic experimentation is a testing procedure in which the dynamic response of the structure is calculated and the obtained displacements are statically applied to the structure in an *on-line* procedure. This technique is essentially identical to traditional time domain analysis but rather than idealizing the nonlinear stiffness characteristics of the structure, the static restoring forces are directly measured from the specimen as the experiment proceeds. Computation of displacements is based on numerical integration of the governing second-order differential equations of motion of a lumped system with assumed mass and damping properties and with a forcing function corresponding to a selected dynamic loading. During the test, actual displacements and restoring forces are measured using the same equipment used for quasi-static experiments. These measured quantities are utilized in subsequent calculations. In this way, both dynamic effects and progressive damage of the specimen are included in the imposed displacements.

The application of the pseudo-dynamic testing procedure allows for an *in-depth* monitoring of the performance of the structure for the entire duration of *realistic* earthquake excitation. This level of monitoring is not possible with quasi-static experiments or shake table testing. In quasi-static experiments, difficulties are encountered, especially for multi-degree of freedom systems, in relating the imposed forces or displacements to those that might occur during an earthquake, and dynamic effects are not included. Shake table testing suffers from difficulties due to the short duration of the experiment and the physical limitations which often mandate testing reduced scale structural models under a single ground motion component.

The pseudo-dynamic setup can be considered as a *loop system* consisting of two cycles, as shown in Figure 2-1. The *calculation cycle* contains the computer and the associated software and hardware for solving the equations of motion, and the *loading cycle* consists of the servo-hydraulic displacement control system which imposes the desired displacements.

The present section summarizes the background of the pseudo-dynamic experimentation. Subsequently, the discussion focuses on the analytical formulation of the pseudo-dynamic experimental technique.

2.1 Background

The pseudo-dynamic technique was first proposed by Takanashi *et al.* [25] at the Institute of Industrial Science of the University of Tokyo and the Building Research Institute of the Ministry of Construction in Japan. Since then, many Japanese researchers have conducted pseudo-dynamic experiments. A comprehensive review of Japanese activities in the devel-

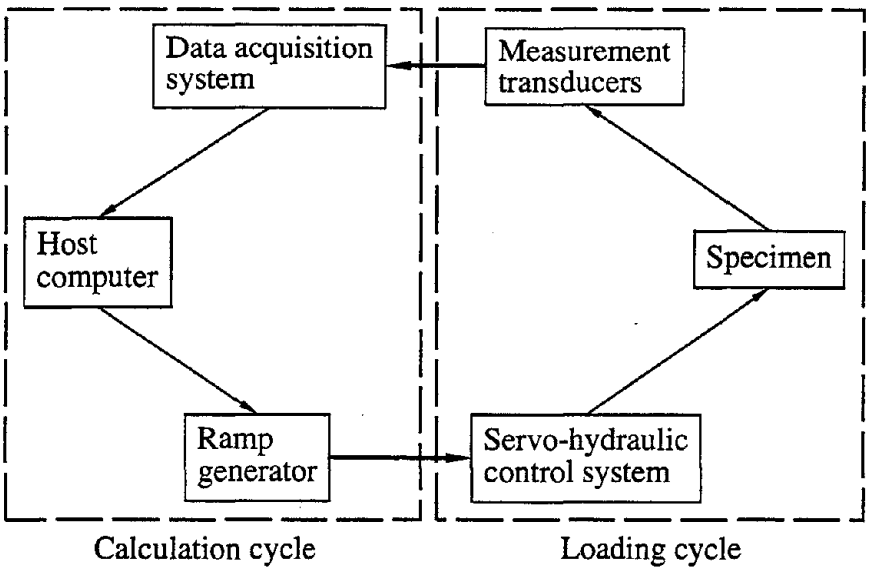

FIGURE 2-1 Block diagram of the pseudo-dynamic test loop.

opment and application of the *on-line* pseudo-dynamic testing is presented in reference [26]. At the University of California, Berkeley, and at the University of Michigan, Ann Arbor, the pseudo-dynamic method has been evaluated and improved as part of the U.S.-Japan Cooperative Earthquake Research Program. Results of these studies are summarized in reference [7]. Whereas the research group at the University of California, Berkeley, concentrated on the time integration [19], the group at the University of Michigan, Ann Arbor focused on the actuator control. A summary of studies on the characteristics of the actuator controller can be found in reference [4].

Different numerical schemes are available to obtain a time stepping approximate solution of the governing equations of motion. Such numerical schemes can be purely explicit (*i.e.* solution depends on the information at previous time steps only, *e.g.* the central difference method), purely implicit (*i.e.* solution depends on the information at previous as well as present time steps, *e.g.* the Newmark β method), or a mixture of implicit/explicit schemes (*e.g.* the operator-splitting method [5]). To avoid the need for iterative solvers, explicit methods predominate in pseudo-dynamic experimentation. Several explicit methods have been examined by Shing and Mahin [18] [19]; they recommend the use of a modified version of the Newmark algorithm which includes frequency-proportional numerical damping. To alleviate the conditional stability problems associated with explicit integration operators, Thewalt and Mahin [27] proposed a fully implicit hybrid solution technique. In their technique, part of the solution is performed digitally and the remainder is solved in an analog form. Shing *et al.* [24] developed an unconditionally stable implicit time integration algorithm based on dual displacement control for pseudo-dynamic tests. This algorithm was successfully applied by Shing *et al.* [23] in testing stiff reinforced masonry walls. An implicit/explicit algorithm formulated by Nakashima *et al.* [10] utilized the

idea of operator-splitting developed by Hughes *et al.* [5]. In this technique, the stiffness matrix is split into linear and nonlinear parts. The explicit predictor-corrector method is employed for the integration associated with the nonlinear stiffness, whereas the implicit unconditionally stable Newmark β method is employed for the integration associated with the linear stiffness.

The results from pseudo-dynamic experimentation can be very sensitive to measurement and control errors. This drawback led several researchers to concentrate on the issue of error analysis. The cumulative nature of experimental errors in pseudo-dynamic tests using explicit numerical integration algorithm was studied by Shing and Mahin [21] [22]. They concluded that the magnitude of the cumulative errors depends on the numerical properties of the algorithm, the frequency characteristics of the specimen and the nature of the experimental errors. The reliability of pseudo-dynamic testing was investigated by Yamazaki *et al.* [31] where experimental error behavior is examined based on an elastic pseudo-dynamic test applied to a full-scale six-story steel structure. An error analysis for implicit integration schemes was performed by Peek and Yi [12] [13]. They concluded that error propagation characteristics of the pseudo-dynamic method based on implicit time-integration schemes are sensitive to details of the implementation. Later, Yi and Peek [32] developed a technique to minimize the cumulative effect of systematic displacement control errors for effective single degree of freedom systems. Recently, Thewalt and Roman [30] presented several new parameters for identifying systematic errors and quantifying their seriousness.

2.2 Pseudo-dynamic Method

The pseudo-dynamic method is potentially advantageous in many circumstances. Some of the situations explored in the literature include the following:

1. It allows large massive structures to be tested (*e.g.* the full-scale five story reinforced masonry research building tested at the University of California, San Diego [17]).

2. Since the test is performed slowly, arbitrarily large ground excitations can be used (*e.g.* applying up to 1.228g of Taft earthquake on 5/48 scale tubular frame specimen [20]).

3. Since the forcing function is analytically prescribed, excitation can be due to generalized multiple component fixed base movement, given the proper form of the equations of motion (*e.g.* the one story structure with rigid diaphragm subjected to five simultaneous components of acceleration: two lateral and three rotational for pitch, roll and twist [28] [29]).

4. Substructuring concepts can also be used to allow a portion of the structure to be tested while the rest of the structure is modeled analytically on the host computer (*e.g.*

converting the inelastic dynamic program DRAIN-2D into a controlling substructure pseudo-dynamic algorithm to test a small subassembly of the first story and the middle bay of a three-bay, eight-story moment resisting steel frame [16]).

The following steps summarize the procedure of pseudo-dynamic experimentation:

1. The tested structure is idealized as a discrete-parameter system.
2. The equations of motion for the system are formulated as usual, *i.e.* a set of second-order ordinary differential equations.
3. The inertial and viscous damping characteristics are assumed and then *numerically* specified.
4. Structural restoring forces are *directly measured* during the experiment and subsequently used in the calculations.
5. Step-by-step numerical integration of the governing differential equations of motion for the tested specimen is performed using an *on-line* computer.
6. The computed displacement response, corresponding to a *specific earthquake* excitation, is imposed on the tested structure by means of servo-hydraulic actuators controlled by the on-line computer.

Following this procedure, the *quasi-statically* imposed displacements of the tested structure will closely resemble those that would actually be developed if the structure were tested dynamically. *Since imposed deformations are statically applied, only appropriate idealization of the stiffness characteristics of the tested structure must be guaranteed in the experimental setup.* Inertial and damping characteristics are only needed for the numerical procedure where *reasonable* assumptions can be made, as discussed in Sections 3.1.2 and 3.1.4.

2.3 Formulation

The dynamic response of an n degrees of freedom system is governed by:

$$[M]\{a\} + [C]\{v\} + [K]\{d\} = \{p\} \tag{2.1}$$

where $[M]$, $[C]$, and $[K]$ are the mass, damping, and stiffness $n \times n$ matrices, respectively; $\{d\}$, $\{v\}$, and $\{a\}$ are the displacement, velocity, and acceleration vectors, respectively and $\{p\}$ is the external force vector. This equation can be discretized in time to give

$$[M]\{a_{i+1}\} + [C]\{v_{i+1}\} + \{r_{i+1}\} = \{p_{i+1}\} \tag{2.2}$$

where $\{r\}$ is the restoring force vector, *i.e.*

$$\{r\} = [K]\{d\} \tag{2.3}$$

In Eq. (2.2), subscript $(i+1)$ indicates the time station $(i+1)(\Delta t)$ where (Δt) is the time interval.

2.3.1 Numerical integration

Stiff structures (*e.g.* steel frames with masonry infill walls) may be classified as short period structures. When the governing differential equations of motion of such structures are integrated using explicit numerical integration methods, stability problems might arise. In the early pseudo-dynamic experimentation, explicit methods were preferred over implicit methods to eliminate the need for iterations with the implicit methods. Since most of the earlier pseudo-dynamic experiments were performed on rather flexible structures (*e.g.* steel cantilevers), use of explicit methods did not cause serious problems. This situation is not the same for short period structures [6]. Accordingly, the recent trend in pseudo-dynamic experimentation aims towards the use of implicit methods, not only for their superior stability properties but also for their desirable spurious energy dissipation properties [6].

The implicit Newmark algorithm developed by Hughes *et al.* [5] is utilized in the present study. In this algorithm the equations of motion (Eq. (2.2)) are satisfied in addition to the following difference relations:

$$\{d_{i+1}\} = \{d^e_{i+1}\} + (\Delta t)^2\beta\{a_{i+1}\} \tag{2.4}$$

$$\{v_{i+1}\} = \{v^e_{i+1}\} + (\Delta t)\gamma\{a_{i+1}\} \tag{2.5}$$

where β and γ are parameters controlling stability and accuracy, respectively. The vectors $\{d^e_{i+1}\}$ and $\{v^e_{i+1}\}$ are explicit forms of displacement and velocity, respectively, *i.e.*

$$\{d^e_{i+1}\} = \{d_i\} + (\Delta t)\{v_i\} + (\Delta t)^2\left(\frac{1}{2} - \beta\right)\{a_i\} \tag{2.6}$$

$$\{v^e_{i+1}\} = \{v_i\} + (\Delta t)(1-\gamma)\{a_i\} \tag{2.7}$$

An expression for $\{a_{i+1}\}$ can be obtained from Eq. (2.4). Upon substitution of this expression in Eq. (2.5) and subsequently, eliminating $\{v_{i+1}\}$ and $\{a_{i+1}\}$ from Eq. (2.2), the following *effective static problem* results:

$$[K^*] = \frac{1}{(\Delta t)^2\beta}[M] + \frac{\gamma}{(\Delta t)\beta}[C] \tag{2.8}$$

$$\{p^{\star}_{i+1}\} = \{p_{i+1}\} - \{r_{i+1}\} + [K^{\star}]\{d^{e}_{i+1}\} - [C]\{v^{e}_{i+1}\} \tag{2.9}$$

$$[K^{\star}]\{d_{i+1}\} = \{p^{\star}_{i+1}\} \tag{2.10}$$

In nonlinear structural analysis, the stiffness matrix $[K]$ depends on the applied displacement $\{d\}$. Since $\{r_{i+1}\}$ depends on $\{d_{i+1}\}$, as shown in Eq. (2.3), an iterative scheme is needed which requires appropriate definition of the evolution of $[K]$ with loading. In general, this definition is unclear due to incomplete knowledge of the material behavior in nonlinear stages.

2.3.2 Conceptual model

The formulation presented in the previous paragraphs is illustrated in an algorithmic form in Figure 2-2 where the superscript m indicates that the specified quantity is measured rather than calculated. The predictor phase in Figure 2-2 is based on the *explicit* part of the displacement vector and on the corresponding measured restoring force vector $\{r^{e}_{i+1}\}$. *Measuring the quantities from the physical specimen eliminates the need for any assumptions on the stiffness matrix of the structure.* In general, the displacement vector $\{d_{i+1}\}$, obtained from the solution of the *effective static problem* given by Eq. (2.10), will differ from its explicit part $\{d^{e}_{i+1}\}$. Therefore, a residual or "out of balance" force vector results; it is eliminated using an iterative scheme. Accordingly, the corrector phase, shown in Figure 2-2, is introduced to eliminate this residual force vector. In general, this corrected phase should be applied until the error $\{d_{i+1} - d^{e}_{i+1}\}$ is eliminated. In the present implementation, a tolerance (TOL = 0.0008 in) is used to check this error quantity. This tolerance is taken as the smallest possible displacement increment which can be applied with the available hydraulic actuators. The reported results in **SECTIONS 4 & 5** are based on applying only one iteration of the correction phase which was sufficient to satisfy the check shown in Figure 2-2. This was possible because of the use of a sufficiently small time step ($\Delta t \leq 0.005$ sec) and special ramping between displacement vectors $\{d_{i-1}\}$ and $\{d_i\}$ as illustrated in Figure 3-2. The numerical stability and the accuracy of several numerical integration schemes, similar to the one adopted herein, have been analyzed by Shing and Mahin [19].

2.4 Summary

The pseudo-dynamic experimentation technique and its analytical formulation is presented. Review of the literature related to different issues of the pseudo-dynamic method is briefly outlined. The presented pseudo-dynamic algorithm utilized the implicit Newmark numerical integration method.

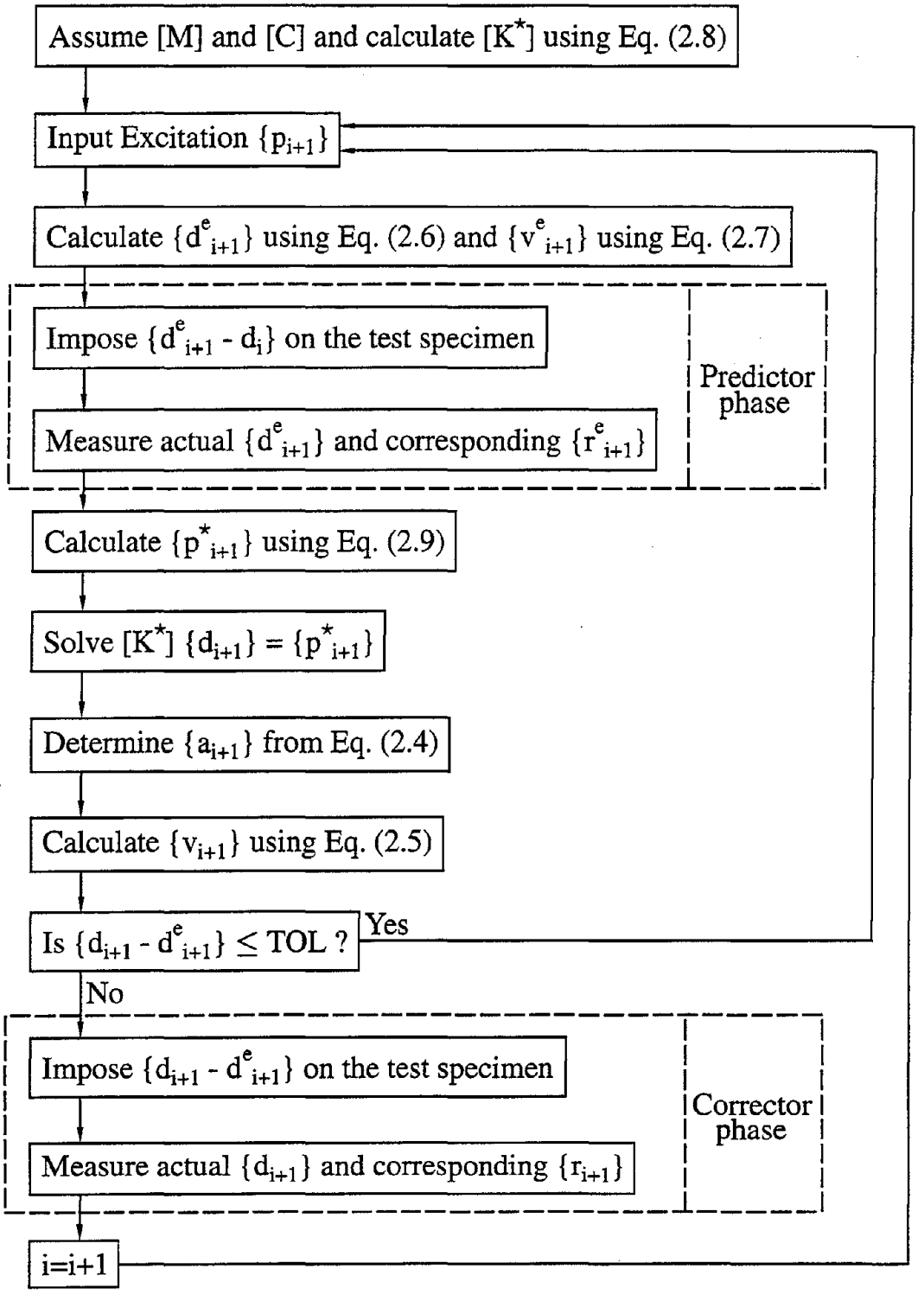

FIGURE 2-2 Pseudo-dynamic algorithm.

SECTION 3

PSEUDO-DYNAMIC APPLICATION

The present section summarizes the application of the pseudo-dynamic experimentation technique for the seismic response evaluation of a two-bay, two-story GLD steel frame infilled with non-integral URM walls. A discussion of the experimental errors encountered in applying the pseudo-dynamic procedure is briefly presented. Finally, numerical verification of the pseudo-dynamic algorithm is illustrated.

3.1 Characteristics of The Tested Structure

The pseudo-dynamic method discussed in the previous section is adopted in testing a quarter scale (*i.e.* the length scale factor $S_l = 4$) two-bay, two-story steel frame infilled with unreinforced concrete block masonry. The geometry of the structure is illustrated in Figure 3-1. The implementation of the pseudo-dynamic procedure is schematically illustrated in Figure 3-2. As shown in Figure 3-2, during the test, distinction is made between external transducers measuring the displacement vector of the structure $\{d_{external}\}$, used in the time integration loop, and internal transducers measuring the displacement vector of the actuators $\{d_{internal}\}$, used to control the actuators in the servo-hydraulic loop. This *dual* displacement control technique has the following advantages:

1. Prevents the deformation of the reaction frame supporting the actuators, or the load transfer mechanism from the actuators to the structure, from affecting the actual displacements of the structure.

2. Avoids any external disturbance to the transducers used in the feed-back control of the servo-hydraulic loop.

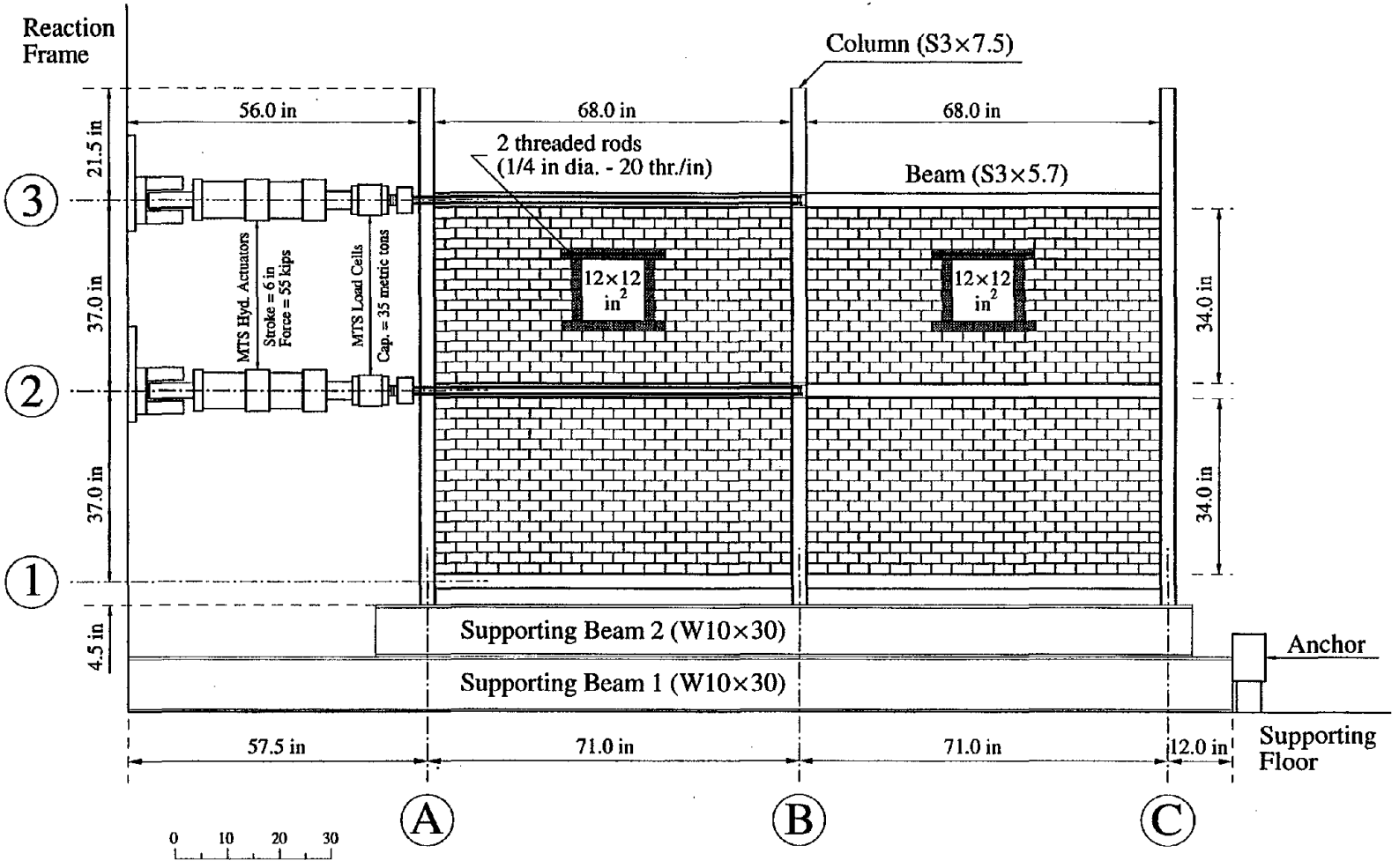

FIGURE 3-1 Layout of the tested specimen.

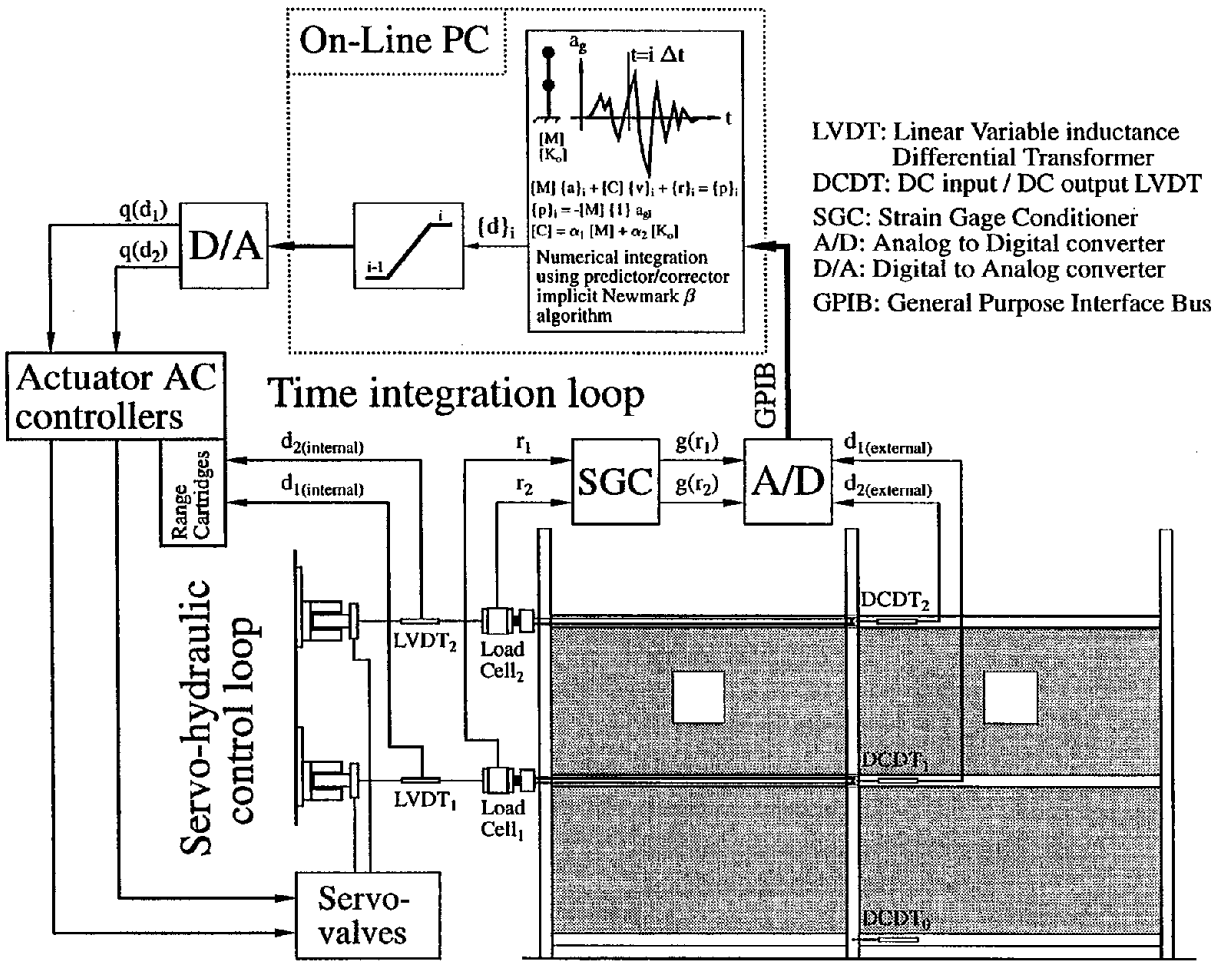

FIGURE 3-2 Schematic illustration of the pseudo-dynamic experiment.

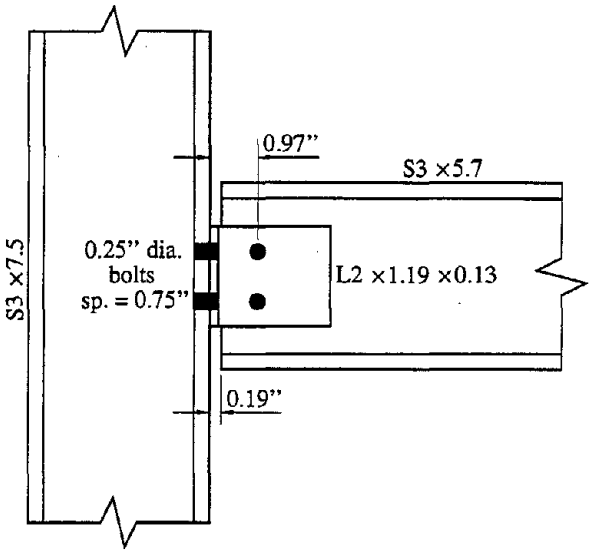

FIGURE 3-3 Detail of ASD-Type 2 (LRFD-Type PR) connection.

3.1.1 Design and construction

The frame members were designed and constructed according to the specifications of the American Institute of Steel Construction (AISC) [1] and connected using bolted framed beam connections. These connections are those designated as "Type 2" according to Allowable Stress Design (ASD) or as "Type PR" (for Partial Restrained) according to Load & Resistance Factor Design (LRFD) [15]. Two *clip angles* L2 × $1\frac{3}{16}$ × $\frac{1}{8}$ with clearance setback of $\frac{3}{16}$ inch were used as shown in Figure 3-3. The specimen was *pinned jointed* to the support structure which consisted of a heavy steel beam supported by the floor anchors (see Figure 3-1).

The out-of-plane instability was prevented by supports perpendicular to the plane of loading using steel channel sections. These supports enclosed layers of grease at the interface between the column and the channel so as to mitigate any in-plane friction and allow free lateral displacements of the specimen. The out-of-plane movements of the tested structures were found to be minimal.

After the complete erection of the steel frame, the infill walls were constructed by an experienced mason using small-scale concrete blocks and model mortar. The mechanical properties of the materials used in constructing the unreinforced concrete block masonry walls are summarized in Table 3-I. Detailed investigation of the mechanical properties of the infill materials can be found in the first report of this three-report-series. The construction of the masonry infill walls followed common practice of ungrouted masonry where mortar on only the face shell of the block was used (*i.e.* face shell bedding). No shear connectors were used between the walls and the surrounding frame members (*i.e.* non-integral walls). The concrete block masonry cells around the openings were grouted. Bond beams on top

TABLE 3-I Mechanical properties of unreinforced masonry components.

f_b [psi]	f_{cyl} [psi]	f_b/f_{cyl}	f_p [psi]	E_p [ksi]
4000	3100	1.29	3300	1500

□ block compressive strength based on net area
△ mortar cylinder compressive strength
◇ masonry prism strength (f_p) & stiffness (E_p) based on the face shell areas

of the openings were reinforced using two threaded rods of $\frac{1}{4}$ inch diameter and 20 threads per inch. The width of the supports of these bond beams was about 4 inches (*i.e.* one block).

3.1.2 Mass properties

As discussed previously, the mass and damping characteristics of the tested structure must assume reasonable values. For this purpose, the layout of the prototype of the tested frame is illustrated in Figure 3-4. From this figure, one can easily calculate the prototype $[M_p]$ and the corresponding model $[M]$ lumped mass matrices,

$$[M_p] = \begin{bmatrix} 0.2 & 0.0 \\ 0.0 & 0.2 \end{bmatrix} \quad \& \quad [M] = \begin{bmatrix} 0.0125 & 0.0000 \\ 0.0000 & 0.0125 \end{bmatrix} \qquad \text{kip.sec}^2/\text{in}$$

It should be noted that the mass in each story accounts for the self weight of the floor and about 25% of the design live load. Since the masses of the walls and the frame are much smaller than the floor mass, they are ignored. To obtain the model mass matrix, the prototype mass matrix is scaled using [14]

$$[M] = \frac{1}{S_l^2}[M_p] \tag{3.1}$$

3.1.3 Stiffness properties

Numerical and experimental studies of the infilled frame require estimation of the stiffness characteristics of the *undamaged* specimen. This estimation is achieved from preliminary experiments on the infilled frame using earthquakes with small Peak Ground Acceleration (PGA) (*e.g.* $0.05g \leq \text{PGA} \leq 0.15g$). These ground motions were large enough to mobilize the composite action of the wall/frame system (*i.e.* provide sufficient lateral displacement

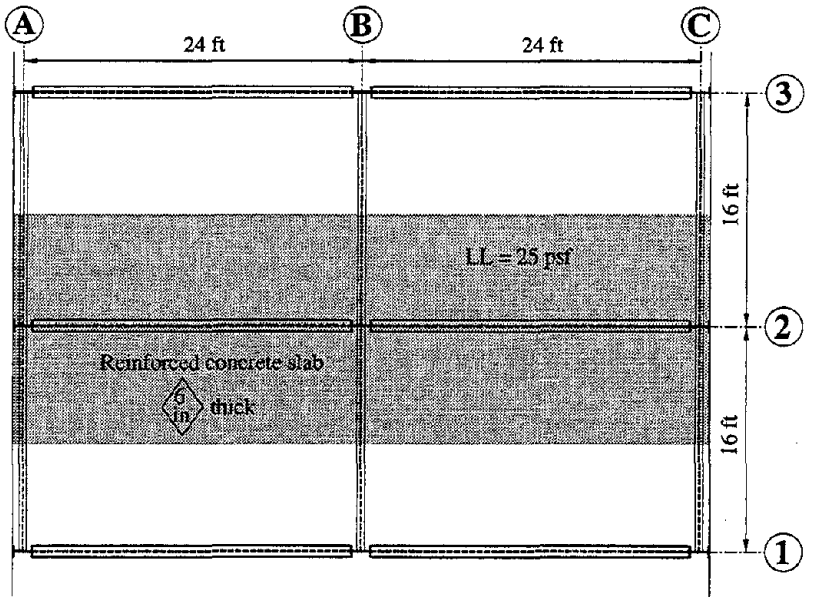

FIGURE 3-4 Plan view of the prototype building.

to overcome the lack of fit between the wall and the frame) without any visible damage to the structure.

A sample result for Taft earthquake S69E component (for information about recorded accelerograms, refer to Table 2-1 of reference [8]) scaled to PGA = $0.1g$ is illustrated in Figure 3-5(a). In this figure, a plot for the story shear versus the inter-story drift is shown for each story. These plots are idealized in Figure 3-5(b) where nonlinear elastic behavior is assumed using the dashed line which follows the back-bone curve of the hysteresis loops. The back-bone curve shown in Figure 3-5(b) is approximated by the symmetric behavior shown in Figure 3-5(c). This approximation is conducted by shifting the origin to the center of the flat region of the plot and by taking the average of the stiffnesses in the positive and negative sides of the loop. The walls are assumed to be inactive during a displacement interval denoted by $2\Delta_{st}$, twice the story *lack of fit* between the infill wall and the bounding frame. This lack of fit is thought to be caused mainly by *shrinkage* of the infill wall as shown in the following section. From Figure 3-5(c), the two main tangent stiffness matrices can be identified as follows,

$$[K^F] = \begin{bmatrix} 25 & -8 \\ -8 & 8 \end{bmatrix} \quad \& \quad [K^{IF}] = \begin{bmatrix} 375 & -177 \\ -177 & 177 \end{bmatrix} \qquad \text{kip/in}$$

where $[K^F]$ and $[K^{IF}]$ are the linear stiffness matrices for the Frame and the Infilled Frame, respectively. These matrices are based on the assumption of rigid floors, *i.e. shear building* approximation. A transition zone exists between the situation of inactive walls, where the stiffness matrix is $[K^F]$, and that of walls in full contact with the bounding frame,

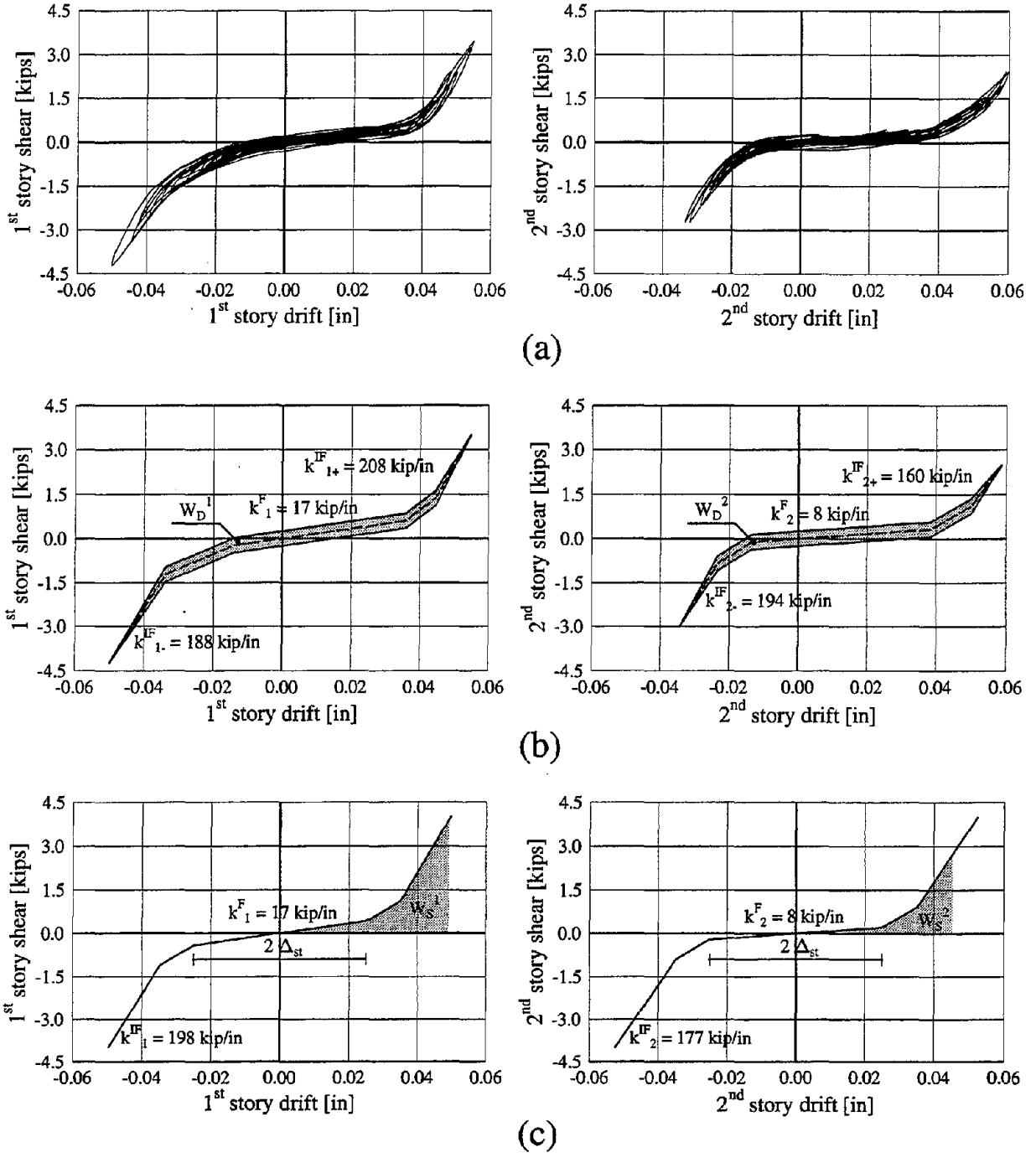

FIGURE 3-5 Stiffness properties. (a) Story shear versus inter-story drift due to Taft ground motion PGA = $0.1g$, (b) idealized hysteretic relations, (c) idealized symmetric back-bone relations. Notations: F (frame); IF (infilled frame); W_D (energy absorbed during one loading cycle); W_S (input energy corresponding to a particular cycle); K (stiffness); Δ_{st} (story lack of fit between the infill wall and the bounding frame).

where the stiffness matrix becomes $[K^{IF}]$. In this transition zone, the roughness along the interface between the walls and the frame members is degraded to provide the infilled frame composite action.

Shrinkage calculations

In the story shear/inter-story drift relations (Figure 3-5(c)), the frame is assumed to carry the full applied lateral load until it starts bearing against the wall. The displacement necessary to start activating the wall/frame behavior Δ_{st} is assumed to depend on the shrinkage of the wall material as shown in Figure 3-6. In this figure, the story lack of fit Δ_{st} is dependent upon the wall geometry, *i.e.* length L and height H, and on the equivalent strain values due to shrinkage in the vertical ϵ_v and horizontal ϵ_h directions. These equivalent strain values are approximately given by

$$\epsilon_v = \frac{\epsilon_{sh}^m \times t_{mb} \times (n_c + 1) + \epsilon_{sh}^b \times h_b \times n_c}{H} \tag{3.2}$$

$$\epsilon_h = \frac{\epsilon_{sh}^m \times t_{mh} \times (\mathrm{INT}(n_b + 0.5) + 1) + \epsilon_{sh}^b \times l_b \times n_b}{L} \tag{3.3}$$

where:

ϵ_{sh}^m = shrinkage strain of the mortar

t_{mb} = thickness of the mortar bed joint

t_{mh} = thickness of the mortar head joint

ϵ_{sh}^b = shrinkage strain of the concrete blocks

h_b = height of a concrete block

l_b = length of a concrete block

n_c = number of courses along the wall height (H)

n_b = number of blocks in one course along the wall length (L)

In Eq. (3.3), INT(•) implies the integer value of •. The parameters needed for the shrinkage calculations are given in Table 3-II. The geometrical parameters are defined in Figure 3-1. The required material parameters are taken from reference [3]. From Eqs. (3.2) and (3.3), Table 3-II and Figure 3-6, one readily obtains the following:

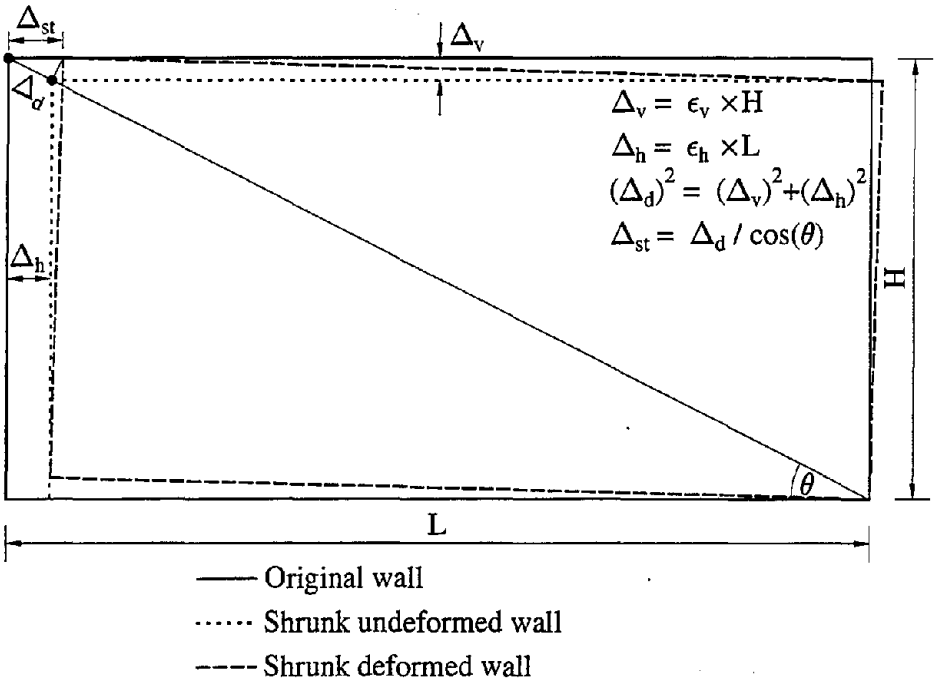

FIGURE 3-6 Lack of fit due to shrinkage.

TABLE 3-II Parameters for shrinkage calculations of one solid infill wall (dim. in inches).

L	H	θ^o	t_{mb}	t_{mh}	h_b	l_b	n_c	n_b	$\epsilon^m_{sh} \times 10^6$	$\epsilon^b_{sh} \times 10^6$
68	34	26.57	$\frac{5}{32}$	$\frac{5}{32}$	$1\frac{27}{32}$	$3\frac{26}{32}$	17	$16\frac{1}{2}$	650 ± 150	330 ± 200

$\epsilon_v = 360 \times 10^{-6}$, $\epsilon_h = 330 \times 10^{-6}$, $\Delta_v = 0.012$ in, $\Delta_h = 0.023$ in,

$\Delta_d = 0.026$ in, $\boxed{\Delta_{st} = 0.029 \pm 0.016 \text{ in}}$

It is interesting to note that the results in Figure 3-5(c) indicate that $\Delta_{st} \approx 0.025$ in, which is close to the calculated mean value. In conducting the shrinkage calculations, it is assumed that the mean shrinkage strain for mortar joints ϵ^m_{sh} and concrete blocks ϵ^b_{sh} are the same in both vertical and horizontal directions. For simplicity, the windows in the top story may be neglected in the calculations of the equivalent strains.

Eigen solution

The eigen problem corresponding to Eq. (2.1) is given by

$$\omega_n^2[M]\{\Phi_n\} = [K]\{\Phi_n\} \tag{3.4}$$

TABLE 3-III Eigen solutions (superscript T denotes transpose).

	f_1 [Hz]	f_2 [Hz]	$\{\Phi_1\}$	$\{\Phi_2\}$
Frame (F)	3.15	7.59	$\{1.00 \quad 2.42\}^T$	$\{1.00 \quad -0.41\}^T$
Infilled Frame (IF)	12.14	31.24	$\{1.00 \quad 1.68\}^T$	$\{1.00 \quad -0.60\}^T$

where ω_n and $\{\Phi_n\}$ are the circular frequency and mode shape, respectively, for the n^{th} mode shape. From the assumed mass matrix $[M]$ and stiffness matrix (either $[K^F]$ or $[K^{IF}]$), one can solve the eigen problem (3.4) to obtain the eigen solution given in Table 3-III where the frequency $f_n = \omega_n/(2\pi)$.

3.1.4 Damping properties

Idealization of damping properties is probably the most uncertain step in structural dynamics. Several sources of material damping exist which makes its accurate idealization extremely difficult. In the present study, the simplest form of damping, namely *proportional damping*, is assumed. In this idealization, the damping matrix $[C]$ is given by,

$$[C] = \alpha_1[M] + \alpha_2[K] \tag{3.5}$$

where α_1 and α_2 are parameters to be determined according to specified damping ratios in two modes. If the circular frequencies in two modes are ω_i and ω_j and the corresponding damping ratios are ξ_i and ξ_j, the constants α_1 and α_2 can be expressed as,

$$\alpha_1 = 2\xi_i\omega_i - \alpha_2\omega_i^2 \qquad \& \qquad \alpha_2 = 2\frac{\omega_j\xi_j - \omega_i\xi_i}{\omega_j^2 - \omega_i^2} \tag{3.6}$$

The damping ratio for any other mode r, with a circular frequency ω_r may be determined from

$$\xi_r = \frac{1}{2}\left(\frac{\alpha_1}{\omega_r} + \alpha_2\,\omega_r\right) \tag{3.7}$$

Equation (3.7) is obtained by converting the equations of motion (Eq. (2.1)) into modal equation for the r^{th} mode (for details, see reference [2]). The second term in Eq. (3.7) maybe based on $[K^F]$ or $[K^{IF}]$. The use of $[K^F]$ is selected in the present study because using $[K^{IF}]$ will lead to an over-estimation of $[C]$ before the walls come in full contact with the bounding frame. On the other hand, it is expected that damping due to hysteresis, produced by sliding between the walls and the frame members, is more important than the viscous damping (refer to section 3.3.1).

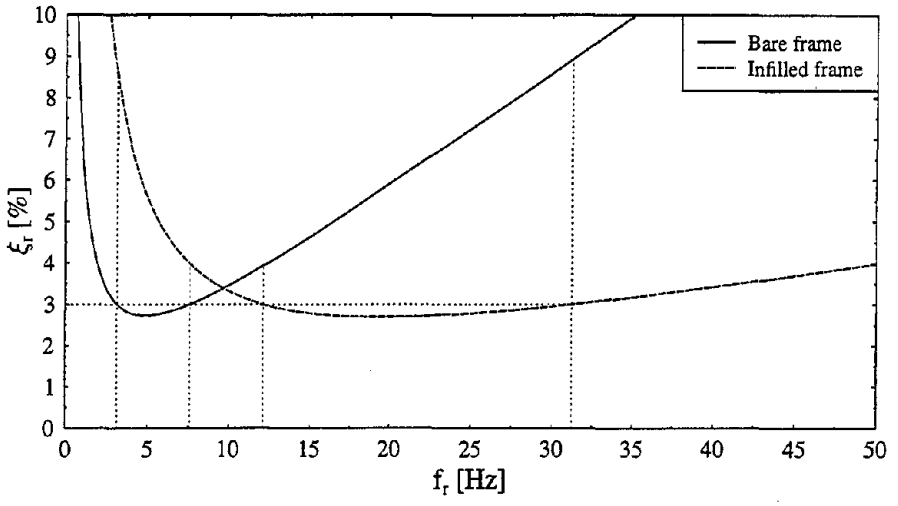

FIGURE 3-7 Effect of frequency on damping ratio (subscript r denotes the r^{th} mode shape).

TABLE 3-IV Damping ratios for the infilled frame (IF) based on assumed damping ratios for the bare frame (F).

	ξ_1^{IF} %	ξ_2^{IF} %
$\xi_1^F = \xi_2^F = 3\%$	3.9	8.9
$\xi_1^F = \xi_2^F = 2\%$	**2.6**	**5.9**

The variation of the damping ratio with frequency is shown in Figure 3-7. In this figure, 3% damping ratio for the two modes is assumed. The solid curve gives the case where the two modes of the bare frame are considered while the dashed line is based on the two modes of the infilled frame. Table (3-IV) gives the damping ratios of the infilled frame based on the assumed ratios for the bare frame. As shown in this table, for the bolted steel frame with concrete block masonry infill walls, 2% damping in the modes of the bare frame produce acceptable values [11] of the damping ratios for the infilled frame. For these ratios, one obtains

$$\alpha_1 = 0.56\,\text{sec}^{-1} \qquad \& \qquad \alpha_2 = 5.9 \times 10^{-4}\,\text{sec}$$

Therefore, the damping matrix becomes

$$[C] = \begin{bmatrix} 2.2 & -0.5 \\ -0.5 & 1.2 \end{bmatrix} \times 10^{-2} \qquad \text{kip.sec/in}$$

3.1.5 Ground motion

Three earthquake records are selected as input ground motion. The first is the one recorded at Taft-Lincoln School, S69E of the event at Kern County, California (July 21, 1952). The second is the one recorded at El-Centro, S00E of the event at Imperial Valley, California (May 18, 1940). These two records represent, respectively, moderate and strong ground shaking typical of the North American west coast earthquakes. The third record is a late 1985 earthquake in the North Nahanni River area of the Northwest Territories of Canada. This record is an intra-plate type of earthquake which is typical of the central and eastern coast regions of North America.

For compliance with the similitude requirements, the record time scale should be compressed by a factor S_t given by [14],

$$S_t = \sqrt{S_l} \tag{3.8}$$

Based on this factor, the compressed earthquake records of the considered three events when scaled to $1g$ PGA are shown in Figure 3-8. The elastic response spectra for the three records are plotted in Figure 3-9 for a damping ratio of 2%. From these plots and the natural periods of the bare and infilled frames, one can observe that the Nahanni record is not likely to produce any inelastic deformation of the bare frame. This is obviously not the case for the other two records. For the infilled frame, as the period of the structure is close to the main peak of the Nahanni spectra, once the system experiences inelastic deformation, the instantaneous period elongates and accordingly significant reduction of the spectral acceleration is expected. Again, this situation does not occur for El-Centro nor Taft where the structural system moves to a higher range of spectral accelerations, particularly under Taft.

3.2 Experimental Errors

Experimental errors are inevitable. This fact has led to their acceptance as long as their relative magnitudes, compared with the measured quantity, are "reasonably small". In the pseudo-dynamic procedure, experimental feedback is adopted in the step-by-step numerical integration. Therefore, errors introduced in any step are carried over to the subsequent computations leading to potentially serious cumulative effects.

Errors are introduced by several sources in the pseudo-dynamic procedure. The errors produced from the experimental environment are usually assumed to be more significant than those due to the numerical environment [18]. Sources of experimental errors include:

1. Inaccurate calibration of displacement transducers used in the closed-loop feedback system which controls the hydraulic actuators.

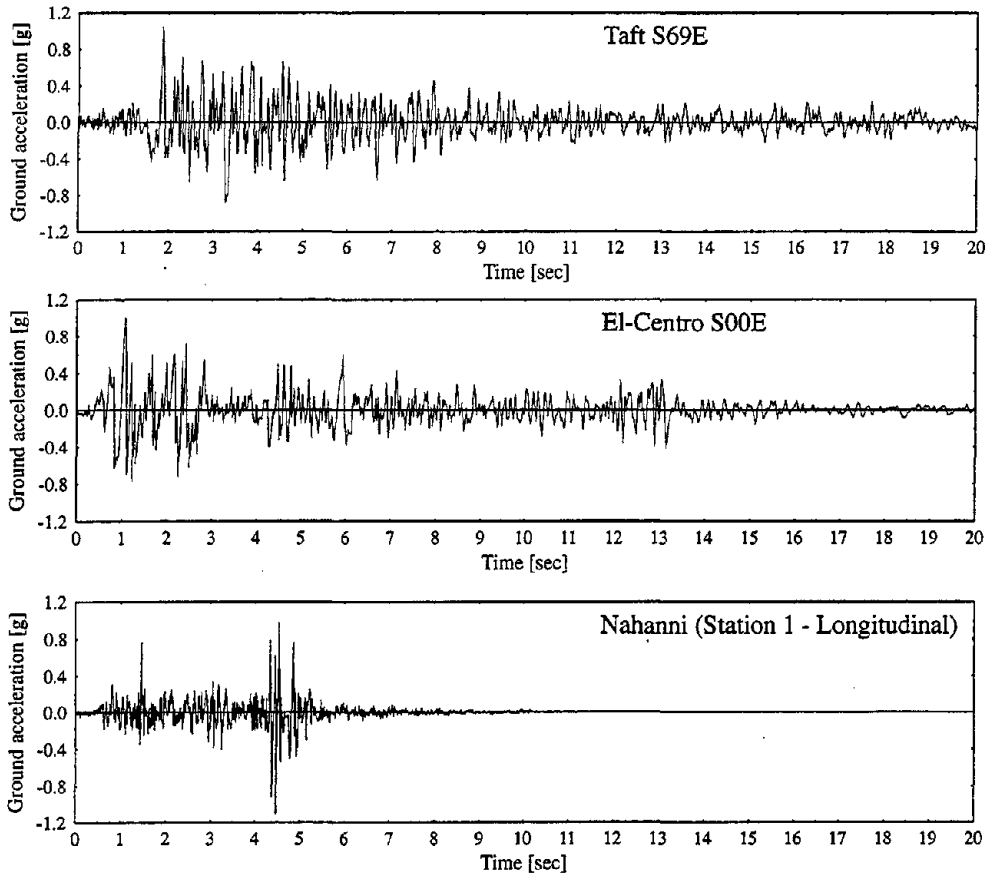

FIGURE 3-8 Ground acceleration scaled to $1g$ and compressed according to Eq. (3.8).

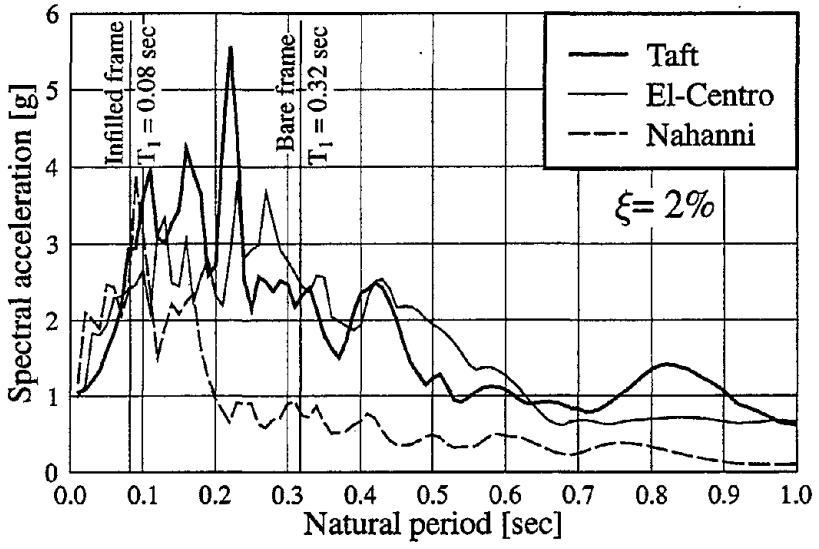

FIGURE 3-9 Elastic response spectra for the considered records.

2. Quantization effects which result from the finite word-length, *i.e.* resolution limits, imposed by the Digital-to-Analog (D/A) conversion of the command signals and the Analog-to-Digital (A/D) conversion of the measured signals.

3. Movement or deformation and friction forces of the supports and connections of the specimen.

4. Lack of hydraulic actuator sensitivity to keep up with the speed of displacement changes.

5. Electrical noise.

Consequently, the actual displacement and force feedback values are likely to deviate from the originally computed and expected quantities. As reported by Peek and Yi [12] [13], the details of the implementation of the implicit time-integration scheme affect the error propagation characteristics. In the present implementation the following conditions gave the best results in minimizing the error propagation:

1. Contrary to what is reported by Peek and Yi [12] [13], use of the previously measured displacements rather than the computed ones led to better control of error propagation. One may speculate that the reason behind this contradiction is the accurate displacement measurements used in the present study and the correction phase added to the pseudo-dynamic algorithm which prevented any accumulation of errors due to the unbalanced force vector. Another important reason for the better control of error propagation with the use of measured displacements rather than calculated ones is attributed to the stiff nature of the tested structure where small changes of the applied displacement produce relatively large changes in the corresponding restoring force. Obviously, with such behavior the accuracy improves by considering the actual measured displacement rather than the previously calculated value.

2. A delay time (0.5 sec) was added between each applied displacement increment to avoid any large sudden impact applied by the actuator to the specimen and to stabilize the hydraulic system before taking the measurements subsequently utilized by the time integration algorithm.

3. The time step was selected as the step at which the compressed earthquake records are digitized (0.005 sec for Taft and El-Centro and 0.0025 sec for Nahanni) to avoid any interpolation of the applied record. These time integration increments were sufficiently small to not cause stability or accuracy problems in the numerical integration algorithm.

4. Deformation of the loading mechanisms and supporting system were continuously monitored and automatically eliminated from the measurements.

5. After the completion of each applied earthquake record, a special procedure was used to bring all the considered degrees of freedom of the structure to their undeformed states and then to bring the specimen to a state of zero load.

6. Ideally, all components of the calculated incremental displacement vector should be simultaneously applied to avoid load reversals due to *hold intervals* of some of the degrees of freedom. This was practically achieved by a special *ramping routine* where the largest displacement increment is executed as a nested loop of the loop corresponding to the smaller displacement increment. The counters of such loops are determined based on the smallest possible displacement increment that can be applied with the available hydraulic actuators ($\approx$ 0.00007in for PGA $\leq 0.15g$ and 0.0008in for PGA $> 0.15g$).

7. Depending on the level of applied PGA, the system (load cells and displacement ranges of actuators) can be adjusted to allow the best possible resolution of the measured forces and applied displacements.

Figure 3-10 shows a sample comparison of the calculated and measured displacements for the two-bay, two-story infilled frame under the Nahanni earthquake scaled to $0.05g$. From such a comparison, it may be concluded that the proposed pseudo-dynamic experimentation technique is reliable as far as experimental error propagation is concerned.

3.3 Numerical Verification of The Pseudo-dynamic Algorithm

The tested infilled frame shows a large change of stiffness due to the activation of the walls beyond the range of displacement needed to overcome the lack of fit between the walls and the bounding frame members. Accordingly, in the elastic stage, the structure is behaving as a *hard spring* which may show complicated response (subharmonic and superharmonic vibrations) even for applied periodic forces (for details refer to Section 1.2 of the book by Moon [9]). This section presents an attempt to numerically obtain the predicted pseudo-dynamic response for the tested infilled frame with undamaged walls. The standard time domain analysis of a simple model (2 degrees of freedom with lumped masses) of the tested structure with the idealized behavior given in Figure 3-5(c) is performed.

To illustrate the idea of the model used for the numerical verification, Figure 3-11 shows the idealization of a three-story frame. The spring stiffness (k_i, $i = 1, 2, 3$) follows one of the curves in Figure 3-5(c) based on the existence or absence of window openings. In Figure 3-11, c_r is the damping coefficient associated with the stiffnesses and c_a is the damping coefficient associated with the masses.

3.3.1 Equivalent viscous damping

The concept of equivalent viscous damping is adopted to calculate the corresponding damping ratio from the hysteresis curves of the infilled frame. This equivalent damping ratio

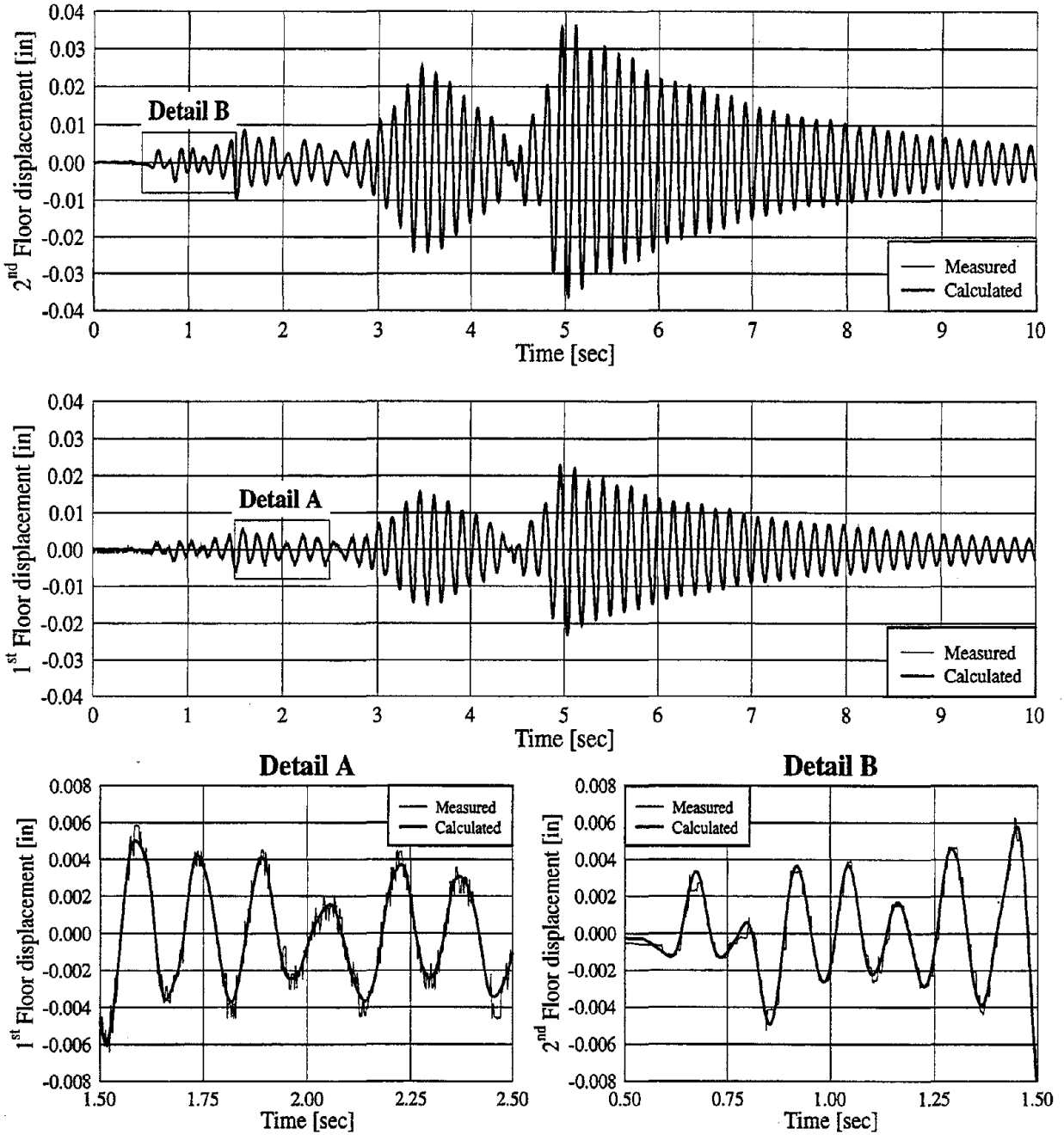

FIGURE 3-10 Comparison between measured and calculated displacements under 0.05g Nahanni earthquake.

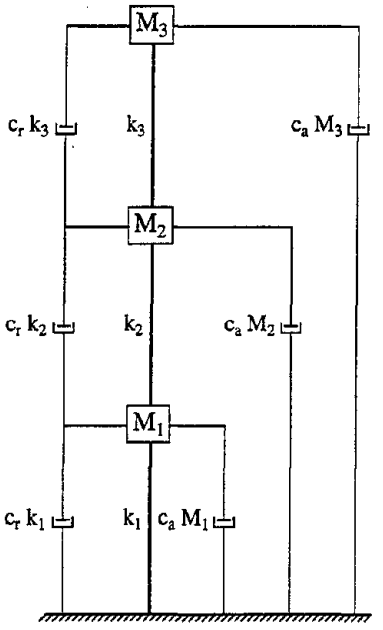

FIGURE 3-11 Model for a three-story frame.

can be expressed as

$$\xi^e = \frac{W_D}{4\pi W_S} \tag{3.9}$$

where ξ^e is the equivalent viscous damping ratio. As indicated in Figures 3-5(b) and 3-5(c), W_D is the area of the hysteresis loop (the amount of energy absorbed during one loading cycle) whereas W_S is the area under the back-bone curve (the amount of input energy at one loading cycle). It should be noted that both W_D and W_S are calculated at the same force level. Applying Eq. (3.9) at the maximum force level under Taft earthquake scaled to $0.1g$, the equivalent viscous damping coefficients (% of the critical damping) obtained for the first and the second stories are 10.5% and 12.2%, respectively. Based on the ratio between the energy absorbed in both stories and the total input energy, ξ^e is determined for the whole structure to be 11.2%.

Assuming equivalent viscous damping ratios in the first two modes as 11.2%, one can obtain the damping coefficients c_r and c_a for the two sets of dampers shown in Figure 3-11. It should be noted that the damping forces are proportional to the *relative velocity* in the first case and to the *absolute velocity* in the second. In general, c_r is more effective in the higher modes and c_a in the lower ones [2]. Using Eq. (3.7) with $\alpha_1 = c_a$ and $\alpha_2 = c_r$ for the two modes $r = 1, 2$, one obtains two equations in the two unknowns c_r and c_a. Assuming $\xi_1^e = \xi_2^e = 10\%$ and using the eigen solution for the two-story frame model, given in Table 3-III, for the bare frame, one obtains

$$c_r = 3.320 \times 10^{-3}\,\text{sec} \qquad \& \qquad c_a = 3.133\,\text{sec}^{-1}$$

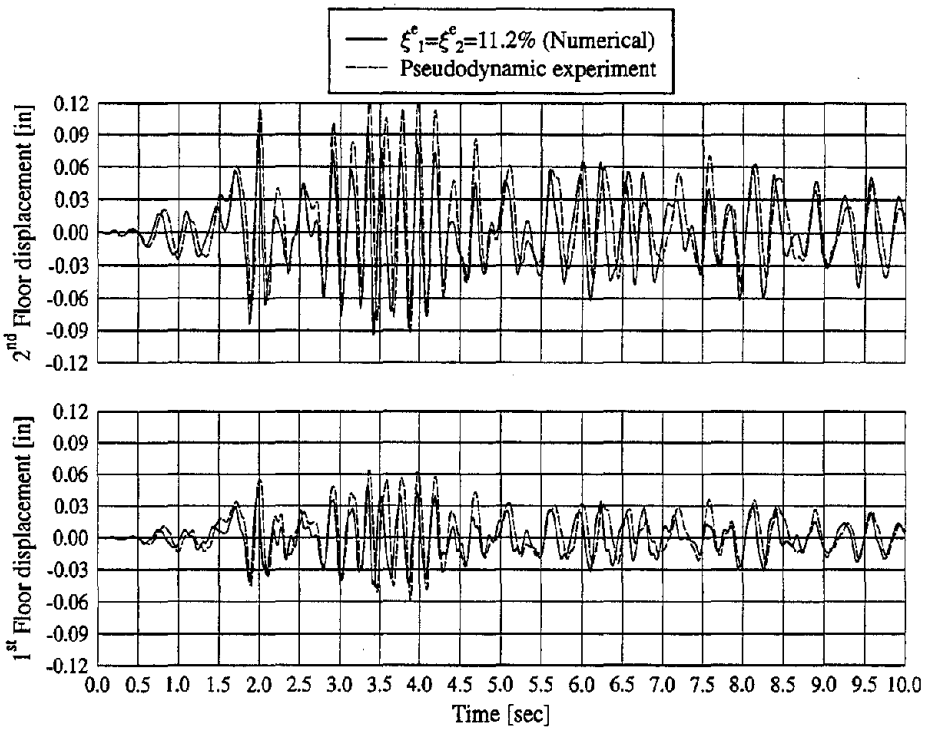

FIGURE 3-12 Time histories of displacements for Taft earthquake scaled to $0.1g$.

Note that, similarly to α_1 and α_2, the units of c_r and c_a are different.

3.3.2 Numerical results

The lumped model shown in Figure 3-11 is specialized for two degrees of freedom following the structural behavior depicted in Figure 3-5(c). Using this model with the equivalent viscous damping ratios determined in the previous section, numerical analysis is performed to obtain the response of the two-bay, two-story infilled frame under the Taft earthquake scaled to $0.1g$. A comparison of the numerically determined time histories of both the first and the second floor displacements, and those obtained pseudo-dynamically (assuming zero viscous damping in the pseudo-dynamic experiment) is shown in Figure 3-12. Since non-zero viscous damping ratios may hide some numerical instabilities, if any are present, it was decided to use zero viscous damping ratios in the pseudo-dynamic experiment for the present case only, *i.e.* to check the stability and accuracy of the implementation of the pseudo-dynamic algorithm.

From Figure 3-12, good agreement between the numerical results and the results from the pseudo-dynamic experiment is evident. It is clear that the symmetry of the assumed structural behavior (refer to Figure 3-5(c)) led to over-estimation of the displacement in one direction (the negative direction) and under-estimation of the displacement in the opposite

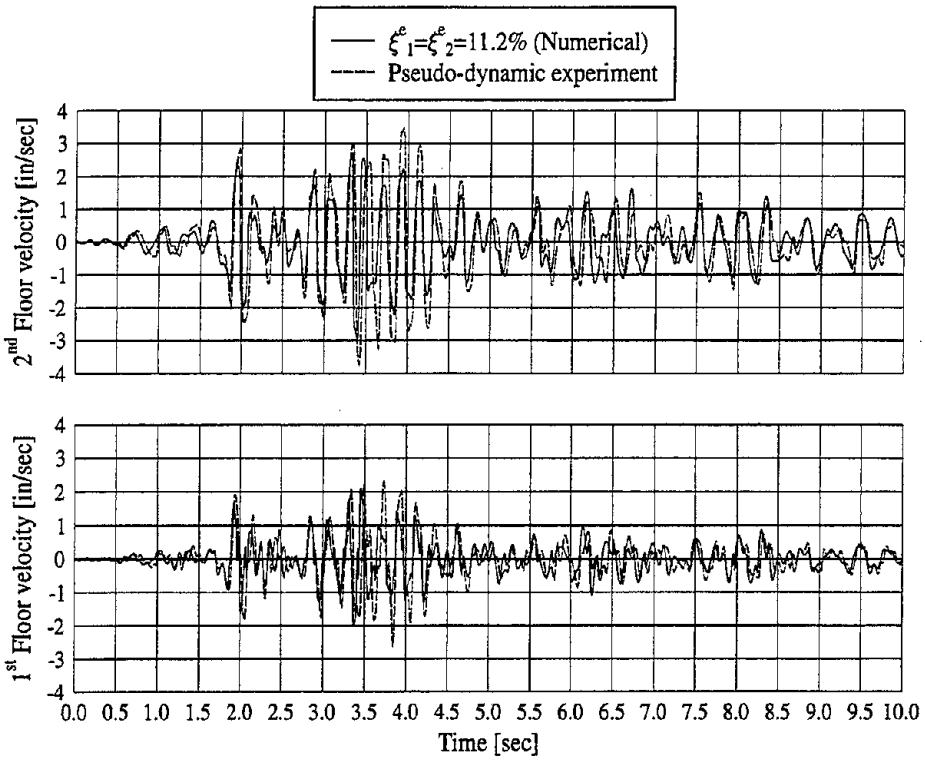

FIGURE 3-13 Time histories of velocities for Taft earthquake scaled to 0.1g.

direction. The good agreement between displacement time histories is also obtained between velocity time histories and acceleration time histories as shown in Figures 3-13 and 3-14, respectively.

3.4 Summary

The pseudo-dynamic algorithm presented in **SECTION 2** is specialized in this section for the case of GLD two-bay, two-story steel frames infilled with URM walls. Evaluation of the experimental errors and the numerical results of a simplified model substantiated the accuracy of this algorithm.

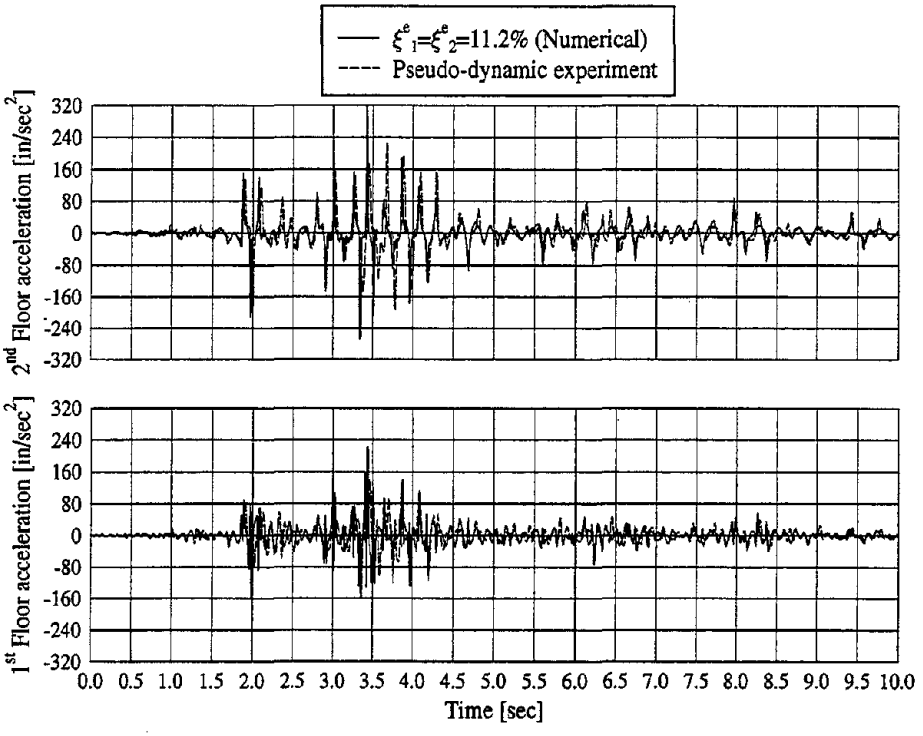

FIGURE 3-14 Time histories of accelerations for Taft earthquake scaled to $0.1g$.

SECTION 4

MEASURED PSEUDO-DYNAMIC RESULTS

The pseudo-dynamic method, discussed in the **SECTION 2**, is applied in **SECTION 3** to test the two-bay, two-story GLD steel frame infilled with URM walls. Here, the descriptions of the testing procedure including the arrangement of instrumentation and the sequence of application of ground motion are given and the experimental results are discussed. The evolution of the cracking in the masonry infill walls and the implication of such cracks on the distribution of forces within the walls are illustrated. Each crack pattern is presented together with a global response measure given by its corresponding story shear/inter-story drift hysteretic relation. On the local level, the straining actions in the frame members are evaluated using the measurements from the strain gages. Finally, comments about the distortion of the different wall panels are given for different loading levels.

4.1 Testing Procedure

The first step in the testing procedure is to establish the layout of the instrumentation. Some of the instruments provided essential data for the pseudo-dynamic procedure. The other instruments provided information useful in understanding the behavior of the frame/wall system. The second step in the testing procedure dealt with the definition of the earthquake load application sequence. The adopted sequence is aimed towards the following goals:

- To consider the effect of the characteristics of different earthquakes in the elastic range of behavior of the structure.

- To understand the performance of a continuously deteriorating structure under the effect of a sequence of earthquakes with the same characteristics but with increasing intensity[1].

4.1.1 Instrumentation

The experimental setup shown in Figure 3-1 was instrumented to provide data for the evaluation of the global and local behavior of the model. Three types of instruments were utilized: (a) load cells, (b) displacement transducers, and (c) strain gages. The load cells (Load Cell_1 & Load Cell_2) provided the information for the restoring force vector $\{r\}$ as shown in Figure 3-2. The displacement transducers (DCDT_1 & DCDT_2) were mounted

[1]In this research, Peak Ground Acceleration (PGA) is the only considered measure for earthquake intensity.

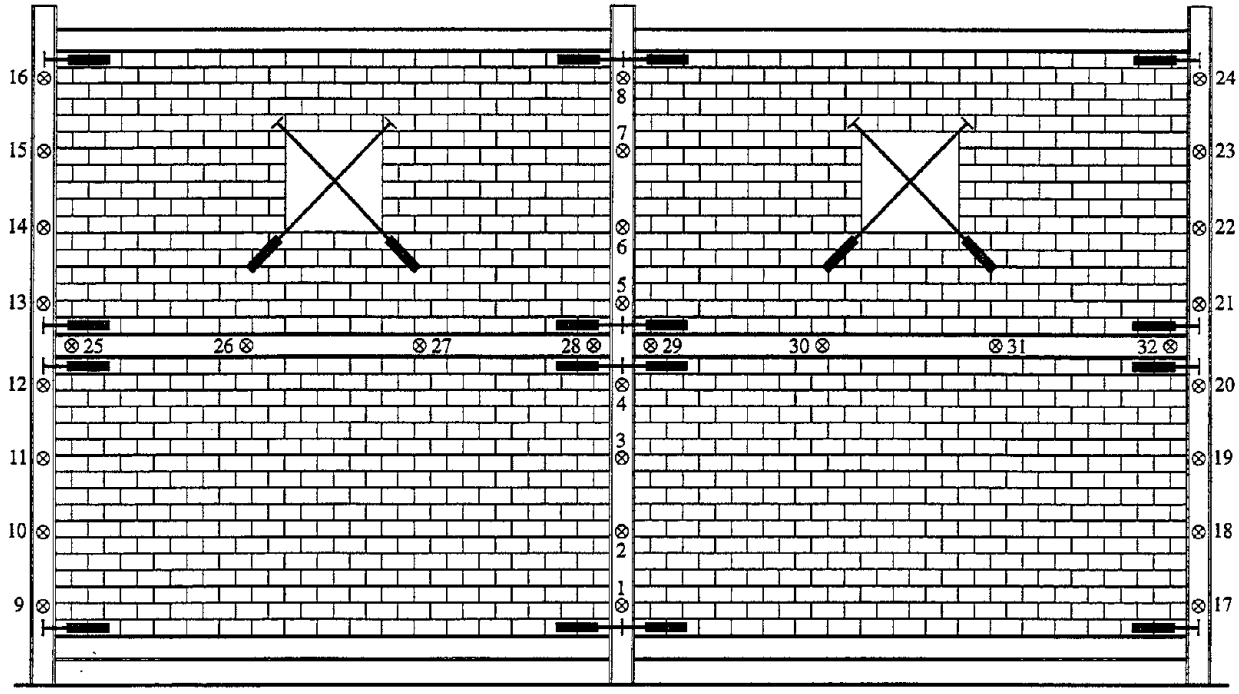

FIGURE 4-1 Experimental setup showing locations of relative displacement transducers and strain gages.

on the structure to provide displacement measurements relative to the supports. These measurements provided the displacement vector $\{d_{(external)}\}$ as shown in Figure 3-2. The transducer $DCDT_0$ shown in Figure 3-2 provided measurements of displacement necessary for the calculation of the net first story drift. The other set of displacement transducers provided relative measurements between two points within the specimen (either two points on one wall or one point on a wall and the other on the frame) for use in determining the gap opening and closing between the frame members and the infills, plus the distortion of window openings. The strain gages in this test were placed only on the steel frame members at different locations. At each location, two gages were placed on the web, one close to each flange, to measure strains in the longitudinal direction of the member. In this way, determination of the member straining actions, normal forces and bending moments at these locations was possible. The locations of the relative displacement transducers and strain gages are shown in Figure 4-1.

4.1.2 Testing sequence

From the elastic response spectra of the selected three earthquake records (scaled to $1.0g$), for the same PGA level (Figure 3-9), the Taft record produced the largest spectral responses.

Therefore, it was chosen as the record to be used once the structure was damaged. The records were scaled on the basis of peak ground acceleration. Before any visible cracking in the masonry walls, the structure was subjected to Taft followed by El-Centro and finally Nahanni earthquake records. Once cracking occurred at Taft scaled to $0.2g$, the structure was subjected to Taft only. In subsequent tests, the Taft record was incremented by $0.025g$ up to PGA $= 0.4g$. After this, a larger increment of $0.05g$ was considered up to PGA $= 0.6g$. Finally, the applied PGA was increased in $0.1g$ increments until PGA $= 0.8g$.

Although the initial state of the structure changed from the application of one record to the other because of the damage accumulation, it is thought that important information regarding structural modeling of degrading infill walls may be obtained from the selected experimental sequence. This is attributed to the fact that the idealization of infill walls and their interaction with the bounding frame members evolve with the level of damage in the walls.

4.2 Analysis of Results

The experimental results are discussed in this section. The discussion is divided into: (a) Global performance in the form of crack patterns and the corresponding story shear/inter-story drift hysteretic relations and (b) Local performance in the form of straining actions in the frame members and panel distorted shapes. Based on the obtained crack patterns, comments are given on possible idealization of the infill walls using the so-called *dual truss system.*

4.2.1 Crack patterns and hysteretic relations

Cracking in masonry infills started at the second story where cracks initiated close to the corners of the window openings. The existence of reinforced bond beams on the top of the windows (see Figure 3-1) moved the cracks slightly away from the corners of the window openings. Because larger inter-story drifts occurred in the first story than the second, cracking in the second story was temporarily arrested while more severe cracking occurred in the first story. General observations on the cracking process in masonry infills are as follows:

- Cracks primarily occur along the interface between the horizontal (bed) mortar joints and the adjacent concrete blocks.
- Adjacent horizontal cracks become connected with cracks occurring along the mortar vertical (head) joints.
- The general form of cracking is a stepped diagonal pattern along the mortar bed and head joints connecting the two diagonally opposite loaded corners of the infill panel.

- Upon load reversal, complete closure of the cracks opposite to the loading direction is attained with new cracks initiating (or existing cracks opening) along the current loaded diagonal.
- Cracks tend to follow the weakest path in the panel. Therefore, upon repeated cyclic loading, most vertical cracks appeared in the mortar head joints rather than in the masonry blocks.
- Crack initiation is always accompanied by a large amount of energy released through hysteresis.

The crack patterns of each pseudo-dynamic run (for successive application of Taft earthquake with increasing PGA) were monitored to distinguish the open cracks from the closed ones for both loading directions (push or pull). The subsequent discussion pertains only to the application of Taft earthquake with different PGA.

At PGA $= 0.2g$, several cracks appeared along the mortar bed and head joints. Horizontal cracks appeared first at the center of the solid infill walls, subsequently, they propagated diagonally towards the loaded corners. A window opening in the center of the panel forces the cracks to initiate at the corners of this opening. The crack pattern, after the completion of the earthquake record, is sketched in Figure 4-2 where open cracks are shown in each loading direction. Increasing the PGA to $0.25g$ produced additional cracks as shown in Figure 4-3. Crack initiation is always accompanied by a large amount of energy released through hysteresis which is clear from the corresponding hysteretic curves where one may notice the sudden drop of story shear or sudden increase of inter-story drift at the onset of cracking. Either effect causes the amount of energy dissipated through hysteresis to significantly increase.

For the test with PGA $= 0.275g$, the main load transfer mechanism, *i.e.* compression-only struts, became evident through monitoring the opening and closing of the cracks upon load reversals. This situation was more obvious in the first story than the second because more damage occurred in the first story and because of the existence of the openings in the second story which makes the definition of the equivalent struts more difficult. The open cracks for each loading direction are illustrated in Figure 4-4. From this figure, one can conclude that the accumulated damage in the first story led to the substantial increase of the area of the hysteretic loops in the story shear/inter-story drift relation of the first story.

At PGA $= 0.325g$, more cracks appeared in the second story as illustrated in Figure 4-5. As shown from the hysteretic curves, the stiffness of the infilled frame and the area of the hysteresis loop decreased, especially for the first story where pronounced levels of damage had developed. This was followed by more severe cracking in the first story at PGA $= 0.4g$ which caused noticeable drop of the load carrying capacity of the structure at that point. The crack patterns after the application of the record scaled to $0.4g$ together with the corresponding hysteretic curves are shown in Figure 4-6.

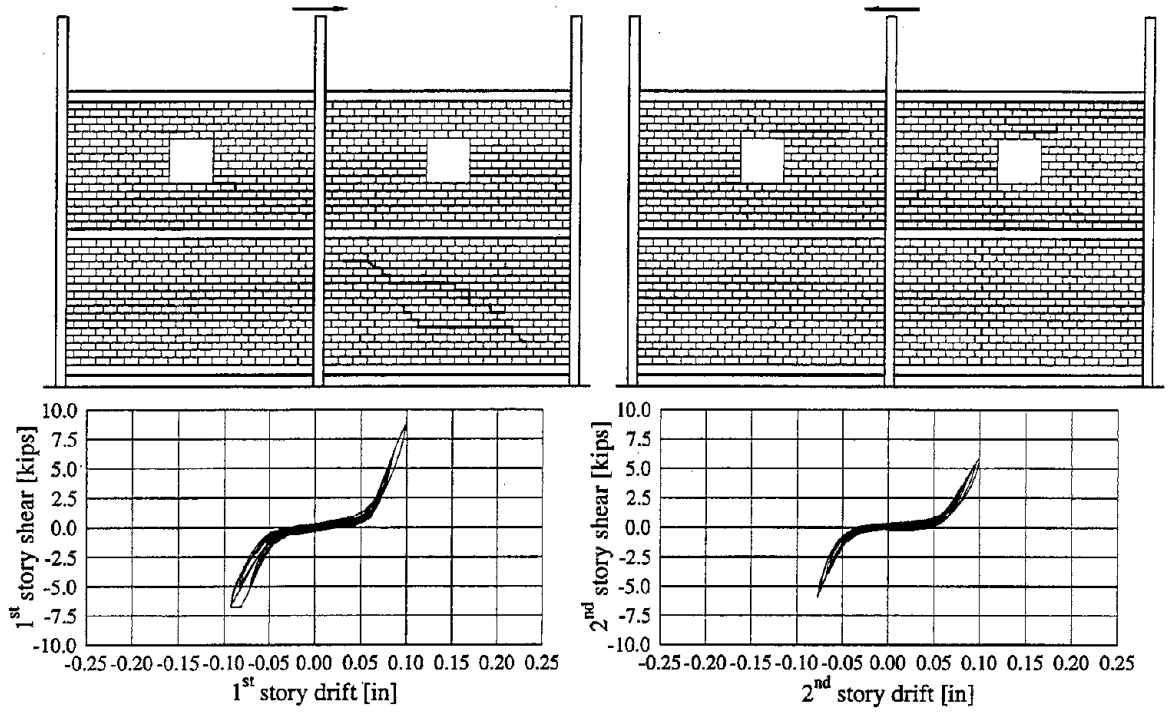

FIGURE 4-2 Crack patterns and hysteretic relations under Taft earthquake scaled to $0.2g$.

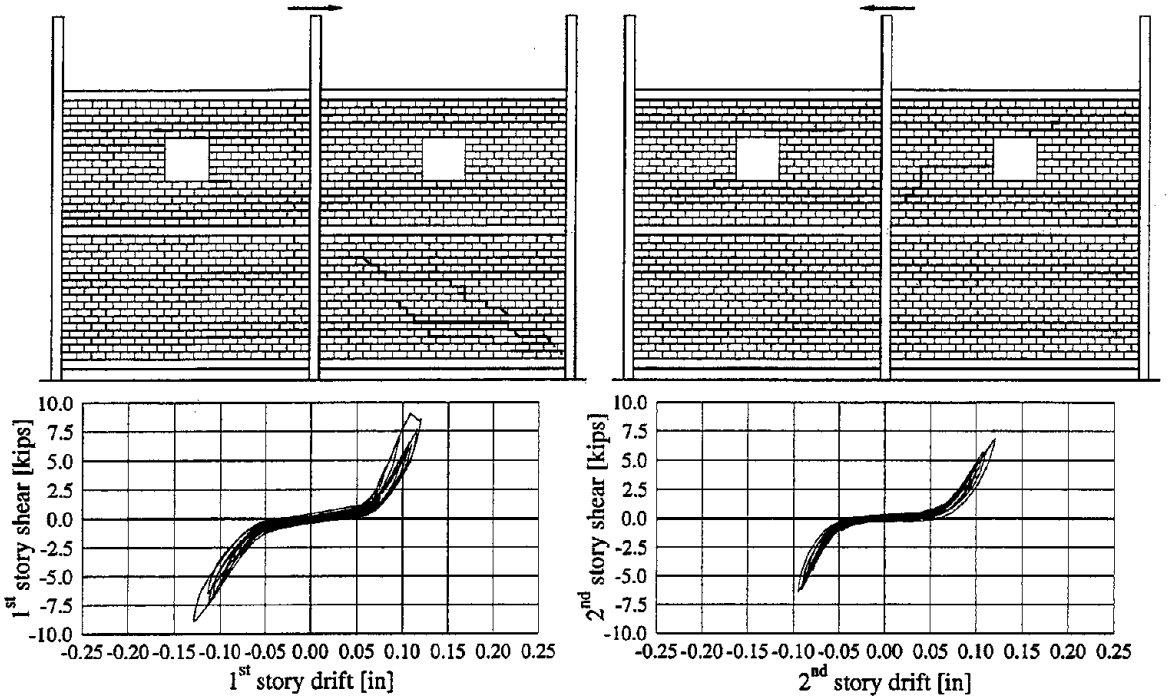

FIGURE 4-3 Crack patterns and hysteretic relations under Taft earthquake scaled to $0.25g$.

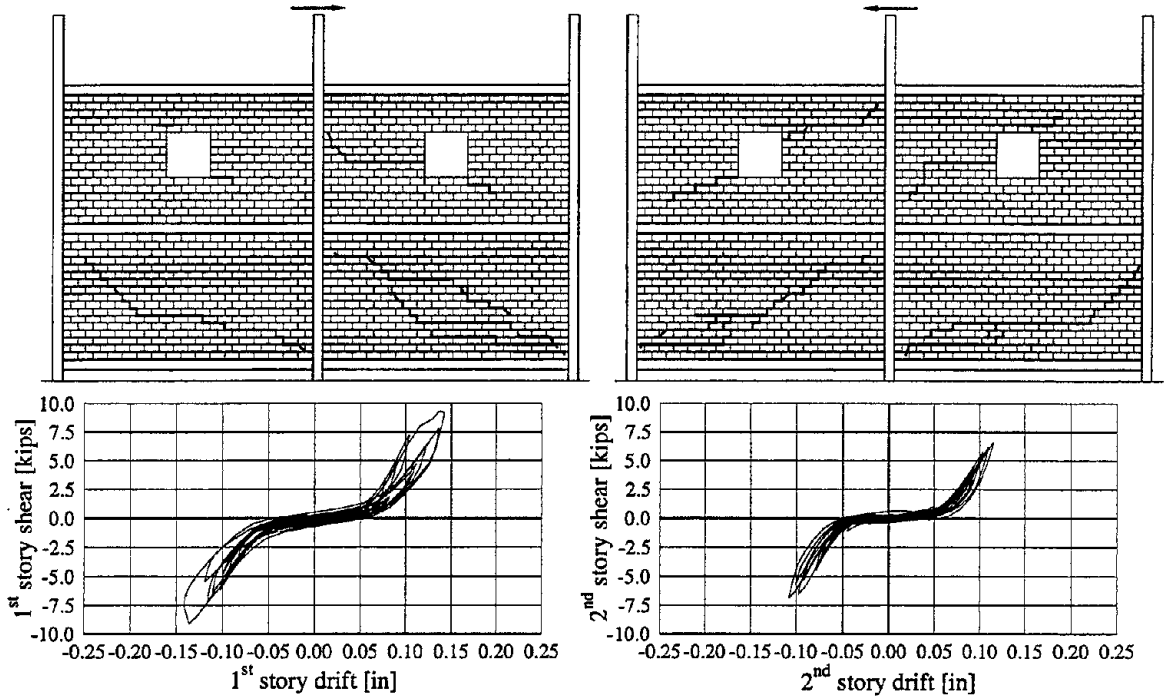

FIGURE 4-4 Crack patterns and hysteretic relations under Taft earthquake scaled to $0.275g$.

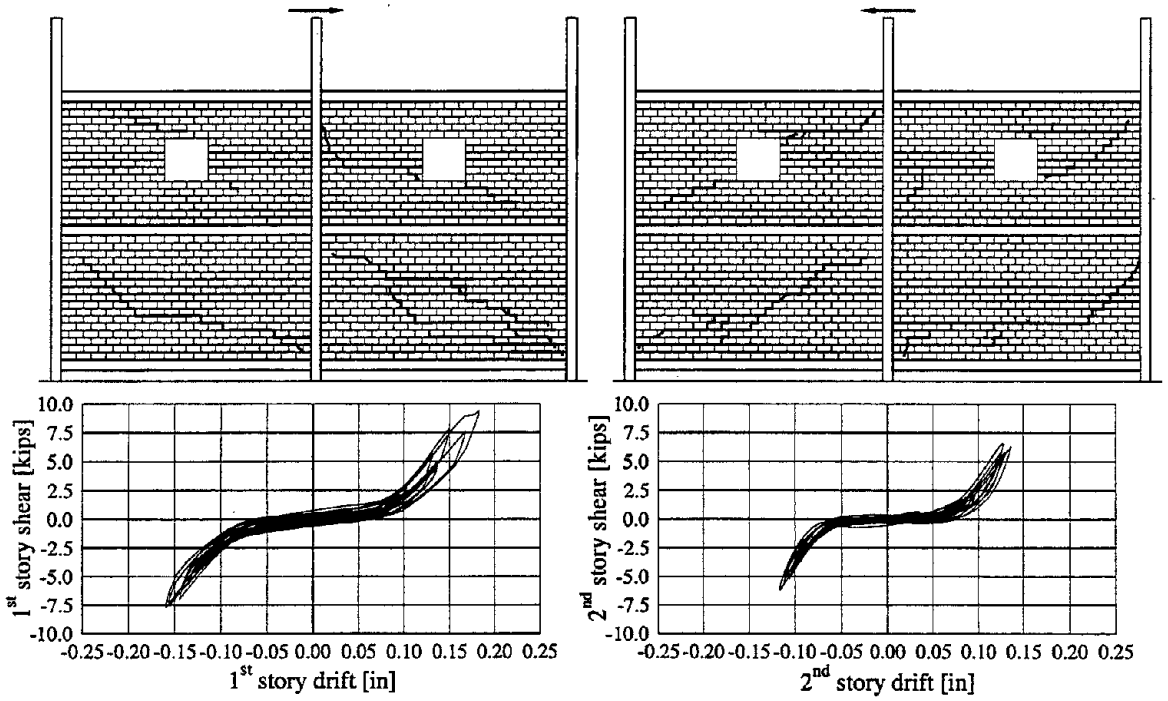

FIGURE 4-5. Crack patterns and hysteretic relations under Taft earthquake scaled to $0.325g$.

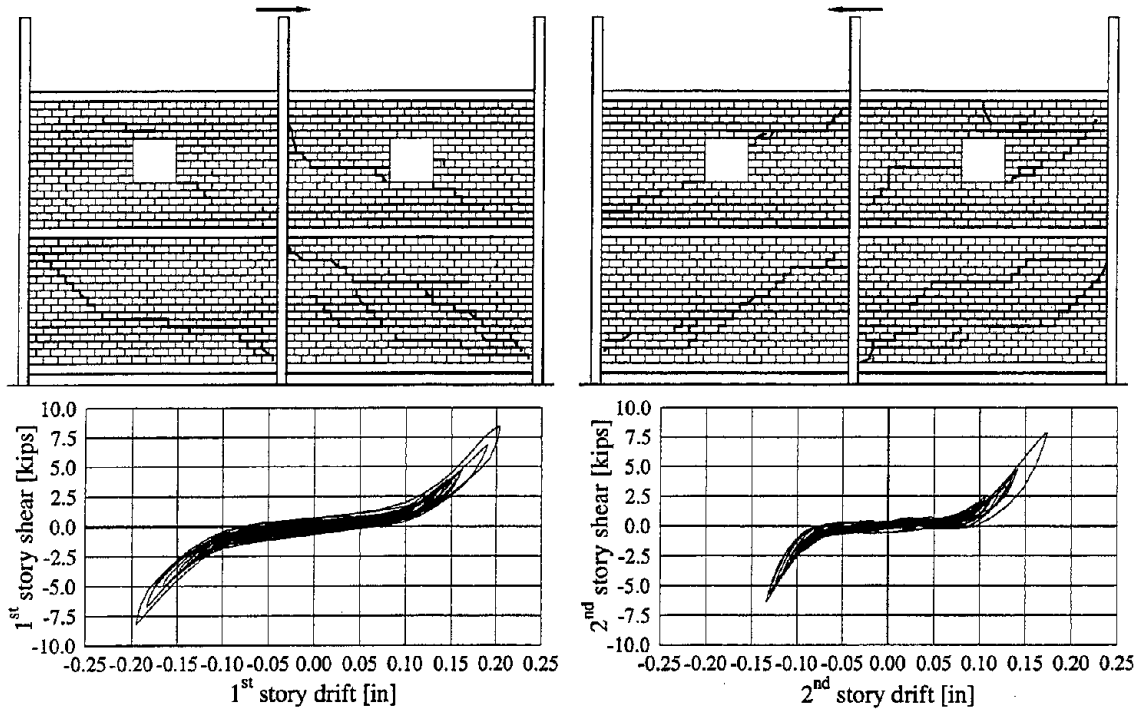

FIGURE 4-6 Crack patterns and hysteretic relations under Taft earthquake scaled to $0.4g$.

The final crack pattern is obtained at PGA = $0.6g$ which is shown in Figure 4-7. The development of the load transfer mechanism was complete at that stage and the equivalent compression struts started to show deterioration in the form of crushed blocks especially in the first story. The first story shear/inter-story drift relation is shown in Figure 4-7; a large amount of hysteretic energy was dissipated. Excessive damage of the equivalent struts followed until PGA = $0.8g$. Beyond $0.6g$, masonry crushing occurred along the compression paths which are sketched in Figure 4-8 and discussed in the following section.

4.2.2 Equivalent truss model

From the crack patterns obtained at PGA = $0.6g$ (Figure 4-7), an *equivalent truss* may be assumed as shown in Figure 4-8. This equivalent truss accounts for the expected compression and tension stress fields in the wall panels according to the loading direction. The material model of the compression struts should account for the capacity of *confined masonry* in axial compression. The tension members are necessary for equilibrium of the *bent* compression fields (struts) and they should be governed by the tensile capacity of the mortar/block interface. Due to the nature of the stepped cracks, significant interlocking is expected. Therefore, sufficient tension softening behavior should be included in the material model.

Each panel is modeled using two *independent* truss systems (*i.e.* a dual system). At one

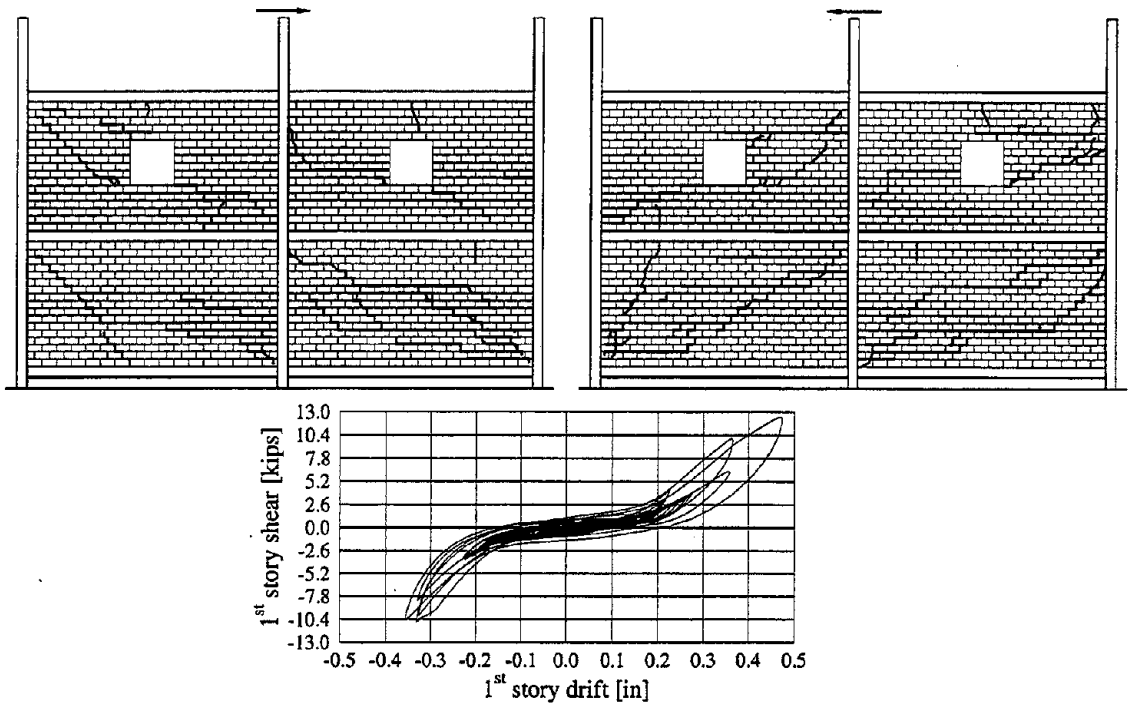

FIGURE 4-7 Crack patterns and hysteretic relation under Taft earthquake scaled to $0.6g$.

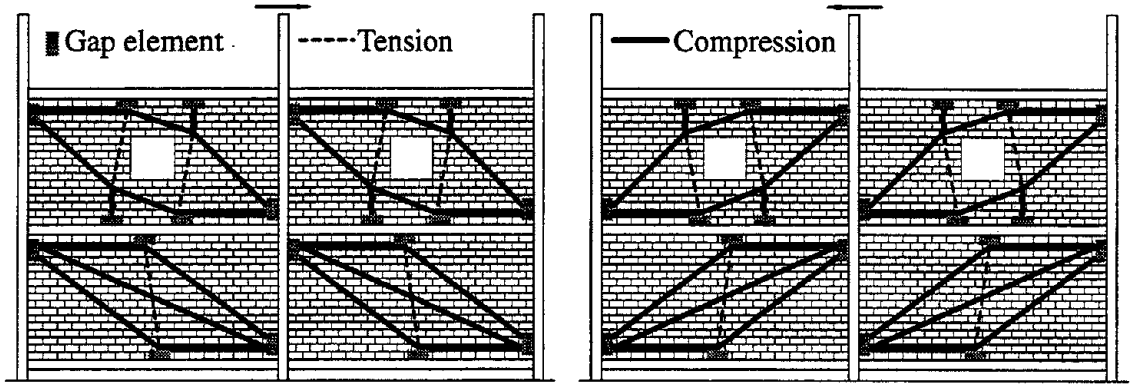

FIGURE 4-8 Loading paths in the infill walls based on the expected stress fields.

instant, only one truss system is active. This may be achieved by adding a gap element at each nodal connection between the truss and the frame members as illustrated in Figure 4-8. The equivalent truss may be connected to the frame members at two or more points to consider *a-priori* the finite *contact length* between the frame members and the infill walls. When the force across such a gap element becomes tensile, the associated truss members are deactivated. Based on the experimental observations, after cracking in the wall panels, significant *dilation* of such cracks produces wall/beam interaction. To account for this interaction, the beams may be connected to the equivalent truss through either compression-only vertical members or gap elements, depending on the topology of the truss.

4.2.3 Straining actions in the frame members

The strain measurements along the frame members and their analyses are presented in this section. The numbering system given in Figure 4-1 will be used to refer to the locations of the strain gages. As an example of the raw measurements, the time histories of the strains at locations 1 and 2, near the base of the middle column, are shown in Figure 4-9 together with the corresponding applied displacements. These results are shown only for the strong motion interval (first 5 seconds) of Taft earthquake scaled to $0.275g$. At each location, two gages designated as 1 and 2 (one close to each flange) measured the strains along the axial direction of the member (ϵ_1, ϵ_2). From these gages, the curvature (Ψ) and the average strain ($\bar{\epsilon}$) at that section are as follows:

$$\Psi = (\epsilon_1 - \epsilon_2)/d \qquad \& \qquad \bar{\epsilon} = (\epsilon_1 + \epsilon_2)/2 \tag{4.1}$$

where d is the distance between the strain gages. The chosen sign convention implies that positive curvature means tension in the fibers close to gage 1 and positive $\bar{\epsilon}$ implies axial tensile strains. The time histories for the calculated curvature along the middle and left columns of the first story under Taft earthquake scaled to $0.275g$ are shown in Figures 4-10 and 4-11, respectively.

The strains and the corresponding stresses in the frame members for all the conducted experiments remained below the *elastic* limit. Therefore, the bending moment (M) and the axial force (N) at any section are *linearly proportional* to the respective curvature (Ψ) and average strain ($\bar{\epsilon}$) at that section. Therefore, one can write

$$M = E_s I \Psi \qquad \& \qquad N = E_s A \bar{\epsilon} \tag{4.2}$$

where E_s is Young's modulus for the steel and I and A are the moment of inertia and the area of the considered section, respectively.

The bending moment diagrams corresponding to the time of maximum base shear under Taft earthquake scaled to $0.275g$ and $0.4g$ are shown in Figures 4-12 and 4-13, respectively.

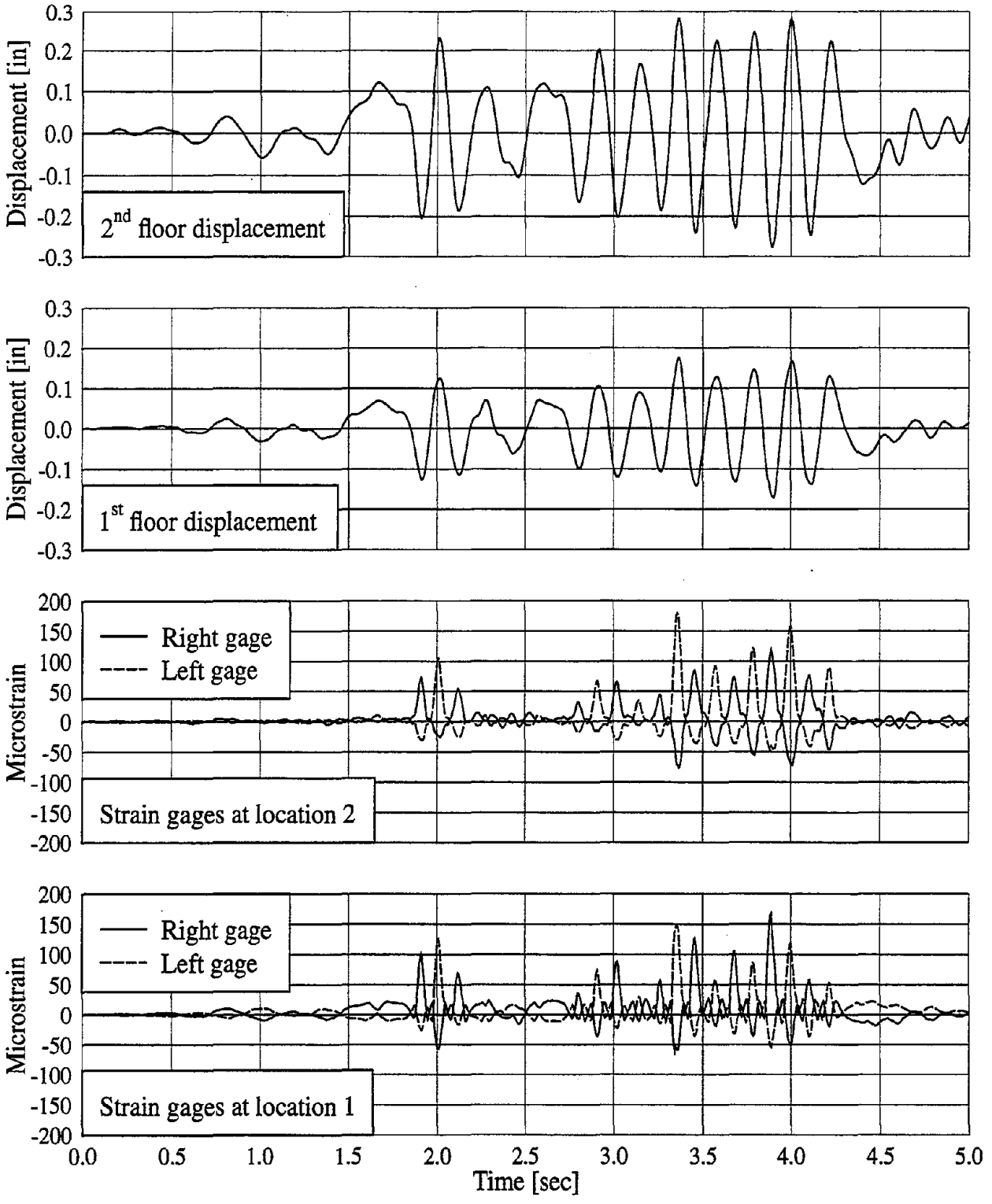

FIGURE 4-9 Time histories for strain measurements and the corresponding applied displacements under Taft earthquake scaled to $0.275g$.

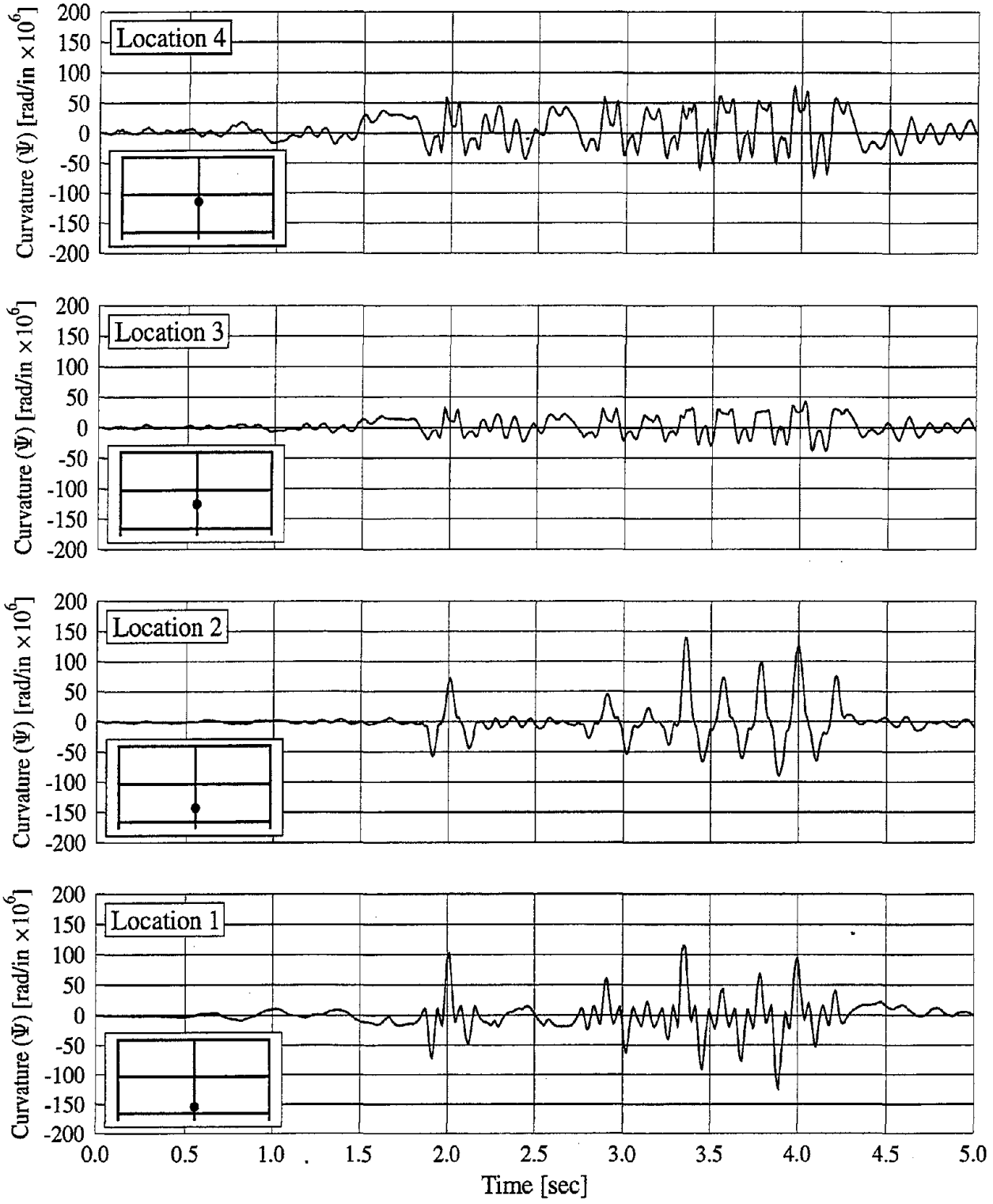

FIGURE 4-10 Time histories for the calculated curvatures along the middle column in the first story under Taft earthquake scaled to $0.275g$.

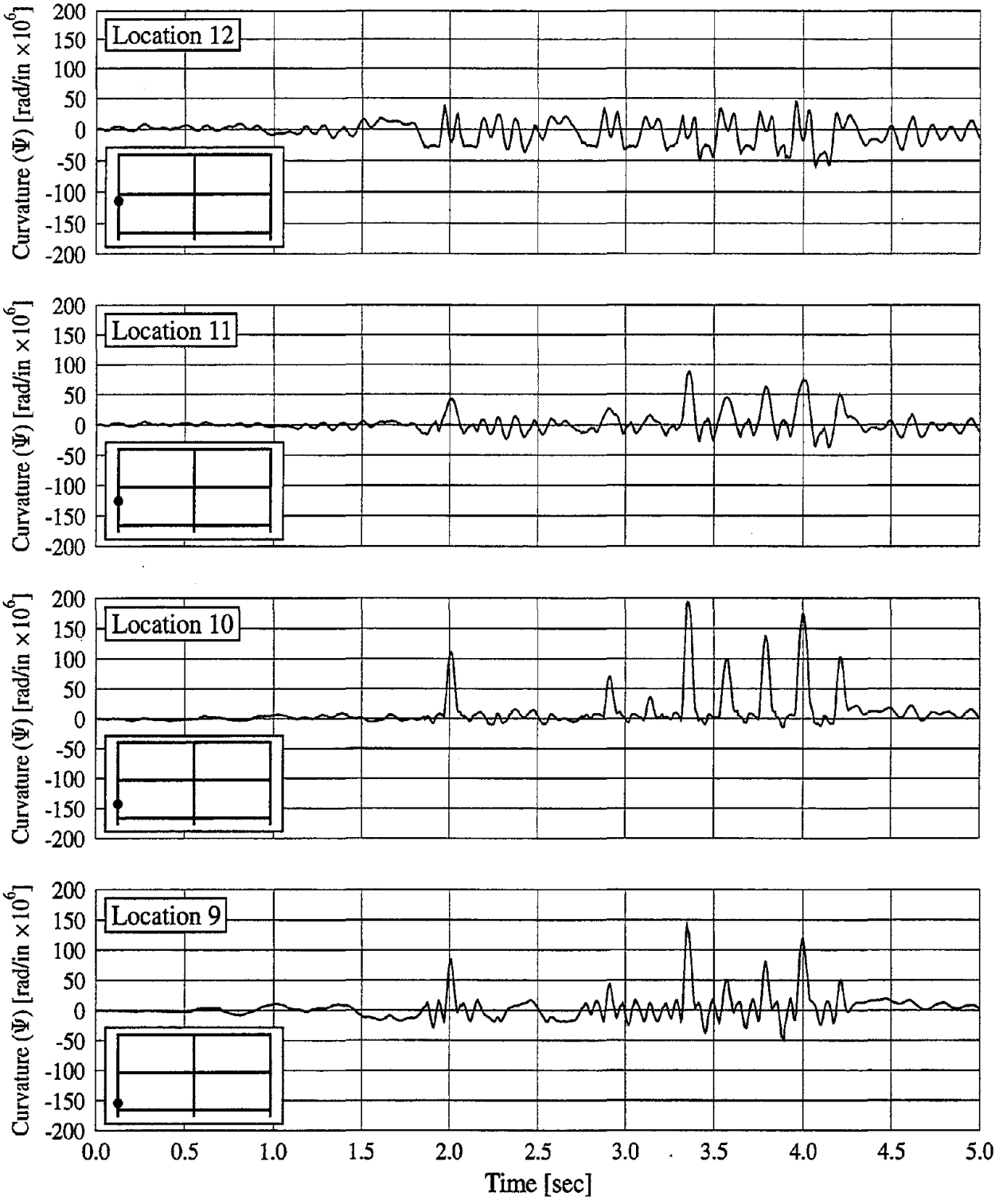

FIGURE 4-11 Time histories for calculated curvatures along the left column in the first story under Taft earthquake scaled to $0.275g$.

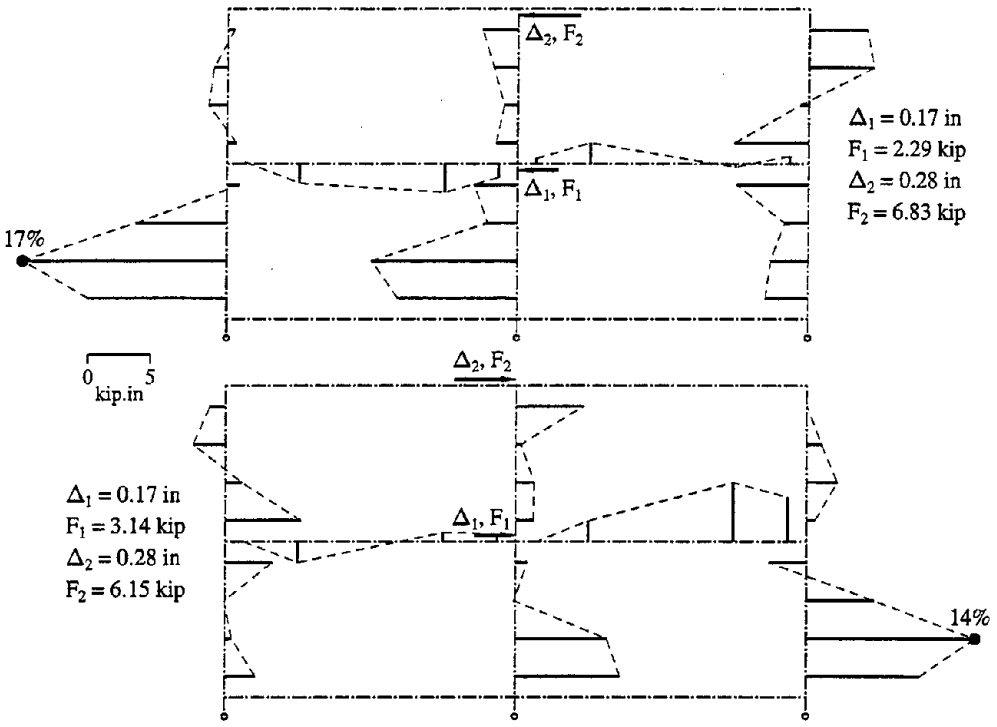

FIGURE 4-12 Bending moment diagram drawn in tension side at maximum base shear under Taft earthquake scaled to $0.275g$ (•: maximum value, given as % of M_y).

In each figure, the diagrams corresponding to both loading directions are shown and the maximum bending moments are indicated as a percentage of the yield moment M_y[2]. The time histories for the normal forces in the locations of maximum bending moment diagrams (*i.e.* locations 2, 10, 18 in the columns and location 26 in the beam) are shown in Figures 4-14 and 4-15 for Taft earthquake scaled to $0.275g$ and $0.4g$, respectively.

Several relevant points may be made regarding the straining actions in the frame members. These are:

1. The bending moment diagram is significantly affected by the interaction between the infill walls and the bounding frame members.

2. Upon load reversal, the bending moment diagram is almost completely reversed even for highly damaged walls.

3. The section of the maximum bending moment is shifted away from the beam to column connections. This observation justifies the need for off-diagonal equivalent

[2]The yield moment is the nominal moment strength when the yield stress is reached at the extreme fibers of the section. For the steel section used in the columns (S 3×7.5), $M_y \approx 97.5$ kip.in.

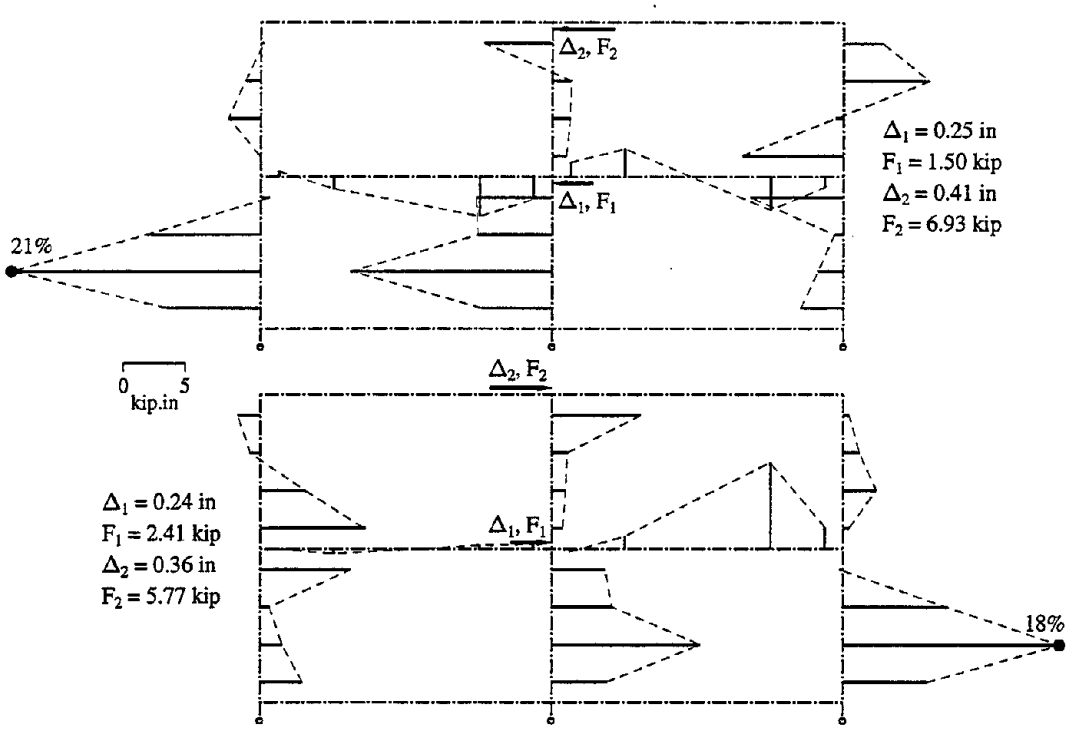

FIGURE 4-13 Bending moment diagram drawn in tension side at maximum base shear under Taft earthquake scaled to $0.4g$ (•: maximum value, given as % of M_y).

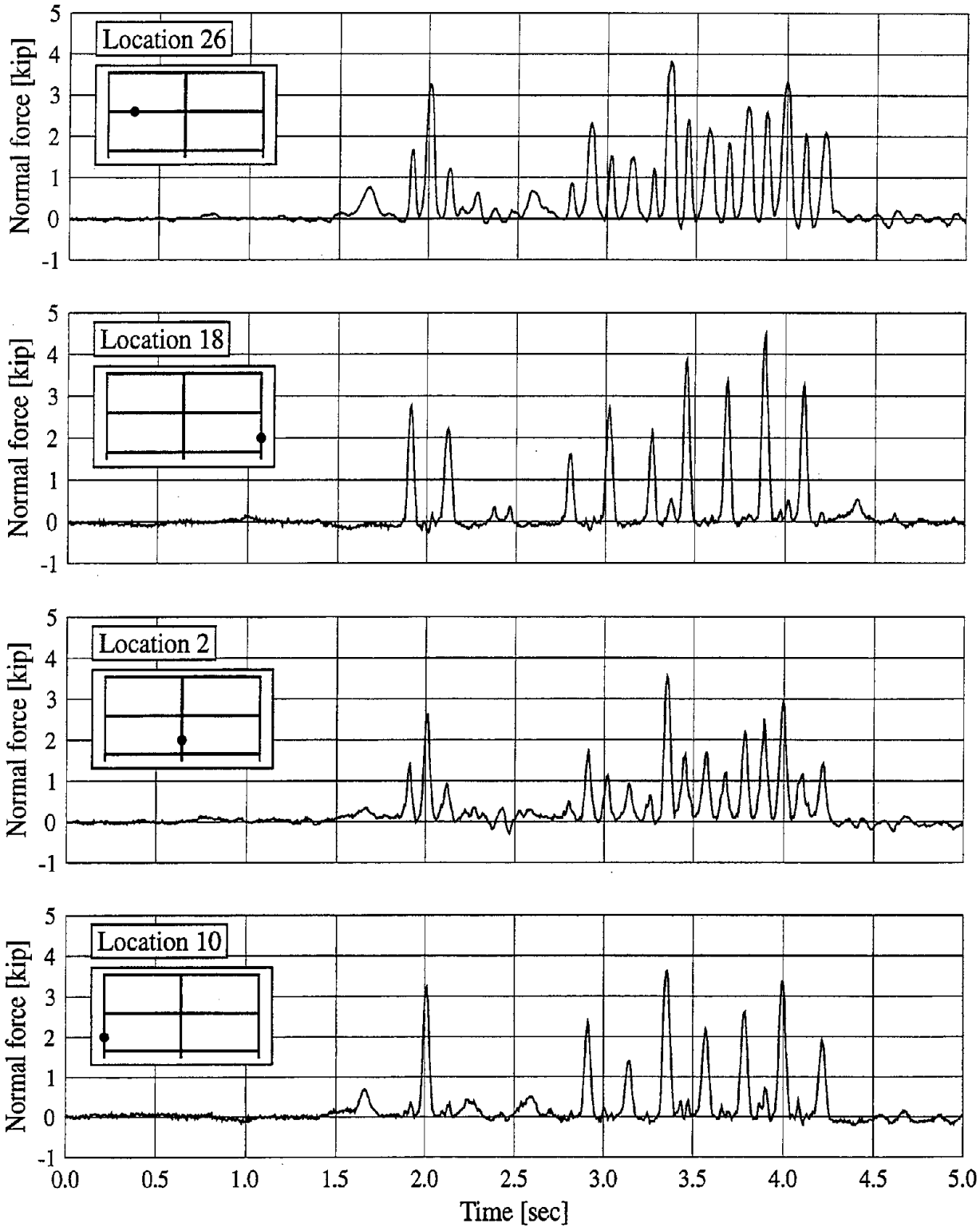

FIGURE 4-14 Time history for axial forces in frame members under Taft earthquake scaled to $0.275g$.

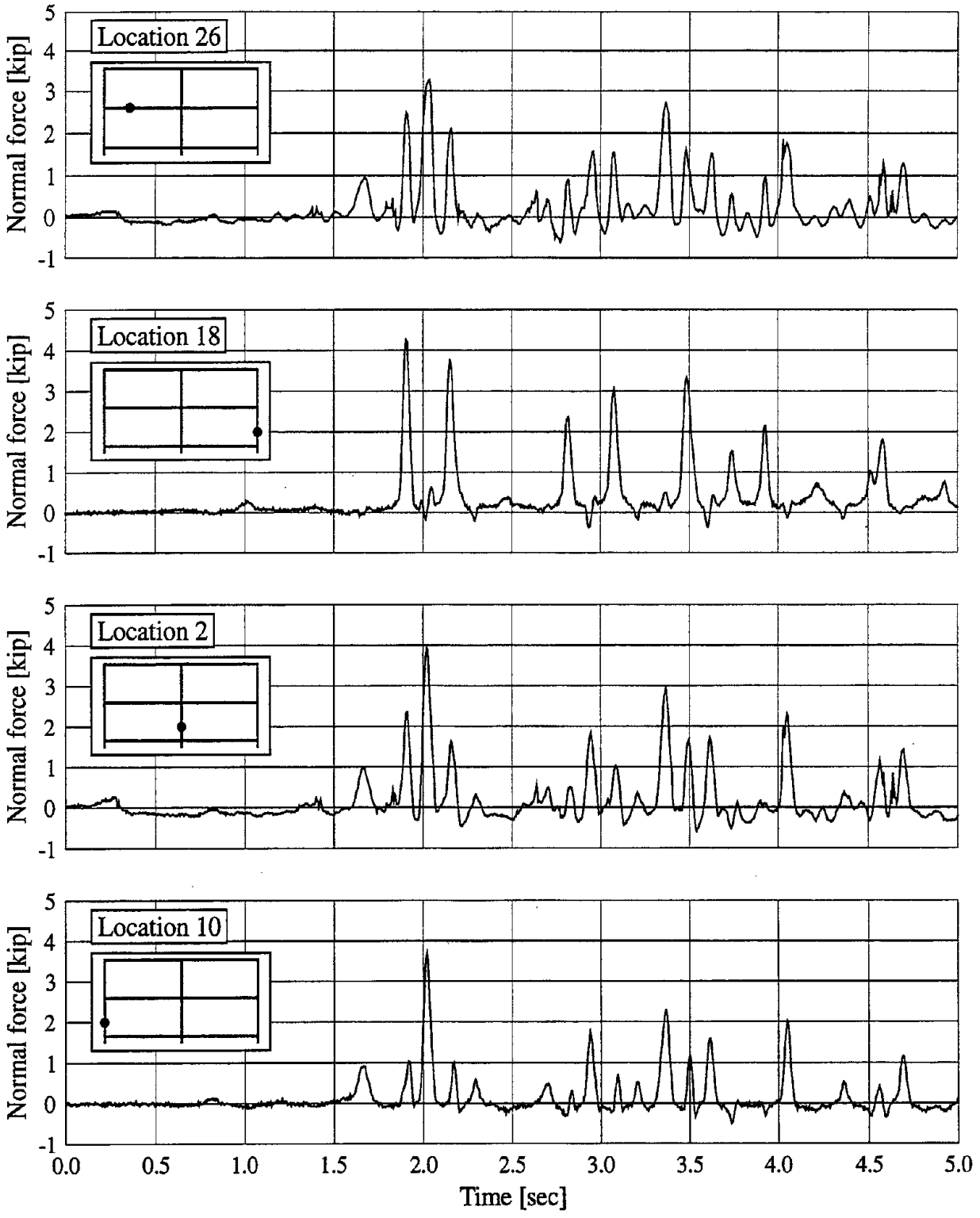

FIGURE 4-15 Time history for axial forces in frame members under Taft earthquake scaled to $0.4g$.

struts to properly account for the effect of infills on the internal forces of the frame members[3].

4. Forces are transmitted between the interior column and the infill walls from both sides. Therefore, the middle column has essentially *single curvature* for both loading directions.

5. Only the first story windward column and the second story leeward column undergo double curvature. This double curvature is more pronounced in the latter. It should be noted that the expected curvature of the bare frame members is quite different.

6. The frame members interact with the infill walls through an equivalent dual truss system as shown in Figure 4-8. This equivalent truss can only transmit compression forces to the frame members. Accordingly, the gap elements shown in the same figure are needed between the truss and the frame members.

7. The normal forces in the frame members are predominantly tension[4] especially for intact walls.

Some of the above points regarding the curvatures of the columns imply different structural behavior than that observed for the single story frames tested quasi-statically, refer to the first report of this series. This may be attributed to the effect of the continuity of the columns because of the second story in the present case. Also, the first story beam confinement provided by the second story infill walls may be another influencing factor in this behavioral difference.

4.2.4 Infill wall panel distortion

The relative displacement measurements taken between the frame members and the infill walls are used to establish the distorted shape of the infill panels *relative* to the bounding frame members. Also, the displacement measurements along the two diagonals of each window opening are utilized to draw the deformed shape of these windows. The measurement devices are shown in Figure 4-1. The results are plotted at the time of maximum applied top floor displacement. As an example, the results obtained from the test with Taft earthquake scaled to $0.275g$ are shown in Figure 4-16. In this figure, the deformations of edges of the infill panels are drawn with respect to fixed frame members. This explains

[3]Reinforced concrete frames designed mainly for gravity loads without considering the infills have splices in the longitudinal reinforcement of the columns. These splices are located just above the upper face of the beams. Accordingly, the observed shift in the location of the maximum moment may lead to serious effects on the performance of reinforcing steel in the spliced region, *i.e.* high bond stress due to the insufficient development length.

[4]For reinforced concrete frames, such observation has a strong impact on the cracking of the frame members when infills are included especially if the gravity loads of upper stories are not considered in testing lower story subassemblages.

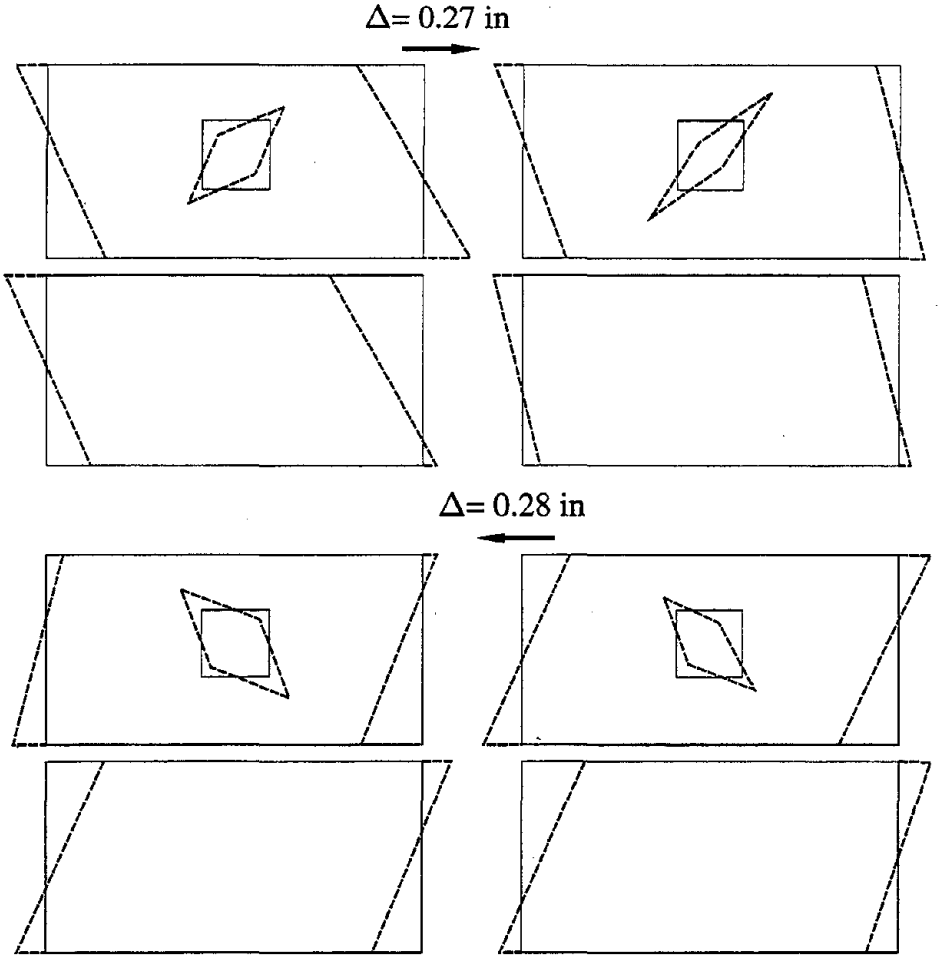

FIGURE 4-16 Distorted shape of the infill panels relative to the frame members and the corresponding window deformation at maximum top floor displacements under Taft earthquake scaled to $0.275g$.

why the direction of deformation in this figure seems to be opposite to the applied lateral displacements. The time histories for the opening and closing of the gaps along the frame columns/walls interface are shown in Figure 4-17. In this figure, four locations are shown: the bottom of the left column with the left wall, the bottom of the right column with the right wall, and the top of the central column with the left and right walls. From this figure, one may notice that the interface undergoes compressive deformation mainly due to the initial gaps between the walls and the frame members. Therefore, the measured contraction is of *finite* nature. On the other hand, the formation of the gap indicates the nature of the compression-only equivalent struts. The deformation time histories of the gap opening and closing indicate that only one system of load transfer is acting in each loading direction. This is clear from the phase of the responses of the top central column/right wall and the bottom right column/right wall interfaces which are shifted half a cycle from the responses of the top central column/left wall and the bottom left column/left wall interfaces.

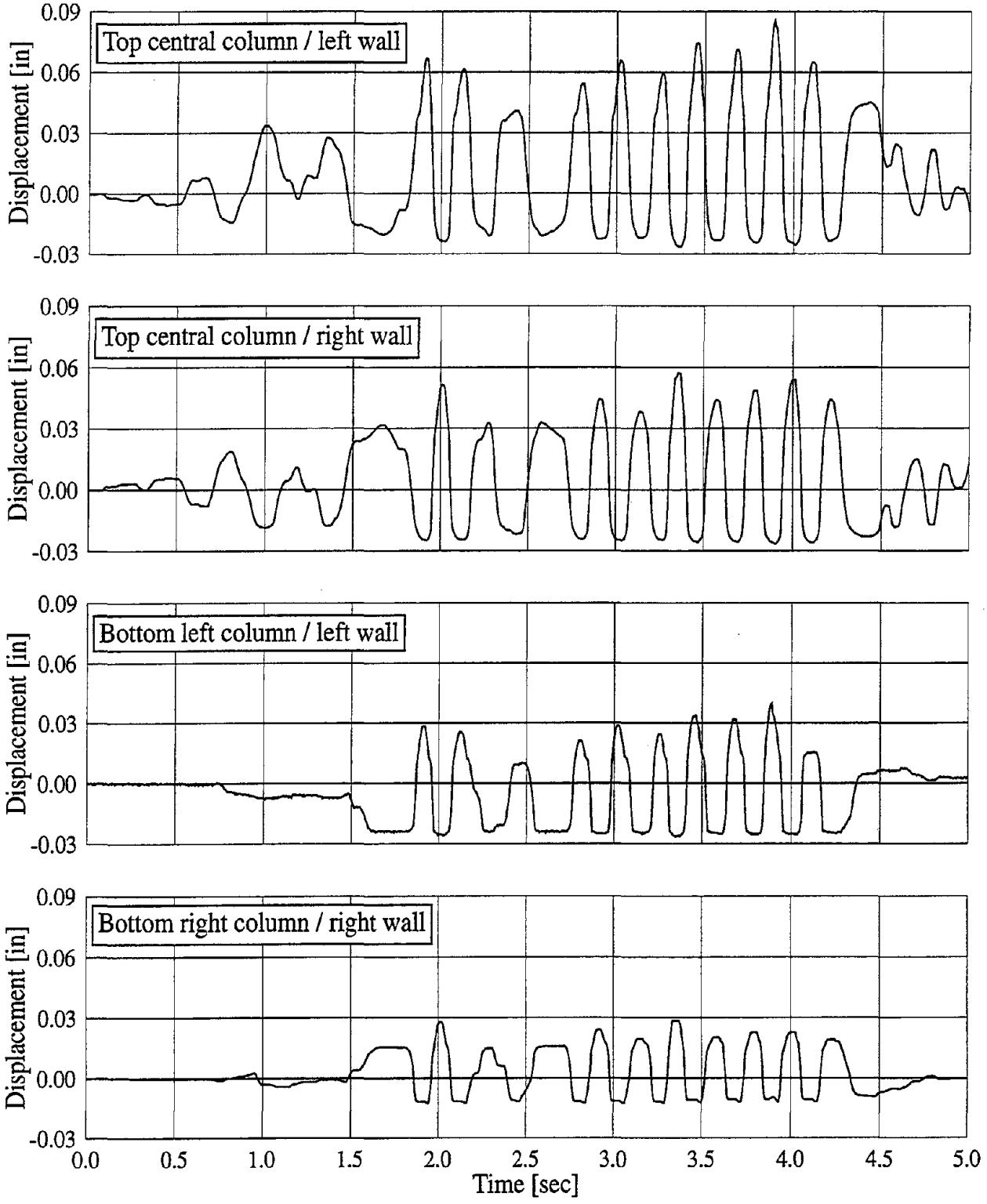

FIGURE 4-17 Time histories of gap opening and closing along the frame/wall interface under Taft earthquake scaled to $0.275g$.

4.3 Summary

The results obtained from the pseudo-dynamic experiments performed on a GLD steel frame with URM infill walls have been presented. The discussion of the results showed the appropriateness of the idealization of masonry infills as an equivalent dual truss system connected to the frame members through gap elements to allow the deactivation of the truss upon the existence of any tension force between the frame members and the infill walls. Inclusion of tension members in the equivalent truss is important to represent the tension fields in the center of the infills. Such tension fields are responsible of initiating cracking in masonry infills and are provided by the interlocking of the stepped crack pattern along the mortar bed and head joints. The straining actions in the frame members were significantly affected by the presence of infills. Infill panel distortion and frame/wall interface conditions revealed the accuracy of modeling the infills as the previously mentioned dual truss system.

SECTION 5

ENERGY-RELATED RESULTS

When a structure is subjected to ground motion, energy (E_I) is *imparted* to it. During the dynamic loading, part of the absorbed energy is *temporarily stored* in the structure in the form of *kinetic* energy (E_K) and *strain* energy (E_S), and the rest is *dissipated* in the form of *damping* energy (E_D) and *hysteretic* energy (E_H) [33].

5.1 Energy Expressions

The expressions for the different types of energy can be obtained by premultiplying all terms in the equation of motion (Eq. (2.1)) by the velocity vector $\{v\}$ and then integrating in time t. Therefore, one obtains the following equation for the *energy balance.*

$$\int_0^t \{v\}^T[M]\{a\}dt + \int_0^t \{v\}^T[C]\{v\}dt + \int_0^t \{v\}^T\{r\}dt = -\int_0^t \{v\}^T[M]\{1\}a_g dt \qquad (5.1)$$

where the superscript T indicates transpose, $\{1\}$ is a unit vector, and all other terms have been previously defined. The following equality holds in Eq. (2.1)

$$\{p\} = -[M]\{1\}a_g \qquad (5.2)$$

where a_g is the ground acceleration. From Eq. (5.1), one can write the following expressions for the different energy terms

$$E_I = -\int_0^t \{v\}^T[M]\{1\}a_g dt \qquad (5.3)$$

$$E_K = \int_0^t \{v\}^T[M]\{a\}dt \qquad (5.4)$$

$$E_D = \int_0^t \{v\}^T[C]\{v\}dt \qquad (5.5)$$

$$E_H + E_S = \int_0^t \{v\}^T\{r\}dt \qquad (5.6)$$

Thus, in terms of the energy components, Eq. (5.1) becomes

$$E_K + E_D + E_H + E_S = E_I \qquad (5.7)$$

To be able to determine a separate expression for the hysteretic energy, one needs to determine the area of the hysteresis loops[1] obtained from the story shear/inter-story drift relationships. This can be achieved using the following expression

$$E_H = \sum_{i=1}^{n} \int_{D_{max}^-}^{D_{max}^+} \left[S_i^{upper} - S_i^{lower} \right] dD_i \tag{5.8}$$

where the summation is carried over the number of stories n. D_i and S_i are the drift and shear of the i^{th} story, respectively. Superscripts (upper) and (lower) refer to the upper and lower curves of the hysteresis loop, respectively. The limits of integration refer to the maximum displacement in the positive and negative sides of the hysteretic loop. Knowing the measured vectors of displacement $\{d\}$ and restoring force $\{r\}$, these story quantities are defined as follows

$$D_i = d_i - d_{i-1} \tag{5.9}$$

$$S_i = \sum_{k=i}^{n} r_k \tag{5.10}$$

where d_i and r_i are the displacement and restoring force of the i^{th} floor, respectively.

5.2 Discussion of Results

Figure 5-1 shows the time histories of the imparted energies obtained from the pseudo-dynamic experiments using Taft, El-Centro and Nahanni earthquakes. In this plot, the PGA is scaled to $0.075g$ and 0% viscous damping ratio is assumed in the pseudo-dynamic experiments for that level of PGA. Comparing this figure with the records given in Figure 3-8, one observes that the evolution of the imparted energy closely follows the distribution of the significant peaks of the ground motion. From the imparted energy of Nahanni earthquake, it is obvious that this record will not produce any significant damage to the tested structure. Based on the elastic response spectrum of the Nahanni record, a similar conclusion was reached in section 3.1.5.

For the Taft earthquake with PGA = $0.15g$, which is the applied intensity level just before initial cracking in the walls occurred, the time histories for the energy terms are given in Figure 5-2. For the loadings and the corresponding crack patterns shown in Figures 4-2, 4-3, 4-4, 4-5, 4-6 and 4-7, the corresponding time histories for the energy terms are given in

[1]Under general loading (*e.g.* earthquakes), the calculation of the hysteretic energy should be carefully implemented because small loading/unloading cycles without complete load reversals may exist which require special attention.

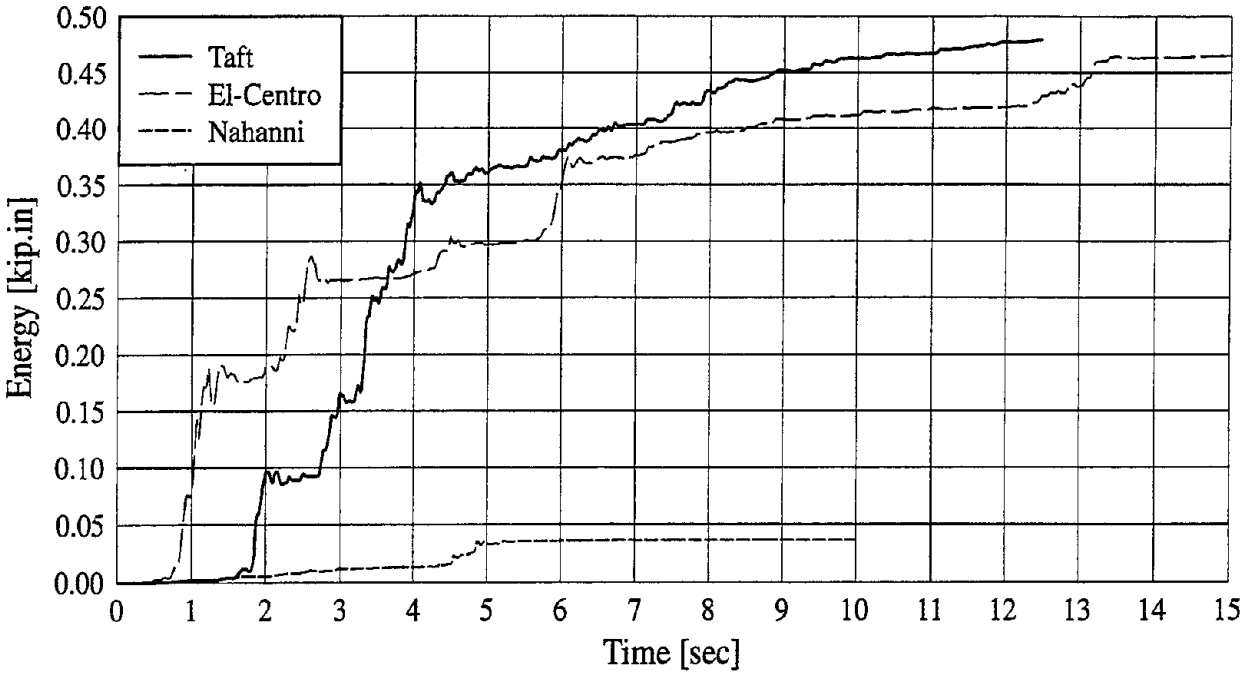

FIGURE 5-1 Imparted Energy for Taft, El-Centro and Nahanni earthquakes scaled to $0.075g$.

Figures 5-3, 5-4, 5-5, 5-6, 5-7 and 5-8, respectively. The energy time histories in the range $0.275g < \text{PGA} \leq 0.4g$ showed oscillation in the maximum magnitudes of the energy terms which may be attributed to the existence of a transition zone before and after the complete formation of the equivalent truss of the infill walls. Beyond PGA $= 0.4g$, the amount of energy imparted to and dissipated from the tested structure showed rapid increase with the increase of PGA. Excessive damage was noticed after $0.6g$ without additional cracking but with crushing of masonry blocks. At PGA $= 0.7g$ and $0.8g$, the time histories for all the energy terms are shown in Figures 5-9 and 5-10, respectively. For clarity and for comparisons, the vertical scale of the time histories of the energy terms for different levels of PGA was kept constant in the ranges PGA $\leq 0.275g$, $0.275g <$ PGA $\leq 0.4g$ and PGA $> 0.4g$.

The variations of the maximum values of the energy terms versus the intensity of the ground motion given by its PGA are illustrated in Figure 5-11. These maximum values were obtained at the end of the applied records. The different energy terms, namely E_I, E_H, and E_{DH} = the dissipated energy = $E_D + E_H$ are shown in this figure. It is obvious that the increase of the hysteretic energy, and consequently the dissipated energy, with increasing PGA becomes rapid at the onset of damage (*i.e.* at PGA $= 0.2g$). A similar trend is obtained for the imparted energy. For the infilled frame with cracked walls, the rate of increase of the damping energy is almost constant with increasing PGA. This is a direct consequence of the numerical modeling of the viscous damping as Rayleigh damping. The corresponding plots of the variation of the maximum top floor displacement and the corresponding story drifts with PGA are shown in Figure 5-12. Also, the story shear

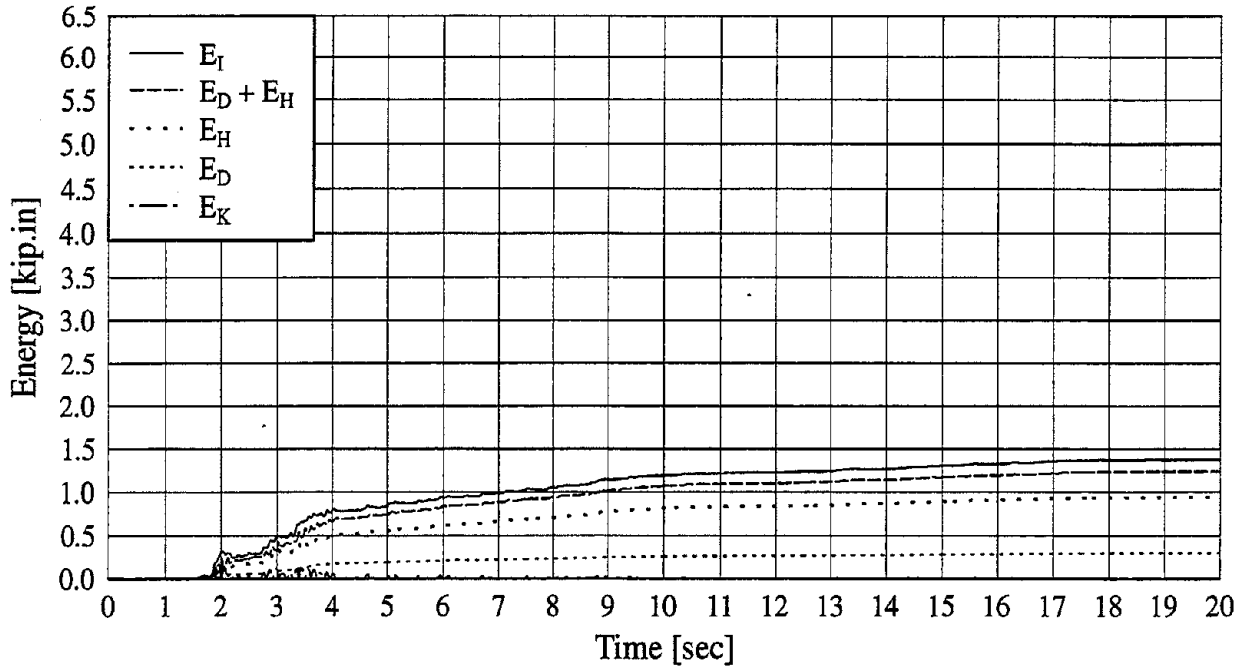

FIGURE 5-2 Time histories for energy terms under Taft earthquake scaled to $0.15g$.

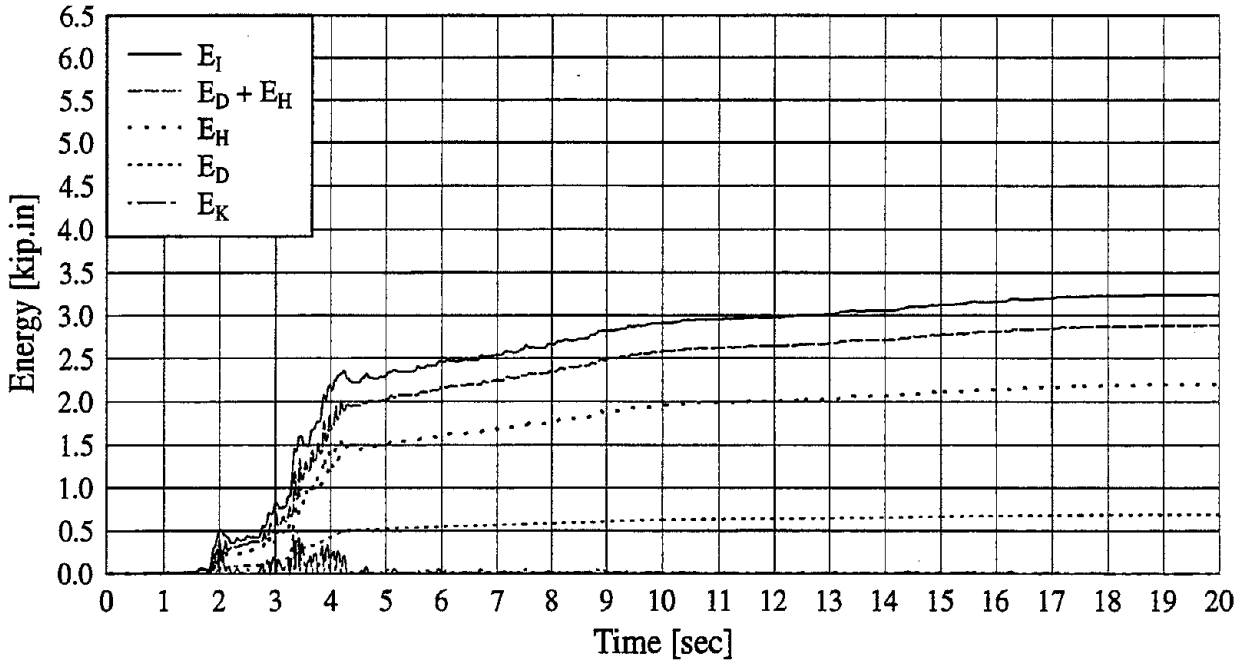

FIGURE 5-3 Time histories for energy terms under Taft earthquake scaled to $0.2g$.

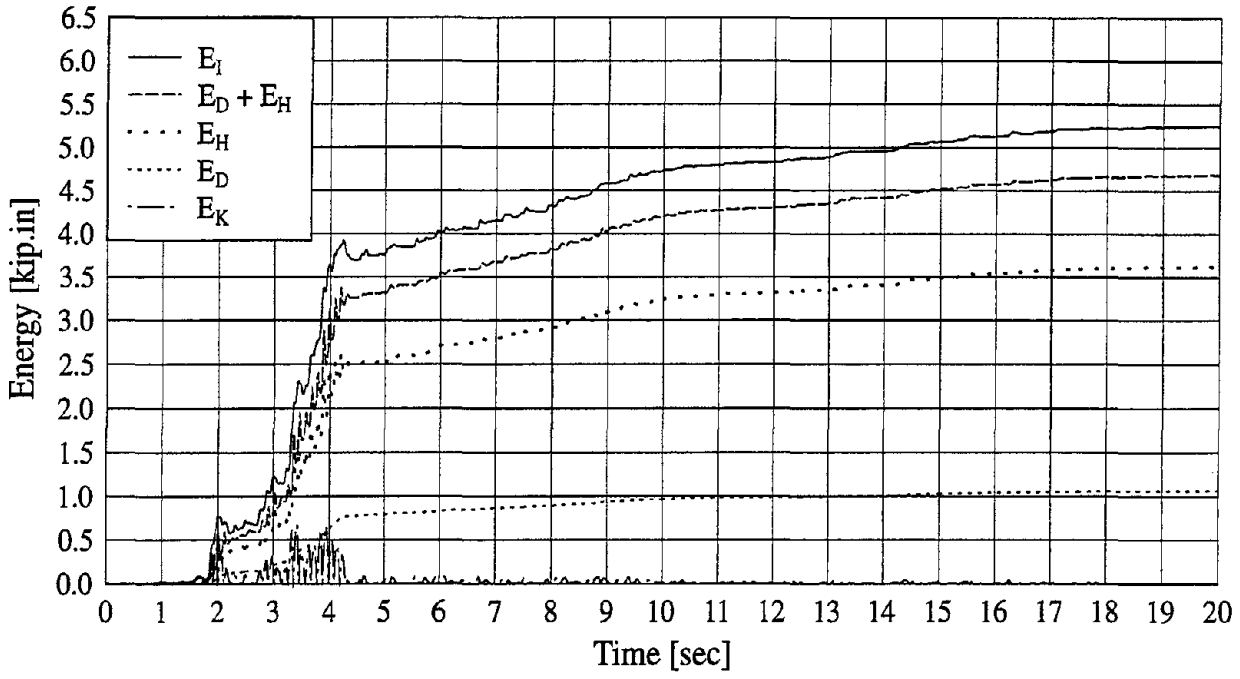

FIGURE 5-4 Time histories for energy terms under Taft earthquake scaled to $0.25g$.

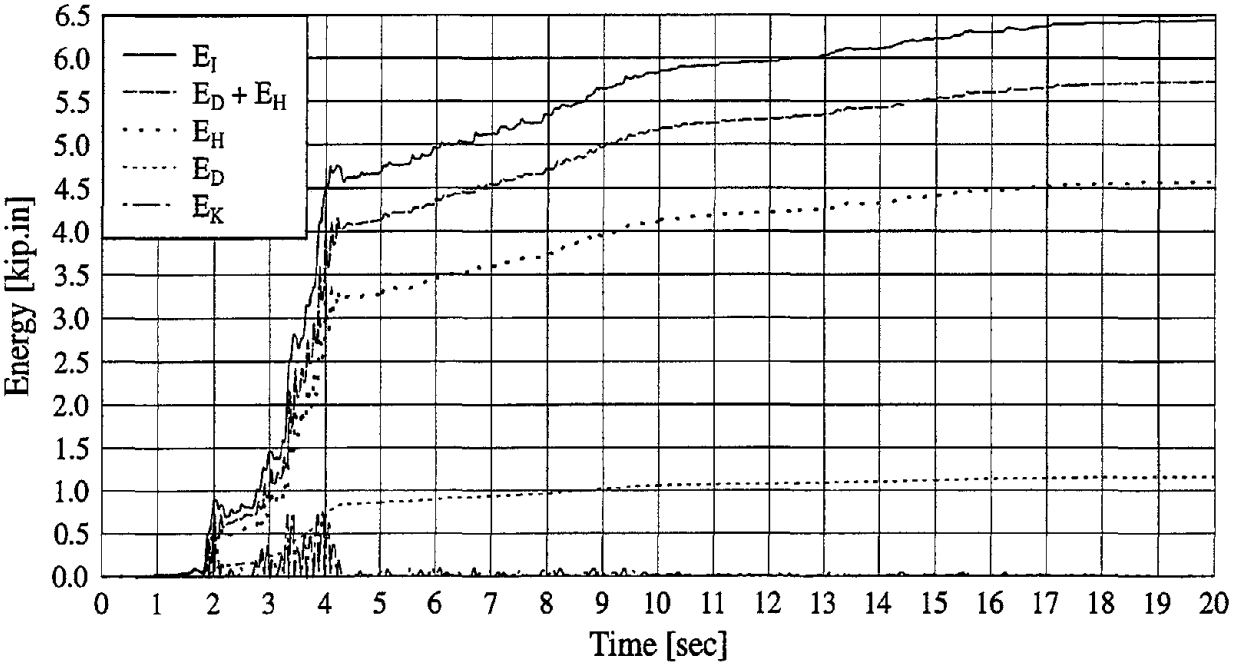

FIGURE 5-5 Time histories for energy terms under Taft earthquake scaled to $0.275g$.

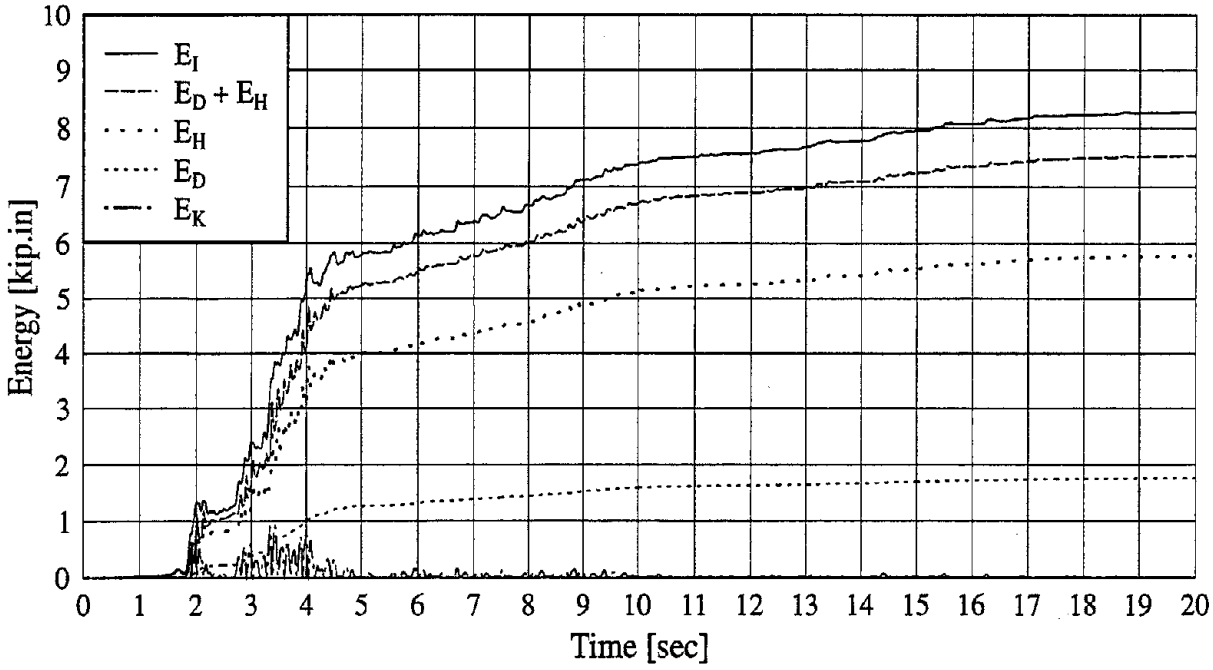

FIGURE 5-6 Time histories for energy terms under Taft earthquake scaled to $0.325g$.

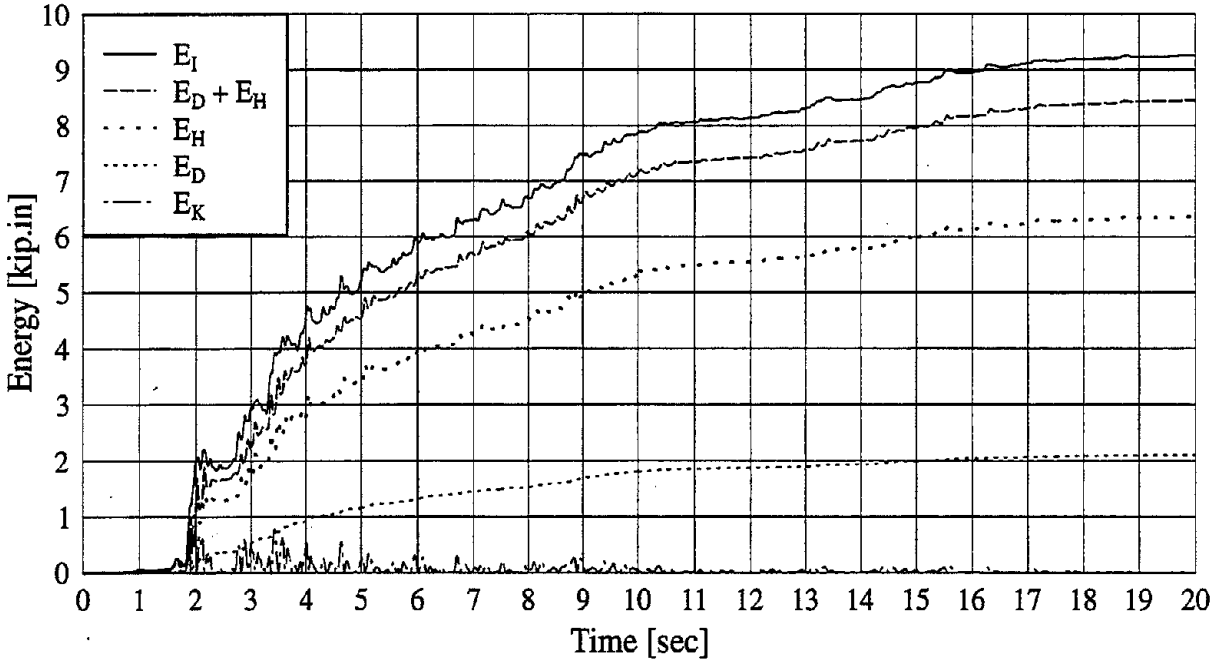

FIGURE 5-7 Time histories for energy terms under Taft earthquake scaled to $0.4g$.

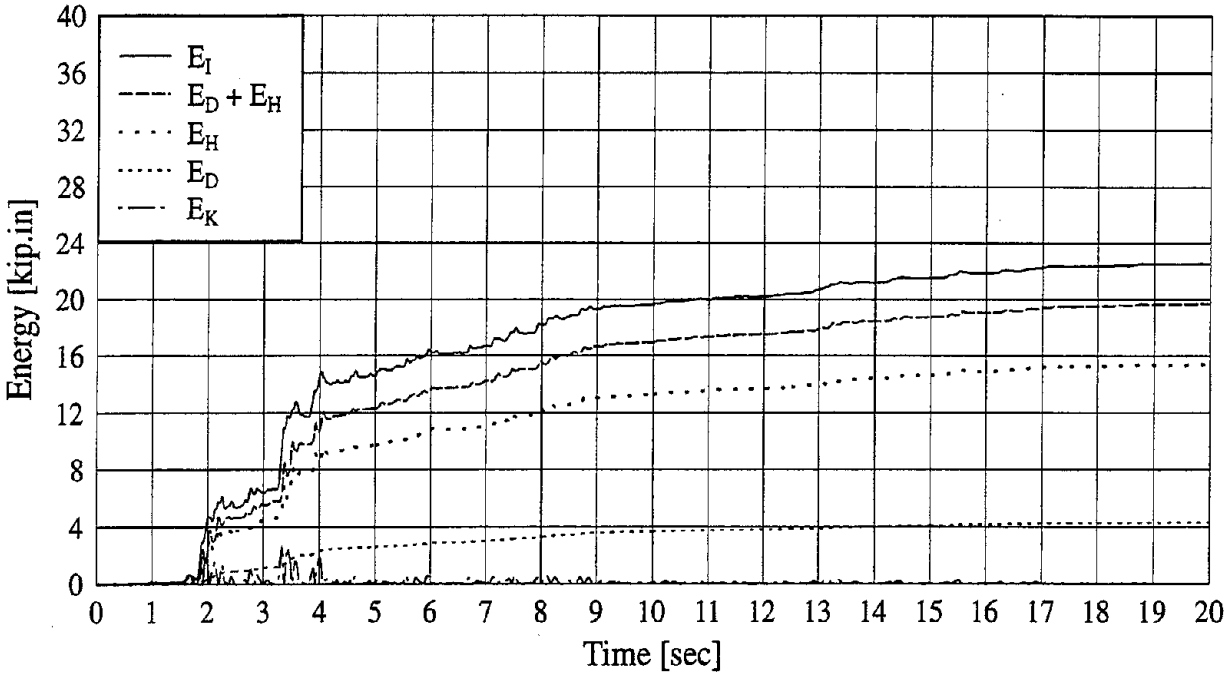

FIGURE 5-8 Time histories for energy terms under Taft earthquake scaled to $0.6g$.

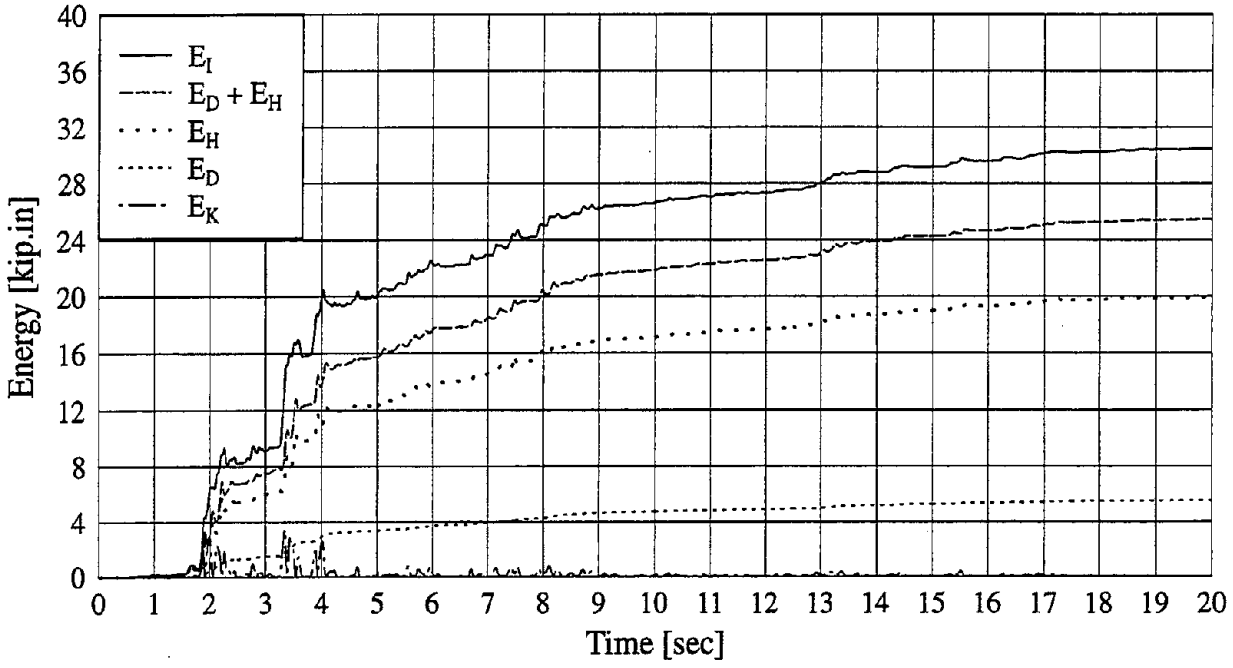

FIGURE 5-9 Time histories for energy terms under Taft earthquake scaled to $0.7g$.

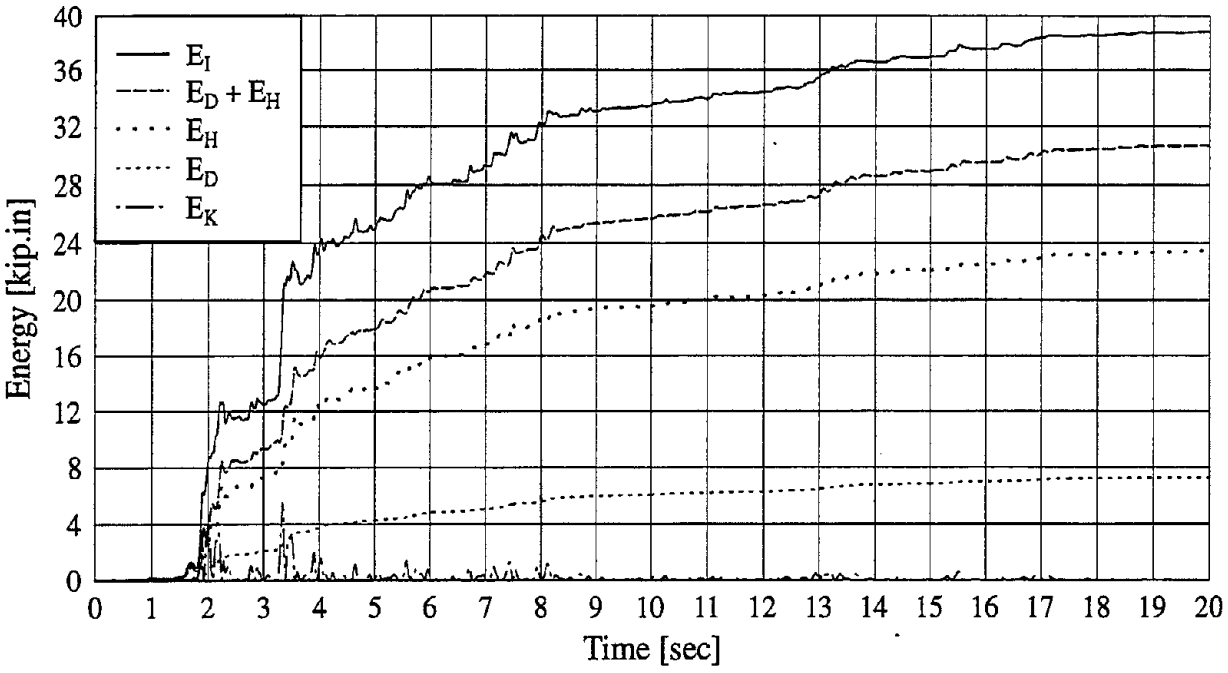

FIGURE 5-10 Time histories for energy terms under Taft earthquake scaled to $0.8g$.

corresponding to the maximum top floor displacement versus PGA relations are plotted in Figure 5-13. These bar charts indicate that inter-story drift or story shear do not correlate well with the amount of energy dissipated from or imparted to the tested structure. This is mainly due to the brittle cracking of the masonry infills which causes large changes in the energy dissipated, and consequently in the energy imparted, with small change of the inter-story drift. Figures 5-14 and 5-15 show the same quantities plotted in Figures 5-12 and 5-13, respectively, but rather than plotting them at the time of maximum roof displacement, they are plotted at the time of maximum base shear. One may observe that the quantities corresponding to maximum base shear correlate better with the maximum energy terms (Figure 5-11), particularly, for the plots of roof displacement and story drifts. This better correlation strengthens the point made about the brittleness of the masonry infill wall cracking.

5.3 Summary

The results obtained from the pseudo-dynamic experiments performed on a GLD steel frame with URM infill walls have been used to evaluate several energy terms. These terms were investigated and their variation with the increase of PGA may be considered as a global measure to quantify the damage state of the structure.

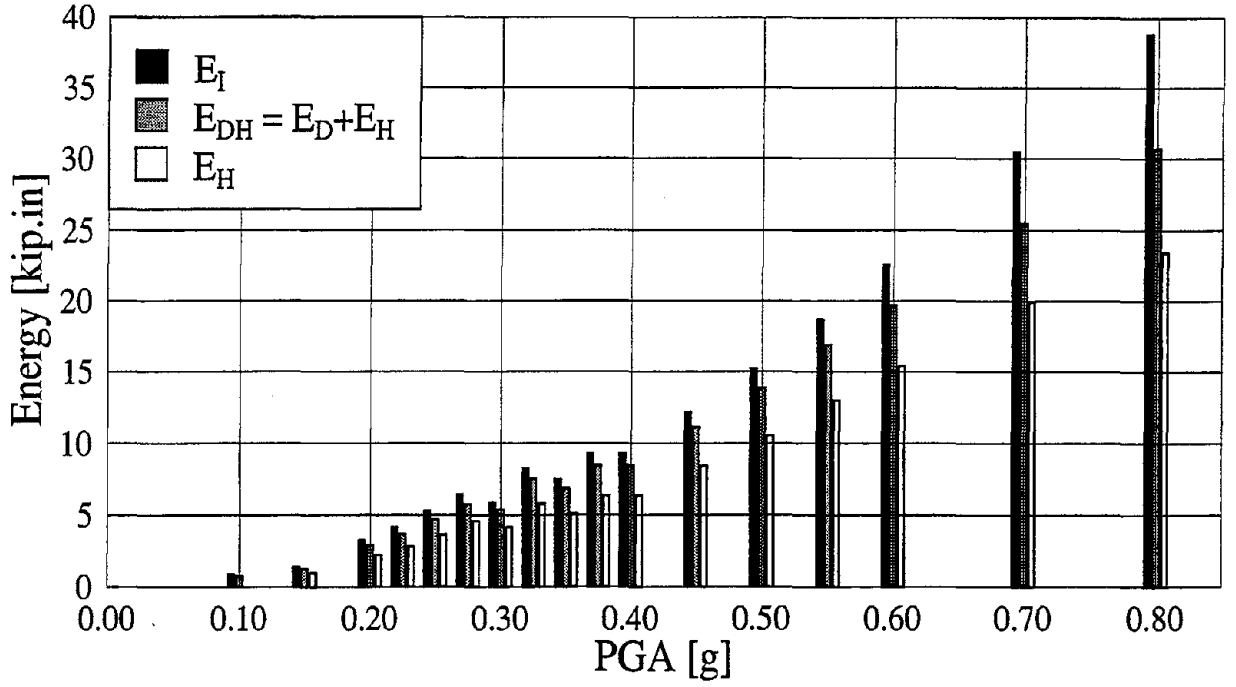

FIGURE 5-11 Variations of maximum values of energy terms with PGA.

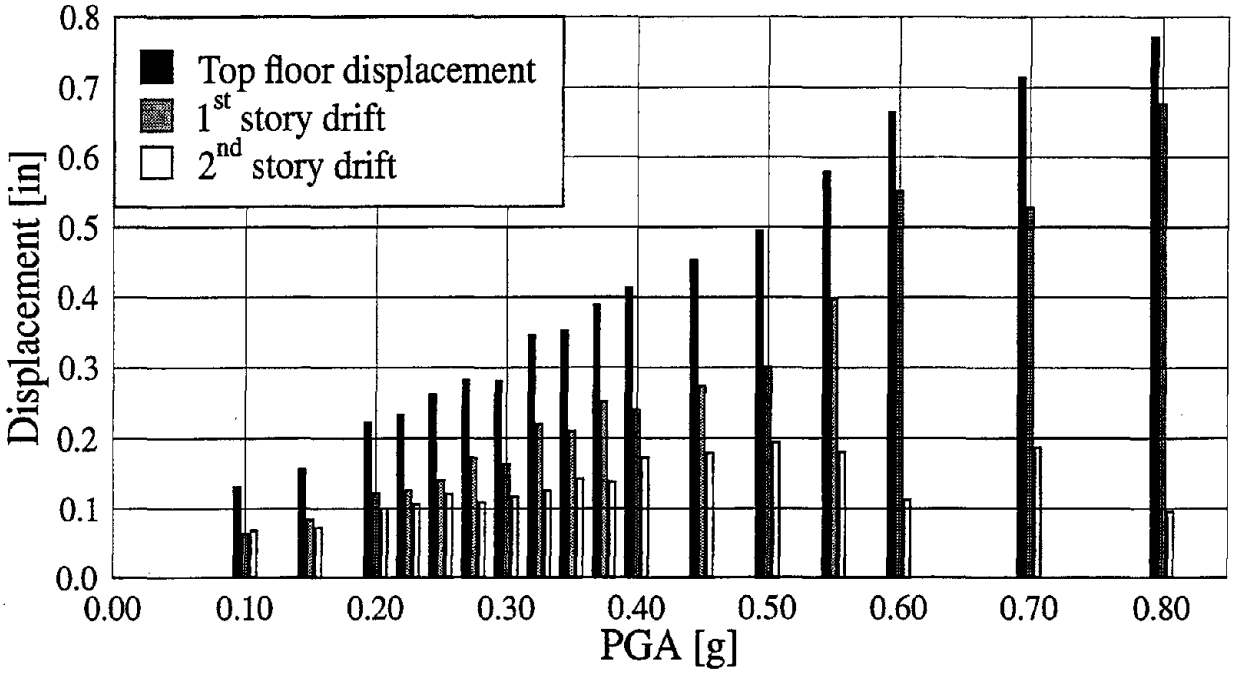

FIGURE 5-12 Variations of the maximum top floor displacement and the corresponding story drifts with PGA.

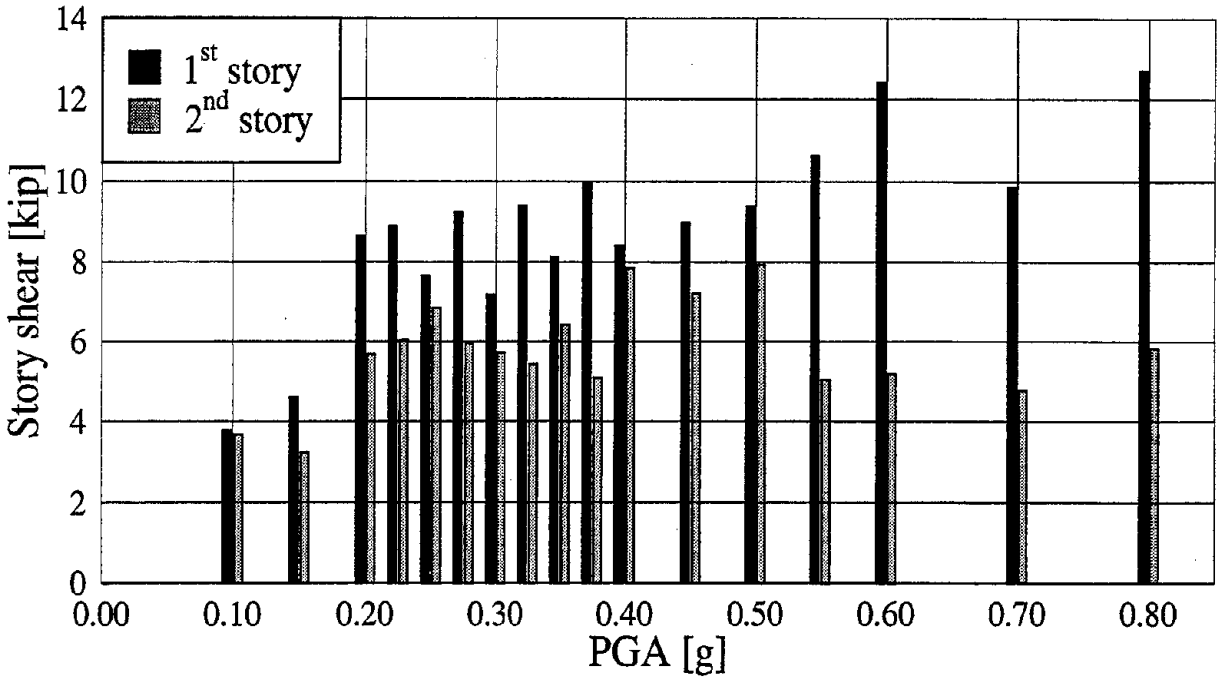

FIGURE 5-13 Variations of the story shears corresponding to the maximum top floor displacement with PGA.

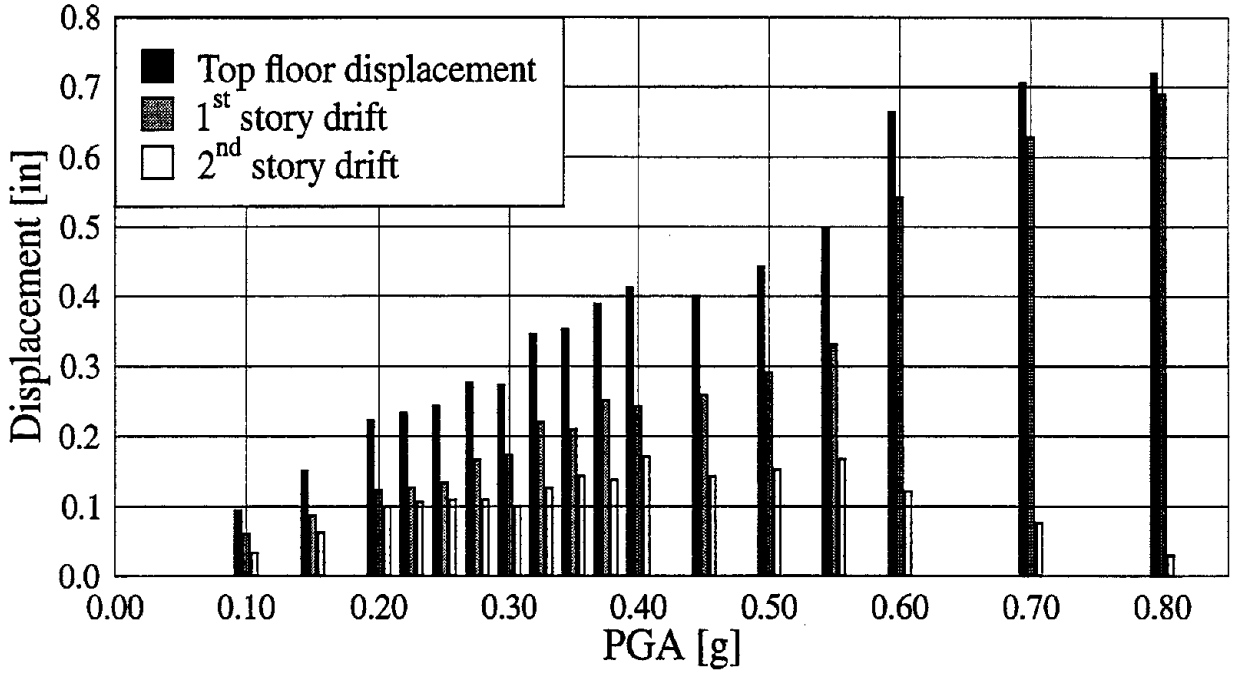

FIGURE 5-14 Variations of the top floor displacement and the inter-story drifts corresponding to maximum base shear with PGA.

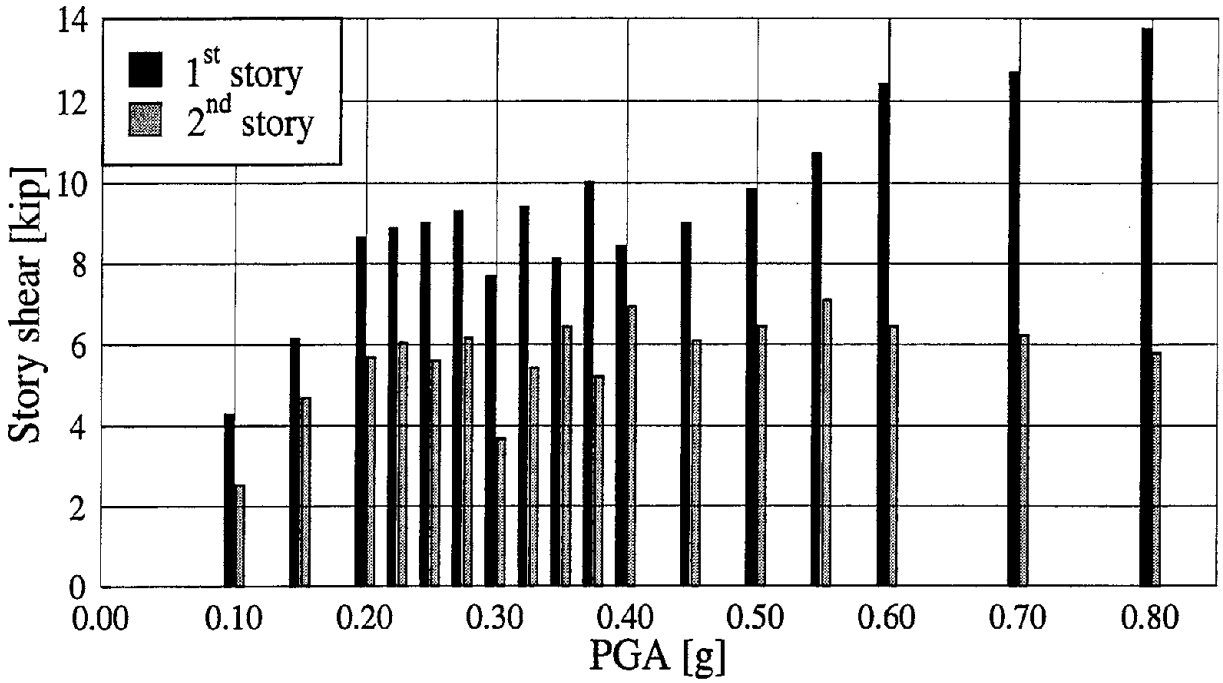

FIGURE 5-15 Variations of the story shears corresponding to the maximum base shear with PGA.

SECTION 6

CONCLUDING REMARKS

6.1 Summary

Unreinforced masonry infill walls can play an important role in the strength and ductility of framed structures, and should be considered in both analysis and design. Accounting for masonry infill walls in the design process mandates knowledge of complicated interaction mechanisms and failure modes. As described in this report, a pseudo-dynamic experimental technique has been developed to provide an improved basis for the evaluation of the dynamic response of frames with masonry infill walls.

In the pseudo-dynamic experimentation not only the structural capacity can be assessed but also the corresponding seismic demand may be predicted. The implementation of this experimental technique proved to be reliable in capturing the seismic response of stiff structures. It was concluded that the implemented predictor-corrector algorithm allows excellent control over the experimental error propagation. The essentially static loading approach used in pseudo-dynamic testing permitted careful documentation of the complex cracking and slipping behavior of the infill walls, and the intricacies of the frame/wall interaction. Regarding the behavior of the infilled frame, it was concluded that imparted energy and hysteretic energy correlate well with the observed damage state and that the initiation and propagation of cracking agreed with the observations of the quasi-static experiments, as conducted and reported in the first part of this study (refer to Figure 1-1). Based on the reported crack patterns, a macro-model is suggested. In this model, equivalent trusses can be used to represent the global effects of the infills on the bounding frame members.

6.2 Suggestions for Future Research

Further application of the pseudo-dynamic techniques should be pursued. Currently, the pseudo-dynamic methodology developed herein is being applied to testing a half scale, two-bay, two-story Lightly Reinforced Concrete (LRC) frame with unreinforced masonry infills. Also, the two-bay, two-story infilled LRC frame analyzed in part III of the present research program (refer to Figure 1-1) is being tested on a shake table under a series of simulated ground motions. The completion of these experiments will provide further information to validate and calibrate the developed models.

The developed pseudo-dynamic algorithm could be implemented as a subroutine for a new "pseudo-dynamic finite element" in finite element programs to allow the testing of sub-assemblages where the rest of the structure is accurately modeled numerically. In this way,

selected parts of the structure, where significant nonlinearities are expected, can be physically modeled while the response of the rest of the structure is obtained numerically. Thus, a new era may begin where the sophistication of advanced computational environments and the realism of physical modeling would be combined in a natural way.

The obtained experimental results provided the necessary means to develop improved simple models for infilled frames such as the equivalent truss model. Further refinements of the model are still needed. Such models are needed for the evaluation of existing infilled structures and the proper design of new ones.

SECTION 7

REFERENCES

[1] American Institute of Steel Construction (AISC), *Manual of Steel Construction, Allowable Stress Design* (ASD), 9th edition, Chicago, Illinois (1989).

[2] J. M. Biggs, *Introduction to structural dynamics*, McGraw-Hill, Inc., New York (1964).

[3] C. T. Grimm, 'Masonry cracks: a review of the literature', *Masonry: materials, design, construction, & maintenance*, H. A. Harris, editor, ASTM, **STP 992**, 257-280 (1988).

[4] R. D. Hanson and N. H. McClamroch, 'Pseudo dynamic test method for inelastic building response', *Proc. 8th U.S. World Conf. Earthquake Engrg.*, San Francisco, California, **VI**, 127-134 (1984).

[5] T. J. R. Hughes, K. S. Pister and R. L. Taylor, 'Implicit-Explicit Finite Elements in Nonlinear Transient Analysis', *Comput. Methods Appl. Mech. Engrg.*, **17/18**, 159-182 (1979).

[6] T. J. R. Hughes, 'Analysis of transient algorithms with particular reference to stability behavior', *Mechanics and mathematics methods: a series of handbooks*, First series: Computations methods in mechanics, Volume 1: Computational methods for transient analysis, T. Belytschko and T. J. R. Hughes (eds.), Elsevier Science Publishers B.V., Chapter 2, 67-156 (1983).

[7] S. A. Mahin, P. B. Shing, C. R. Thewalt and R. D. Hanson, 'Pseudodynamic test method - Current status and future directions', *J. Struct. Engrg.*, ASCE, **115**, 8, 2113-2128 (1989).

[8] B. Mohraz and F. E. Elghadamsi, 'Chapter 2: Earthquake ground motion and response spectra', *The seismic design handbook*, F. Naeim (ed.), Van Nostrand Reinhold, New York, 32-80 (1989).

[9] F. C. Moon, *Chaotic and fractal dynamics*, John Wiley & Sons, Inc., New York (1992).

[10] M. Nakashima, T. Kaminosono, M. Ishida and K. Ando, 'Integration techniques for substructure pseudo dynamic testing', *Proc. 4th U.S. Natl. Conf. Earthquake Engrg.*, Palm Springs, California, **II**, 515-524 (1990).

[11] N. M. Newmark and W. J. Hall, 'Procedures and criteria for earthquake resistant design', *Building Science Series 46*, Building Practices for Disaster Mitigation, U. S. Departement of Commerce (1973).

[12] R. Peek and W. H. Yi, 'Error analysis for pseudodynamic test method. I: Analysis', *J. Struct. Engrg.*, ASCE, **116**, 7, 1618-1637 (1990).

[13] R. Peek and W. H. Yi, 'Error analysis for pseudodynamic test method. II: Application', *J. Struct. Engrg.*, ASCE, **116**, 7, 1638-1658 (1990).

[14] G. M. Sabnis, H. G. Harris, R. N. White and M. S. Mirza, *Structural modeling and experimental techniques*, Prentice-Hall, Inc., New Jersy (1983).

[15] C. G. Salmon and J. E. Johnson, *Steel structures: design and behavior emphasizing load and resistance factor design*, Harper & Row, Publishers, New York (1990).

[16] S. P. Schneider and C. W. Roeder 'An inelastic substructure technique for the pseudodynamic test method', *Earthquake Engrg. Struct. Dyn.*, **23**, 761-775 (1994).

[17] F. Seible, G. Hegemier and A. Igarashi, 'Simulated seismic laboratory load testing of full-scale buildings', *Earthquake SPECTRA*, **12**, 1, 57-86 (1996).

[18] P. B. Shing and S. A. Mahin, 'Experimental error propagation in pseudodynamic testing', *Report No. UCB/EERC-83/12*, Earthquake Engrg. Res. Ctr., Univ. of California, Berkeley (1983).

[19] P. B. Shing and S. A. Mahin, 'Pseudodynamic test method for seismic performance evaluation: Theory and implementation', *Report No. UCB/EERC-84/12*, Earthquake Engrg. Res. Ctr., Univ. of California, Berkeley (1984).

[20] P. B. Shing, S. A. Mahin and S. N. Dermitzakis, 'Evaluation of on-line computer methods for seismic performance testing', *Proc. 8th U.S. World Conf. Earthquake Engrg.*, San Francisco, California, **VI**, 135-142 (1984).

[21] P. B. Shing and S. A. Mahin, 'Cumulative experimental errors in pseudodynamic tests', *Earthquake Engrg. Struct. Dyn.*, **15**, 409-424 (1987).

[22] P. B. Shing and S. A. Mahin, 'Experimental error effects in pseudodynamic testing', *J. Struct. Engrg.*, ASCE, **116**, 4, 805-821 (1989).

[23] P. B. Shing, M. T. Vannan and E. Carter, 'Evaluation of reinforced masonry shear wall components by pseudodynamic testing', *Proc. 4th U.S. Natl. Conf. Earthquake Engrg.*, Palm Springs, California, **II**, 829-838 (1990).

[24] P. B. Shing, M. T. Vannan and E. Carter, 'Implicit time integration for pseudodynamic tests', *Earthquake Engrg. Struct. Dyn.*, **20**, 551-576 (1991).

[25] K. Takanashi, K. Udagawa, M. Seki, T. Okada and H. Tanaka, 'Nonlinear earthquake response analysis of structures by a computer-actuator on-line system', *Bull. earthquake resist. struct. res. center*, Tokyo, **8** (1975).

[26] K. Takanashi and M. Nakashima, 'Japanese activities on on-Line testing', *J. Struct. Engrg.*, ASCE, **113**, 7, 1014-1032 (1987).

[27] C. R. Thewalt and S. A. Mahin, 'Hybrid solution techniques for generalized pseudodynamic testing', *Report No. UCB/EERC-87/09*, Earthquake Engrg. Res. Ctr., Univ. of California, Berkeley (1987).

[28] C. R. Thewalt and S. A. Mahin, 'The pseudodynamic test method: Numerical aspects', *Reliability and risk analysis*, **2**, Experimental and numerical methods in earthquake engineering, J. Donea and P. M. Jones (eds.), Kluwer Academic Publishers, The Netherlands, 47-62 (1991).

[29] C. R. Thewalt and S. A. Mahin, 'The pseudodynamic test method: Verification and extensions', *Reliability and risk analysis*, **2**, Experimental and numerical methods in earthquake engineering, J. Donea and P. M. Jones (eds.), Kluwer Academic Publishers, The Netherlands, 101-118 (1991).

[30] C. Thewalt and M. Roman, 'Performance parameters for pseudodynamic tests', *J. Struct. Engrg.*, ASCE, **120**, 9, 2768-2781 (1994).

[31] Y. Yamazaki, M. Nakashima and T. Kaminosono, 'Reliability of pseudodynamic test in earthquake response simulation', *J. Struct. Engrg.*, ASCE, **115**, 8, 2098-2112 (1989).

[32] W. H. Yi and R. Peek, 'Posterior time-step adjustment in pseudodynamic testing', *J. Engrg. Mech.*, ASCE, **119**, 7, 1376-1386 (1993).

[33] T. F. Zahrah and W. J. Hall, 'Earthquake energy absorption in SDOF structures', *J. Struct. Engrg.*, ASCE, **110**, 8, 1757-1772 (1984).

NATIONAL CENTER FOR EARTHQUAKE ENGINEERING RESEARCH
LIST OF TECHNICAL REPORTS

The National Center for Earthquake Engineering Research (NCEER) publishes technical reports on a variety of subjects related to earthquake engineering written by authors funded through NCEER. These reports are available from both NCEER Publications and the National Technical Information Service (NTIS). Requests for reports should be directed to NCEER Publications, National Center for Earthquake Engineering Research, State University of New York at Buffalo, Red Jacket Quadrangle, Buffalo, New York 14261. Reports can also be requested through NTIS, 5285 Port Royal Road, Springfield, Virginia 22161. NTIS accession numbers are shown in parenthesis, if available.

NCEER-87-0001 "First-Year Program in Research, Education and Technology Transfer," 3/5/87, (PB88-134275, A04, MF-A01).

NCEER-87-0002 "Experimental Evaluation of Instantaneous Optimal Algorithms for Structural Control," by R.C. Lin, T.T. Soong and A.M. Reinhorn, 4/20/87, (PB88-134341, A04, MF-A01).

NCEER-87-0003 "Experimentation Using the Earthquake Simulation Facilities at University at Buffalo," by A.M. Reinhorn and R.L. Ketter, to be published.

NCEER-87-0004 "The System Characteristics and Performance of a Shaking Table," by J.S. Hwang, K.C. Chang and G.C. Lee, 6/1/87, (PB88-134259, A03, MF-A01). This report is available only through NTIS (see address given above).

NCEER-87-0005 "A Finite Element Formulation for Nonlinear Viscoplastic Material Using a Q Model," by O. Gyebi and G. Dasgupta, 11/2/87, (PB88-213764, A08, MF-A01).

NCEER-87-0006 "Symbolic Manipulation Program (SMP) - Algebraic Codes for Two and Three Dimensional Finite Element Formulations," by X. Lee and G. Dasgupta, 11/9/87, (PB88-218522, A05, MF-A01).

NCEER-87-0007 "Instantaneous Optimal Control Laws for Tall Buildings Under Seismic Excitations," by J.N. Yang, A. Akbarpour and P. Ghaemmaghami, 6/10/87, (PB88-134333, A06, MF-A01). This report is only available through NTIS (see address given above).

NCEER-87-0008 "IDARC: Inelastic Damage Analysis of Reinforced Concrete Frame - Shear-Wall Structures," by Y.J. Park, A.M. Reinhorn and S.K. Kunnath, 7/20/87, (PB88-134325, A09, MF-A01). This report is only available through NTIS (see address given above).

NCEER-87-0009 "Liquefaction Potential for New York State: A Preliminary Report on Sites in Manhattan and Buffalo," by M. Budhu, V. Vijayakumar, R.F. Giese and L. Baumgras, 8/31/87, (PB88-163704, A03, MF-A01). This report is available only through NTIS (see address given above).

NCEER-87-0010 "Vertical and Torsional Vibration of Foundations in Inhomogeneous Media," by A.S. Veletsos and K.W. Dotson, 6/1/87, (PB88-134291, A03, MF-A01). This report is only available through NTIS (see address given above).

NCEER-87-0011 "Seismic Probabilistic Risk Assessment and Seismic Margins Studies for Nuclear Power Plants," by Howard H.M. Hwang, 6/15/87, (PB88-134267, A03, MF-A01). This report is only available through NTIS (see address given above).

NCEER-87-0012 "Parametric Studies of Frequency Response of Secondary Systems Under Ground-Acceleration Excitations," by Y. Yong and Y.K. Lin, 6/10/87, (PB88-134309, A03, MF-A01). This report is only available through NTIS (see address given above).

NCEER-87-0013 "Frequency Response of Secondary Systems Under Seismic Excitation," by J.A. HoLung, J. Cai and Y.K. Lin, 7/31/87, (PB88-134317, A05, MF-A01). This report is only available through NTIS (see address given above).

NCEER-87-0014 "Modelling Earthquake Ground Motions in Seismically Active Regions Using Parametric Time Series Methods," by G.W. Ellis and A.S. Cakmak, 8/25/87, (PB88-134283, A08, MF-A01). This report is only available through NTIS (see address given above).

NCEER-87-0015 "Detection and Assessment of Seismic Structural Damage," by E. DiPasquale and A.S. Cakmak, 8/25/87, (PB88-163712, A05, MF-A01). This report is only available through NTIS (see address given above).

NCEER-87-0016 "Pipeline Experiment at Parkfield, California," by J. Isenberg and E. Richardson, 9/15/87, (PB88-163720, A03, MF-A01). This report is available only through NTIS (see address given above).

NCEER-87-0017 "Digital Simulation of Seismic Ground Motion," by M. Shinozuka, G. Deodatis and T. Harada, 8/31/87, (PB88-155197, A04, MF-A01). This report is available only through NTIS (see address given above).

NCEER-87-0018 "Practical Considerations for Structural Control: System Uncertainty, System Time Delay and Truncation of Small Control Forces," J.N. Yang and A. Akbarpour, 8/10/87, (PB88-163738, A08, MF-A01). This report is only available through NTIS (see address given above).

NCEER-87-0019 "Modal Analysis of Nonclassically Damped Structural Systems Using Canonical Transformation," by J.N. Yang, S. Sarkani and F.X. Long, 9/27/87, (PB88-187851, A04, MF-A01).

NCEER-87-0020 "A Nonstationary Solution in Random Vibration Theory," by J.R. Red-Horse and P.D. Spanos, 11/3/87, (PB88-163746, A03, MF-A01).

NCEER-87-0021 "Horizontal Impedances for Radially Inhomogeneous Viscoelastic Soil Layers," by A.S. Veletsos and K.W. Dotson, 10/15/87, (PB88-150859, A04, MF-A01).

NCEER-87-0022 "Seismic Damage Assessment of Reinforced Concrete Members," by Y.S. Chung, C. Meyer and M. Shinozuka, 10/9/87, (PB88-150867, A05, MF-A01). This report is available only through NTIS (see address given above).

NCEER-87-0023 "Active Structural Control in Civil Engineering," by T.T. Soong, 11/11/87, (PB88-187778, A03, MF-A01).

NCEER-87-0024 "Vertical and Torsional Impedances for Radially Inhomogeneous Viscoelastic Soil Layers," by K.W. Dotson and A.S. Veletsos, 12/87, (PB88-187786, A03, MF-A01).

NCEER-87-0025 "Proceedings from the Symposium on Seismic Hazards, Ground Motions, Soil-Liquefaction and Engineering Practice in Eastern North America," October 20-22, 1987, edited by K.H. Jacob, 12/87, (PB88-188115, A23, MF-A01).

NCEER-87-0026 "Report on the Whittier-Narrows, California, Earthquake of October 1, 1987," by J. Pantelic and A. Reinhorn, 11/87, (PB88-187752, A03, MF-A01). This report is available only through NTIS (see address given above).

NCEER-87-0027 "Design of a Modular Program for Transient Nonlinear Analysis of Large 3-D Building Structures," by S. Srivastav and J.F. Abel, 12/30/87, (PB88-187950, A05, MF-A01). This report is only available through NTIS (see address given above).

NCEER-87-0028 "Second-Year Program in Research, Education and Technology Transfer," 3/8/88, (PB88-219480, A04, MF-A01).

NCEER-88-0001 "Workshop on Seismic Computer Analysis and Design of Buildings With Interactive Graphics," by W. McGuire, J.F. Abel and C.H. Conley, 1/18/88, (PB88-187760, A03, MF-A01). This report is only available through NTIS (see address given above).

NCEER-88-0002 "Optimal Control of Nonlinear Flexible Structures," by J.N. Yang, F.X. Long and D. Wong, 1/22/88, (PB88-213772, A06, MF-A01).

NCEER-88-0003 "Substructuring Techniques in the Time Domain for Primary-Secondary Structural Systems," by G.D. Manolis and G. Juhn, 2/10/88, (PB88-213780, A04, MF-A01).

NCEER-88-0004 "Iterative Seismic Analysis of Primary-Secondary Systems," by A. Singhal, L.D. Lutes and P.D. Spanos, 2/23/88, (PB88-213798, A04, MF-A01).

NCEER-88-0005 "Stochastic Finite Element Expansion for Random Media," by P.D. Spanos and R. Ghanem, 3/14/88, (PB88-213806, A03, MF-A01).

NCEER-88-0006 "Combining Structural Optimization and Structural Control," by F.Y. Cheng and C.P. Pantelides, 1/10/88, (PB88-213814, A05, MF-A01).

NCEER-88-0007 "Seismic Performance Assessment of Code-Designed Structures," by H.H-M. Hwang, J-W. Jaw and H-J. Shau, 3/20/88, (PB88-219423, A04, MF-A01). This report is only available through NTIS (see address given above).

NCEER-88-0008 "Reliability Analysis of Code-Designed Structures Under Natural Hazards," by H.H-M. Hwang, H. Ushiba and M. Shinozuka, 2/29/88, (PB88-229471, A07, MF-A01). This report is only available through NTIS (see address given above).

NCEER-88-0009 "Seismic Fragility Analysis of Shear Wall Structures," by J-W Jaw and H.H-M. Hwang, 4/30/88, (PB89-102867, A04, MF-A01).

NCEER-88-0010 "Base Isolation of a Multi-Story Building Under a Harmonic Ground Motion - A Comparison of Performances of Various Systems," by F-G Fan, G. Ahmadi and I.G. Tadjbakhsh, 5/18/88, (PB89-122238, A06, MF-A01). This report is only available through NTIS (see address given above).

NCEER-88-0011 "Seismic Floor Response Spectra for a Combined System by Green's Functions," by F.M. Lavelle, L.A. Bergman and P.D. Spanos, 5/1/88, (PB89-102875, A03, MF-A01).

NCEER-88-0012 "A New Solution Technique for Randomly Excited Hysteretic Structures," by G.Q. Cai and Y.K. Lin, 5/16/88, (PB89-102883, A03, MF-A01).

NCEER-88-0013 "A Study of Radiation Damping and Soil-Structure Interaction Effects in the Centrifuge," by K. Weissman, supervised by J.H. Prevost, 5/24/88, (PB89-144703, A06, MF-A01).

NCEER-88-0014 "Parameter Identification and Implementation of a Kinematic Plasticity Model for Frictional Soils," by J.H. Prevost and D.V. Griffiths, to be published.

NCEER-88-0015 "Two- and Three- Dimensional Dynamic Finite Element Analyses of the Long Valley Dam," by D.V. Griffiths and J.H. Prevost, 6/17/88, (PB89-144711, A04, MF-A01).

NCEER-88-0016 "Damage Assessment of Reinforced Concrete Structures in Eastern United States," by A.M. Reinhorn, M.J. Seidel, S.K. Kunnath and Y.J. Park, 6/15/88, (PB89-122220, A04, MF-A01). This report is only available through NTIS (see address given above).

NCEER-88-0017 "Dynamic Compliance of Vertically Loaded Strip Foundations in Multilayered Viscoelastic Soils," by S. Ahmad and A.S.M. Israil, 6/17/88, (PB89-102891, A04, MF-A01).

NCEER-88-0018 "An Experimental Study of Seismic Structural Response With Added Viscoelastic Dampers," by R.C. Lin, Z. Liang, T.T. Soong and R.H. Zhang, 6/30/88, (PB89-122212, A05, MF-A01). This report is available only through NTIS (see address given above).

NCEER-88-0019 "Experimental Investigation of Primary - Secondary System Interaction," by G.D. Manolis, G. Juhn and A.M. Reinhorn, 5/27/88, (PB89-122204, A04, MF-A01).

NCEER-88-0020 "A Response Spectrum Approach For Analysis of Nonclassically Damped Structures," by J.N. Yang, S. Sarkani and F.X. Long, 4/22/88, (PB89-102909, A04, MF-A01).

NCEER-88-0021 "Seismic Interaction of Structures and Soils: Stochastic Approach," by A.S. Veletsos and A.M. Prasad, 7/21/88, (PB89-122196, A04, MF-A01). This report is only available through NTIS (see address given above).

NCEER-88-0022 "Identification of the Serviceability Limit State and Detection of Seismic Structural Damage," by E. DiPasquale and A.S. Cakmak, 6/15/88, (PB89-122188, A05, MF-A01). This report is available only through NTIS (see address given above).

NCEER-88-0023 "Multi-Hazard Risk Analysis: Case of a Simple Offshore Structure," by B.K. Bhartia and E.H. Vanmarcke, 7/21/88, (PB89-145213, A05, MF-A01).

NCEER-88-0024 "Automated Seismic Design of Reinforced Concrete Buildings," by Y.S. Chung, C. Meyer and M. Shinozuka, 7/5/88, (PB89-122170, A06, MF-A01). This report is available only through NTIS (see address given above).

NCEER-88-0025 "Experimental Study of Active Control of MDOF Structures Under Seismic Excitations," by L.L. Chung, R.C. Lin, T.T. Soong and A.M. Reinhorn, 7/10/88, (PB89-122600, A04, MF-A01).

NCEER-88-0026 "Earthquake Simulation Tests of a Low-Rise Metal Structure," by J.S. Hwang, K.C. Chang, G.C. Lee and R.L. Ketter, 8/1/88, (PB89-102917, A04, MF-A01).

NCEER-88-0027 "Systems Study of Urban Response and Reconstruction Due to Catastrophic Earthquakes," by F. Kozin and H.K. Zhou, 9/22/88, (PB90-162348, A04, MF-A01).

NCEER-88-0028 "Seismic Fragility Analysis of Plane Frame Structures," by H.H-M. Hwang and Y.K. Low, 7/31/88, (PB89-131445, A06, MF-A01).

NCEER-88-0029 "Response Analysis of Stochastic Structures," by A. Kardara, C. Bucher and M. Shinozuka, 9/22/88, (PB89-174429, A04, MF-A01).

NCEER-88-0030 "Nonnormal Accelerations Due to Yielding in a Primary Structure," by D.C.K. Chen and L.D. Lutes, 9/19/88, (PB89-131437, A04, MF-A01).

NCEER-88-0031 "Design Approaches for Soil-Structure Interaction," by A.S. Veletsos, A.M. Prasad and Y. Tang, 12/30/88, (PB89-174437, A03, MF-A01). This report is available only through NTIS (see address given above).

NCEER-88-0032 "A Re-evaluation of Design Spectra for Seismic Damage Control," by C.J. Turkstra and A.G. Tallin, 11/7/88, (PB89-145221, A05, MF-A01).

NCEER-88-0033 "The Behavior and Design of Noncontact Lap Splices Subjected to Repeated Inelastic Tensile Loading," by V.E. Sagan, P. Gergely and R.N. White, 12/8/88, (PB89-163737, A08, MF-A01).

NCEER-88-0034 "Seismic Response of Pile Foundations," by S.M. Mamoon, P.K. Banerjee and S. Ahmad, 11/1/88, (PB89-145239, A04, MF-A01).

NCEER-88-0035 "Modeling of R/C Building Structures With Flexible Floor Diaphragms (IDARC2)," by A.M. Reinhorn, S.K. Kunnath and N. Panahshahi, 9/7/88, (PB89-207153, A07, MF-A01).

NCEER-88-0036 "Solution of the Dam-Reservoir Interaction Problem Using a Combination of FEM, BEM with Particular Integrals, Modal Analysis, and Substructuring," by C-S. Tsai, G.C. Lee and R.L. Ketter, 12/31/88, (PB89-207146, A04, MF-A01).

NCEER-88-0037 "Optimal Placement of Actuators for Structural Control," by F.Y. Cheng and C.P. Pantelides, 8/15/88, (PB89-162846, A05, MF-A01).

NCEER-88-0038 "Teflon Bearings in Aseismic Base Isolation: Experimental Studies and Mathematical Modeling," by A. Mokha, M.C. Constantinou and A.M. Reinhorn, 12/5/88, (PB89-218457, A10, MF-A01). This report is available only through NTIS (see address given above).

NCEER-88-0039 "Seismic Behavior of Flat Slab High-Rise Buildings in the New York City Area," by P. Weidlinger and M. Ettouney, 10/15/88, (PB90-145681, A04, MF-A01).

NCEER-88-0040 "Evaluation of the Earthquake Resistance of Existing Buildings in New York City," by P. Weidlinger and M. Ettouney, 10/15/88, to be published.

NCEER-88-0041 "Small-Scale Modeling Techniques for Reinforced Concrete Structures Subjected to Seismic Loads," by W. Kim, A. El-Attar and R.N. White, 11/22/88, (PB89-189625, A05, MF-A01).

NCEER-88-0042 "Modeling Strong Ground Motion from Multiple Event Earthquakes," by G.W. Ellis and A.S. Cakmak, 10/15/88, (PB89-174445, A03, MF-A01).

NCEER-88-0043 "Nonstationary Models of Seismic Ground Acceleration," by M. Grigoriu, S.E. Ruiz and E. Rosenblueth, 7/15/88, (PB89-189617, A04, MF-A01).

NCEER-88-0044 "SARCF User's Guide: Seismic Analysis of Reinforced Concrete Frames," by Y.S. Chung, C. Meyer and M. Shinozuka, 11/9/88, (PB89-174452, A08, MF-A01).

NCEER-88-0045 "First Expert Panel Meeting on Disaster Research and Planning," edited by J. Pantelic and J. Stoyle, 9/15/88, (PB89-174460, A05, MF-A01). This report is only available through NTIS (see address given above).

NCEER-88-0046 "Preliminary Studies of the Effect of Degrading Infill Walls on the Nonlinear Seismic Response of Steel Frames," by C.Z. Chrysostomou, P. Gergely and J.F. Abel, 12/19/88, (PB89-208383, A05, MF-A01).

NCEER-88-0047 "Reinforced Concrete Frame Component Testing Facility - Design, Construction, Instrumentation and Operation," by S.P. Pessiki, C. Conley, T. Bond, P. Gergely and R.N. White, 12/16/88, (PB89-174478, A04, MF-A01).

NCEER-89-0001 "Effects of Protective Cushion and Soil Compliancy on the Response of Equipment Within a Seismically Excited Building," by J.A. HoLung, 2/16/89, (PB89-207179, A04, MF-A01).

NCEER-89-0002 "Statistical Evaluation of Response Modification Factors for Reinforced Concrete Structures," by H.H-M. Hwang and J-W. Jaw, 2/17/89, (PB89-207187, A05, MF-A01).

NCEER-89-0003 "Hysteretic Columns Under Random Excitation," by G-Q. Cai and Y.K. Lin, 1/9/89, (PB89-196513, A03, MF-A01).

NCEER-89-0004 "Experimental Study of `Elephant Foot Bulge' Instability of Thin-Walled Metal Tanks," by Z-H. Jia and R.L. Ketter, 2/22/89, (PB89-207195, A03, MF-A01).

NCEER-89-0005 "Experiment on Performance of Buried Pipelines Across San Andreas Fault," by J. Isenberg, E. Richardson and T.D. O'Rourke, 3/10/89, (PB89-218440, A04, MF-A01). This report is available only through NTIS (see address given above).

NCEER-89-0006 "A Knowledge-Based Approach to Structural Design of Earthquake-Resistant Buildings," by M. Subramani, P. Gergely, C.H. Conley, J.F. Abel and A.H. Zaghw, 1/15/89, (PB89-218465, A06, MF-A01).

NCEER-89-0007 "Liquefaction Hazards and Their Effects on Buried Pipelines," by T.D. O'Rourke and P.A. Lane, 2/1/89, (PB89-218481, A09, MF-A01).

NCEER-89-0008 "Fundamentals of System Identification in Structural Dynamics," by H. Imai, C-B. Yun, O. Maruyama and M. Shinozuka, 1/26/89, (PB89-207211, A04, MF-A01).

NCEER-89-0009 "Effects of the 1985 Michoacan Earthquake on Water Systems and Other Buried Lifelines in Mexico," by A.G. Ayala and M.J. O'Rourke, 3/8/89, (PB89-207229, A06, MF-A01).

NCEER-89-R010 "NCEER Bibliography of Earthquake Education Materials," by K.E.K. Ross, Second Revision, 9/1/89, (PB90-125352, A05, MF-A01). This report is replaced by NCEER-92-0018.

NCEER-89-0011 "Inelastic Three-Dimensional Response Analysis of Reinforced Concrete Building Structures (IDARC-3D), Part I - Modeling," by S.K. Kunnath and A.M. Reinhorn, 4/17/89, (PB90-114612, A07, MF-A01).

NCEER-89-0012 "Recommended Modifications to ATC-14," by C.D. Poland and J.O. Malley, 4/12/89, (PB90-108648, A15, MF-A01).

NCEER-89-0013 "Repair and Strengthening of Beam-to-Column Connections Subjected to Earthquake Loading," by M. Corazao and A.J. Durrani, 2/28/89, (PB90-109885, A06, MF-A01).

NCEER-89-0014 "Program EXKAL2 for Identification of Structural Dynamic Systems," by O. Maruyama, C-B. Yun, M. Hoshiya and M. Shinozuka, 5/19/89, (PB90-109877, A09, MF-A01).

NCEER-89-0015 "Response of Frames With Bolted Semi-Rigid Connections, Part I - Experimental Study and Analytical Predictions," by P.J. DiCorso, A.M. Reinhorn, J.R. Dickerson, J.B. Radziminski and W.L. Harper, 6/1/89, to be published.

NCEER-89-0016 "ARMA Monte Carlo Simulation in Probabilistic Structural Analysis," by P.D. Spanos and M.P. Mignolet, 7/10/89, (PB90-109893, A03, MF-A01).

NCEER-89-P017 "Preliminary Proceedings from the Conference on Disaster Preparedness - The Place of Earthquake Education in Our Schools," Edited by K.E.K. Ross, 6/23/89, (PB90-108606, A03, MF-A01).

NCEER-89-0017 "Proceedings from the Conference on Disaster Preparedness - The Place of Earthquake Education in Our Schools," Edited by K.E.K. Ross, 12/31/89, (PB90-207895, A012, MF-A02). This report is available only through NTIS (see address given above).

NCEER-89-0018 "Multidimensional Models of Hysteretic Material Behavior for Vibration Analysis of Shape Memory Energy Absorbing Devices, by E.J. Graesser and F.A. Cozzarelli, 6/7/89, (PB90-164146, A04, MF-A01).

NCEER-89-0019 "Nonlinear Dynamic Analysis of Three-Dimensional Base Isolated Structures (3D-BASIS)," by S. Nagarajaiah, A.M. Reinhorn and M.C. Constantinou, 8/3/89, (PB90-161936, A06, MF-A01). This report has been replaced by NCEER-93-0011.

NCEER-89-0020 "Structural Control Considering Time-Rate of Control Forces and Control Rate Constraints," by F.Y. Cheng and C.P. Pantelides, 8/3/89, (PB90-120445, A04, MF-A01).

NCEER-89-0021 "Subsurface Conditions of Memphis and Shelby County," by K.W. Ng, T-S. Chang and H-H.M. Hwang, 7/26/89, (PB90-120437, A03, MF-A01).

NCEER-89-0022 "Seismic Wave Propagation Effects on Straight Jointed Buried Pipelines," by K. Elhmadi and M.J. O'Rourke, 8/24/89, (PB90-162322, A10, MF-A02).

NCEER-89-0023 "Workshop on Serviceability Analysis of Water Delivery Systems," edited by M. Grigoriu, 3/6/89, (PB90-127424, A03, MF-A01).

NCEER-89-0024 "Shaking Table Study of a 1/5 Scale Steel Frame Composed of Tapered Members," by K.C. Chang, J.S. Hwang and G.C. Lee, 9/18/89, (PB90-160169, A04, MF-A01).

NCEER-89-0025 "DYNA1D: A Computer Program for Nonlinear Seismic Site Response Analysis - Technical Documentation," by Jean H. Prevost, 9/14/89, (PB90-161944, A07, MF-A01). This report is available only through NTIS (see address given above).

NCEER-89-0026 "1:4 Scale Model Studies of Active Tendon Systems and Active Mass Dampers for Aseismic Protection," by A.M. Reinhorn, T.T. Soong, R.C. Lin, Y.P. Yang, Y. Fukao, H. Abe and M. Nakai, 9/15/89, (PB90-173246, A10, MF-A02).

NCEER-89-0027 "Scattering of Waves by Inclusions in a Nonhomogeneous Elastic Half Space Solved by Boundary Element Methods," by P.K. Hadley, A. Askar and A.S. Cakmak, 6/15/89, (PB90-145699, A07, MF-A01).

NCEER-89-0028 "Statistical Evaluation of Deflection Amplification Factors for Reinforced Concrete Structures," by H.H.M. Hwang, J-W. Jaw and A.L. Ch'ng, 8/31/89, (PB90-164633, A05, MF-A01).

NCEER-89-0029 "Bedrock Accelerations in Memphis Area Due to Large New Madrid Earthquakes," by H.H.M. Hwang, C.H.S. Chen and G. Yu, 11/7/89, (PB90-162330, A04, MF-A01).

NCEER-89-0030 "Seismic Behavior and Response Sensitivity of Secondary Structural Systems," by Y.Q. Chen and T.T. Soong, 10/23/89, (PB90-164658, A08, MF-A01).

NCEER-89-0031 "Random Vibration and Reliability Analysis of Primary-Secondary Structural Systems," by Y. Ibrahim, M. Grigoriu and T.T. Soong, 11/10/89, (PB90-161951, A04, MF-A01).

NCEER-89-0032 "Proceedings from the Second U.S. - Japan Workshop on Liquefaction, Large Ground Deformation and Their Effects on Lifelines, September 26-29, 1989," Edited by T.D. O'Rourke and M. Hamada, 12/1/89, (PB90-209388, A22, MF-A03).

NCEER-89-0033 "Deterministic Model for Seismic Damage Evaluation of Reinforced Concrete Structures," by J.M. Bracci, A.M. Reinhorn, J.B. Mander and S.K. Kunnath, 9/27/89, (PB91-108803, A06, MF-A01).

NCEER-89-0034 "On the Relation Between Local and Global Damage Indices," by E. DiPasquale and A.S. Cakmak, 8/15/89, (PB90-173865, A05, MF-A01).

NCEER-89-0035 "Cyclic Undrained Behavior of Nonplastic and Low Plasticity Silts," by A.J. Walker and H.E. Stewart, 7/26/89, (PB90-183518, A10, MF-A01).

NCEER-89-0036 "Liquefaction Potential of Surficial Deposits in the City of Buffalo, New York," by M. Budhu, R. Giese and L. Baumgrass, 1/17/89, (PB90-208455, A04, MF-A01).

NCEER-89-0037 "A Deterministic Assessment of Effects of Ground Motion Incoherence," by A.S. Veletsos and Y. Tang, 7/15/89, (PB90-164294, A03, MF-A01).

NCEER-89-0038 "Workshop on Ground Motion Parameters for Seismic Hazard Mapping," July 17-18, 1989, edited by R.V. Whitman, 12/1/89, (PB90-173923, A04, MF-A01).

NCEER-89-0039 "Seismic Effects on Elevated Transit Lines of the New York City Transit Authority," by C.J. Costantino, C.A. Miller and E. Heymsfield, 12/26/89, (PB90-207887, A06, MF-A01).

NCEER-89-0040 "Centrifugal Modeling of Dynamic Soil-Structure Interaction," by K. Weissman, Supervised by J.H. Prevost, 5/10/89, (PB90-207879, A07, MF-A01).

NCEER-89-0041 "Linearized Identification of Buildings With Cores for Seismic Vulnerability Assessment," by I-K. Ho and A.E. Aktan, 11/1/89, (PB90-251943, A07, MF-A01).

NCEER-90-0001 "Geotechnical and Lifeline Aspects of the October 17, 1989 Loma Prieta Earthquake in San Francisco," by T.D. O'Rourke, H.E. Stewart, F.T. Blackburn and T.S. Dickerman, 1/90, (PB90-208596, A05, MF-A01).

NCEER-90-0002 "Nonnormal Secondary Response Due to Yielding in a Primary Structure," by D.C.K. Chen and L.D. Lutes, 2/28/90, (PB90-251976, A07, MF-A01).

NCEER-90-0003 "Earthquake Education Materials for Grades K-12," by K.E.K. Ross, 4/16/90, (PB91-251984, A05, MF-A05). This report has been replaced by NCEER-92-0018.

NCEER-90-0004 "Catalog of Strong Motion Stations in Eastern North America," by R.W. Busby, 4/3/90, (PB90-251984, A05, MF-A01).

NCEER-90-0005 "NCEER Strong-Motion Data Base: A User Manual for the GeoBase Release (Version 1.0 for the Sun3)," by P. Friberg and K. Jacob, 3/31/90 (PB90-258062, A04, MF-A01).

NCEER-90-0006 "Seismic Hazard Along a Crude Oil Pipeline in the Event of an 1811-1812 Type New Madrid Earthquake," by H.H.M. Hwang and C-H.S. Chen, 4/16/90, (PB90-258054, A04, MF-A01).

NCEER-90-0007 "Site-Specific Response Spectra for Memphis Sheahan Pumping Station," by H.H.M. Hwang and C.S. Lee, 5/15/90, (PB91-108811, A05, MF-A01).

NCEER-90-0008 "Pilot Study on Seismic Vulnerability of Crude Oil Transmission Systems," by T. Ariman, R. Dobry, M. Grigoriu, F. Kozin, M. O'Rourke, T. O'Rourke and M. Shinozuka, 5/25/90, (PB91-108837, A06, MF-A01).

NCEER-90-0009 "A Program to Generate Site Dependent Time Histories: EQGEN," by G.W. Ellis, M. Srinivasan and A.S. Cakmak, 1/30/90, (PB91-108829, A04, MF-A01).

NCEER-90-0010 "Active Isolation for Seismic Protection of Operating Rooms," by M.E. Talbott, Supervised by M. Shinozuka, 6/8/9, (PB91-110205, A05, MF-A01).

NCEER-90-0011 "Program LINEARID for Identification of Linear Structural Dynamic Systems," by C-B. Yun and M. Shinozuka, 6/25/90, (PB91-110312, A08, MF-A01).

NCEER-90-0012 "Two-Dimensional Two-Phase Elasto-Plastic Seismic Response of Earth Dams," by A.N. Yiagos, Supervised by J.H. Prevost, 6/20/90, (PB91-110197, A13, MF-A02).

NCEER-90-0013 "Secondary Systems in Base-Isolated Structures: Experimental Investigation, Stochastic Response and Stochastic Sensitivity," by G.D. Manolis, G. Juhn, M.C. Constantinou and A.M. Reinhorn, 7/1/90, (PB91-110320, A08, MF-A01).

NCEER-90-0014 "Seismic Behavior of Lightly-Reinforced Concrete Column and Beam-Column Joint Details," by S.P. Pessiki, C.H. Conley, P. Gergely and R.N. White, 8/22/90, (PB91-108795, A11, MF-A02).

NCEER-90-0015 "Two Hybrid Control Systems for Building Structures Under Strong Earthquakes," by J.N. Yang and A. Danielians, 6/29/90, (PB91-125393, A04, MF-A01).

NCEER-90-0016 "Instantaneous Optimal Control with Acceleration and Velocity Feedback," by J.N. Yang and Z. Li, 6/29/90, (PB91-125401, A03, MF-A01).

NCEER-90-0017 "Reconnaissance Report on the Northern Iran Earthquake of June 21, 1990," by M. Mehrain, 10/4/90, (PB91-125377, A03, MF-A01).

NCEER-90-0018 "Evaluation of Liquefaction Potential in Memphis and Shelby County," by T.S. Chang, P.S. Tang, C.S. Lee and H. Hwang, 8/10/90, (PB91-125427, A09, MF-A01).

NCEER-90-0019 "Experimental and Analytical Study of a Combined Sliding Disc Bearing and Helical Steel Spring Isolation System," by M.C. Constantinou, A.S. Mokha and A.M. Reinhorn, 10/4/90, (PB91-125385, A06, MF-A01). This report is available only through NTIS (see address given above).

NCEER-90-0020 "Experimental Study and Analytical Prediction of Earthquake Response of a Sliding Isolation System with a Spherical Surface," by A.S. Mokha, M.C. Constantinou and A.M. Reinhorn, 10/11/90, (PB91-125419, A05, MF-A01).

NCEER-90-0021 "Dynamic Interaction Factors for Floating Pile Groups," by G. Gazetas, K. Fan, A. Kaynia and E. Kausel, 9/10/90, (PB91-170381, A05, MF-A01).

NCEER-90-0022 "Evaluation of Seismic Damage Indices for Reinforced Concrete Structures," by S. Rodriguez-Gomez and A.S. Cakmak, 9/30/90, PB91-171322, A06, MF-A01).

NCEER-90-0023 "Study of Site Response at a Selected Memphis Site," by H. Desai, S. Ahmad, E.S. Gazetas and M.R. Oh, 10/11/90, (PB91-196857, A03, MF-A01).

NCEER-90-0024 "A User's Guide to Strongmo: Version 1.0 of NCEER's Strong-Motion Data Access Tool for PCs and Terminals," by P.A. Friberg and C.A.T. Susch, 11/15/90, (PB91-171272, A03, MF-A01).

NCEER-90-0025 "A Three-Dimensional Analytical Study of Spatial Variability of Seismic Ground Motions," by L-L. Hong and A.H.-S. Ang, 10/30/90, (PB91-170399, A09, MF-A01).

NCEER-90-0026 "MUMOID User's Guide - A Program for the Identification of Modal Parameters," by S. Rodriguez-Gomez and E. DiPasquale, 9/30/90, (PB91-171298, A04, MF-A01).

NCEER-90-0027 "SARCF-II User's Guide - Seismic Analysis of Reinforced Concrete Frames," by S. Rodriguez-Gomez, Y.S. Chung and C. Meyer, 9/30/90, (PB91-171280, A05, MF-A01).

NCEER-90-0028 "Viscous Dampers: Testing, Modeling and Application in Vibration and Seismic Isolation," by N. Makris and M.C. Constantinou, 12/20/90 (PB91-190561, A06, MF-A01).

NCEER-90-0029 "Soil Effects on Earthquake Ground Motions in the Memphis Area," by H. Hwang, C.S. Lee, K.W. Ng and T.S. Chang, 8/2/90, (PB91-190751, A05, MF-A01).

NCEER-91-0001 "Proceedings from the Third Japan-U.S. Workshop on Earthquake Resistant Design of Lifeline Facilities and Countermeasures for Soil Liquefaction, December 17-19, 1990," edited by T.D. O'Rourke and M. Hamada, 2/1/91, (PB91-179259, A99, MF-A04).

NCEER-91-0002 "Physical Space Solutions of Non-Proportionally Damped Systems," by M. Tong, Z. Liang and G.C. Lee, 1/15/91, (PB91-179242, A04, MF-A01).

NCEER-91-0003 "Seismic Response of Single Piles and Pile Groups," by K. Fan and G. Gazetas, 1/10/91, (PB92-174994, A04, MF-A01).

NCEER-91-0004 "Damping of Structures: Part 1 - Theory of Complex Damping," by Z. Liang and G. Lee, 10/10/91, (PB92-197235, A12, MF-A03).

NCEER-91-0005 "3D-BASIS - Nonlinear Dynamic Analysis of Three Dimensional Base Isolated Structures: Part II," by S. Nagarajaiah, A.M. Reinhorn and M.C. Constantinou, 2/28/91, (PB91-190553, A07, MF-A01). This report has been replaced by NCEER-93-0011.

NCEER-91-0006 "A Multidimensional Hysteretic Model for Plasticity Deforming Metals in Energy Absorbing Devices," by E.J. Graesser and F.A. Cozzarelli, 4/9/91, (PB92-108364, A04, MF-A01).

NCEER-91-0007 "A Framework for Customizable Knowledge-Based Expert Systems with an Application to a KBES for Evaluating the Seismic Resistance of Existing Buildings," by E.G. Ibarra-Anaya and S.J. Fenves, 4/9/91, (PB91-210930, A08, MF-A01).

NCEER-91-0008 "Nonlinear Analysis of Steel Frames with Semi-Rigid Connections Using the Capacity Spectrum Method," by G.G. Deierlein, S-H. Hsieh, Y-J. Shen and J.F. Abel, 7/2/91, (PB92-113828, A05, MF-A01).

NCEER-91-0009 "Earthquake Education Materials for Grades K-12," by K.E.K. Ross, 4/30/91, (PB91-212142, A06, MF-A01). This report has been replaced by NCEER-92-0018.

NCEER-91-0010 "Phase Wave Velocities and Displacement Phase Differences in a Harmonically Oscillating Pile," by N. Makris and G. Gazetas, 7/8/91, (PB92-108356, A04, MF-A01).

NCEER-91-0011 "Dynamic Characteristics of a Full-Size Five-Story Steel Structure and a 2/5 Scale Model," by K.C. Chang, G.C. Yao, G.C. Lee, D.S. Hao and Y.C. Yeh," 7/2/91, (PB93-116648, A06, MF-A02).

NCEER-91-0012 "Seismic Response of a 2/5 Scale Steel Structure with Added Viscoelastic Dampers," by K.C. Chang, T.T. Soong, S-T. Oh and M.L. Lai, 5/17/91, (PB92-110816, A05, MF-A01).

NCEER-91-0013 "Earthquake Response of Retaining Walls; Full-Scale Testing and Computational Modeling," by S. Alampalli and A-W.M. Elgamal, 6/20/91, to be published.

NCEER-91-0014 "3D-BASIS-M: Nonlinear Dynamic Analysis of Multiple Building Base Isolated Structures," by P.C. Tsopelas, S. Nagarajaiah, M.C. Constantinou and A.M. Reinhorn, 5/28/91, (PB92-113885, A09, MF-A02).

NCEER-91-0015 "Evaluation of SEAOC Design Requirements for Sliding Isolated Structures," by D. Theodossiou and M.C. Constantinou, 6/10/91, (PB92-114602, A11, MF-A03).

NCEER-91-0016 "Closed-Loop Modal Testing of a 27-Story Reinforced Concrete Flat Plate-Core Building," by H.R. Somaprasad, T. Toksoy, H. Yoshiyuki and A.E. Aktan, 7/15/91, (PB92-129980, A07, MF-A02).

NCEER-91-0017 "Shake Table Test of a 1/6 Scale Two-Story Lightly Reinforced Concrete Building," by A.G. El-Attar, R.N. White and P. Gergely, 2/28/91, (PB92-222447, A06, MF-A02).

NCEER-91-0018 "Shake Table Test of a 1/8 Scale Three-Story Lightly Reinforced Concrete Building," by A.G. El-Attar, R.N. White and P. Gergely, 2/28/91, (PB93-116630, A08, MF-A02).

NCEER-91-0019 "Transfer Functions for Rigid Rectangular Foundations," by A.S. Veletsos, A.M. Prasad and W.H. Wu, 7/31/91, to be published.

NCEER-91-0020 "Hybrid Control of Seismic-Excited Nonlinear and Inelastic Structural Systems," by J.N. Yang, Z. Li and A. Danielians, 8/1/91, (PB92-143171, A06, MF-A02).

NCEER-91-0021 "The NCEER-91 Earthquake Catalog: Improved Intensity-Based Magnitudes and Recurrence Relations for U.S. Earthquakes East of New Madrid," by L. Seeber and J.G. Armbruster, 8/28/91, (PB92-176742, A06, MF-A02).

NCEER-91-0022 "Proceedings from the Implementation of Earthquake Planning and Education in Schools: The Need for Change - The Roles of the Changemakers," by K.E.K. Ross and F. Winslow, 7/23/91, (PB92-129998, A12, MF-A03).

NCEER-91-0023 "A Study of Reliability-Based Criteria for Seismic Design of Reinforced Concrete Frame Buildings," by H.H.M. Hwang and H-M. Hsu, 8/10/91, (PB92-140235, A09, MF-A02).

NCEER-91-0024 "Experimental Verification of a Number of Structural System Identification Algorithms," by R.G. Ghanem, H. Gavin and M. Shinozuka, 9/18/91, (PB92-176577, A18, MF-A04).

NCEER-91-0025 "Probabilistic Evaluation of Liquefaction Potential," by H.H.M. Hwang and C.S. Lee," 11/25/91, (PB92-143429, A05, MF-A01).

NCEER-91-0026 "Instantaneous Optimal Control for Linear, Nonlinear and Hysteretic Structures - Stable Controllers," by J.N. Yang and Z. Li, 11/15/91, (PB92-163807, A04, MF-A01).

NCEER-91-0027 "Experimental and Theoretical Study of a Sliding Isolation System for Bridges," by M.C. Constantinou, A. Kartoum, A.M. Reinhorn and P. Bradford, 11/15/91, (PB92-176973, A10, MF-A03).

NCEER-92-0001 "Case Studies of Liquefaction and Lifeline Performance During Past Earthquakes, Volume 1: Japanese Case Studies," Edited by M. Hamada and T. O'Rourke, 2/17/92, (PB92-197243, A18, MF-A04).

NCEER-92-0002 "Case Studies of Liquefaction and Lifeline Performance During Past Earthquakes, Volume 2: United States Case Studies," Edited by T. O'Rourke and M. Hamada, 2/17/92, (PB92-197250, A20, MF-A04).

NCEER-92-0003 "Issues in Earthquake Education," Edited by K. Ross, 2/3/92, (PB92-222389, A07, MF-A02).

NCEER-92-0004 "Proceedings from the First U.S. - Japan Workshop on Earthquake Protective Systems for Bridges," Edited by I.G. Buckle, 2/4/92, (PB94-142239, A99, MF-A06).

NCEER-92-0005 "Seismic Ground Motion from a Haskell-Type Source in a Multiple-Layered Half-Space," A.P. Theoharis, G. Deodatis and M. Shinozuka, 1/2/92, to be published.

NCEER-92-0006 "Proceedings from the Site Effects Workshop," Edited by R. Whitman, 2/29/92, (PB92-197201, A04, MF-A01).

NCEER-92-0007 "Engineering Evaluation of Permanent Ground Deformations Due to Seismically-Induced Liquefaction," by M.H. Baziar, R. Dobry and A-W.M. Elgamal, 3/24/92, (PB92-222421, A13, MF-A03).

NCEER-92-0008 "A Procedure for the Seismic Evaluation of Buildings in the Central and Eastern United States," by C.D. Poland and J.O. Malley, 4/2/92, (PB92-222439, A20, MF-A04).

NCEER-92-0009 "Experimental and Analytical Study of a Hybrid Isolation System Using Friction Controllable Sliding Bearings," by M.Q. Feng, S. Fujii and M. Shinozuka, 5/15/92, (PB93-150282, A06, MF-A02).

NCEER-92-0010 "Seismic Resistance of Slab-Column Connections in Existing Non-Ductile Flat-Plate Buildings," by A.J. Durrani and Y. Du, 5/18/92, (PB93-116812, A06, MF-A02).

NCEER-92-0011 "The Hysteretic and Dynamic Behavior of Brick Masonry Walls Upgraded by Ferrocement Coatings Under Cyclic Loading and Strong Simulated Ground Motion," by H. Lee and S.P. Prawel, 5/11/92, to be published.

NCEER-92-0012 "Study of Wire Rope Systems for Seismic Protection of Equipment in Buildings," by G.F. Demetriades, M.C. Constantinou and A.M. Reinhorn, 5/20/92, (PB93-116655, A08, MF-A02).

NCEER-92-0013 "Shape Memory Structural Dampers: Material Properties, Design and Seismic Testing," by P.R. Witting and F.A. Cozzarelli, 5/26/92, (PB93-116663, A05, MF-A01).

NCEER-92-0014 "Longitudinal Permanent Ground Deformation Effects on Buried Continuous Pipelines," by M.J. O'Rourke, and C. Nordberg, 6/15/92, (PB93-116671, A08, MF-A02).

NCEER-92-0015 "A Simulation Method for Stationary Gaussian Random Functions Based on the Sampling Theorem," by M. Grigoriu and S. Balopoulou, 6/11/92, (PB93-127496, A05, MF-A01).

NCEER-92-0016 "Gravity-Load-Designed Reinforced Concrete Buildings: Seismic Evaluation of Existing Construction and Detailing Strategies for Improved Seismic Resistance," by G.W. Hoffmann, S.K. Kunnath, A.M. Reinhorn and J.B. Mander, 7/15/92, (PB94-142007, A08, MF-A02).

NCEER-92-0017 "Observations on Water System and Pipeline Performance in the Limón Area of Costa Rica Due to the April 22, 1991 Earthquake," by M. O'Rourke and D. Ballantyne, 6/30/92, (PB93-126811, A06, MF-A02).

NCEER-92-0018 "Fourth Edition of Earthquake Education Materials for Grades K-12," Edited by K.E.K. Ross, 8/10/92, (PB93-114023, A07, MF-A02).

NCEER-92-0019 "Proceedings from the Fourth Japan-U.S. Workshop on Earthquake Resistant Design of Lifeline Facilities and Countermeasures for Soil Liquefaction," Edited by M. Hamada and T.D. O'Rourke, 8/12/92, (PB93-163939, A99, MF-E11).

NCEER-92-0020 "Active Bracing System: A Full Scale Implementation of Active Control," by A.M. Reinhorn, T.T. Soong, R.C. Lin, M.A. Riley, Y.P. Wang, S. Aizawa and M. Higashino, 8/14/92, (PB93-127512, A06, MF-A02).

NCEER-92-0021 "Empirical Analysis of Horizontal Ground Displacement Generated by Liquefaction-Induced Lateral Spreads," by S.F. Bartlett and T.L. Youd, 8/17/92, (PB93-188241, A06, MF-A02).

NCEER-92-0022 "IDARC Version 3.0: Inelastic Damage Analysis of Reinforced Concrete Structures," by S.K. Kunnath, A.M. Reinhorn and R.F. Lobo, 8/31/92, (PB93-227502, A07, MF-A02).

NCEER-92-0023 "A Semi-Empirical Analysis of Strong-Motion Peaks in Terms of Seismic Source, Propagation Path and Local Site Conditions, by M. Kamiyama, M.J. O'Rourke and R. Flores-Berrones, 9/9/92, (PB93-150266, A08, MF-A02).

NCEER-92-0024 "Seismic Behavior of Reinforced Concrete Frame Structures with Nonductile Details, Part I: Summary of Experimental Findings of Full Scale Beam-Column Joint Tests," by A. Beres, R.N. White and P. Gergely, 9/30/92, (PB93-227783, A05, MF-A01).

NCEER-92-0025 "Experimental Results of Repaired and Retrofitted Beam-Column Joint Tests in Lightly Reinforced Concrete Frame Buildings," by A. Beres, S. El-Borgi, R.N. White and P. Gergely, 10/29/92, (PB93-227791, A05, MF-A01).

NCEER-92-0026 "A Generalization of Optimal Control Theory: Linear and Nonlinear Structures," by J.N. Yang, Z. Li and S. Vongchavalitkul, 11/2/92, (PB93-188621, A05, MF-A01).

NCEER-92-0027 "Seismic Resistance of Reinforced Concrete Frame Structures Designed Only for Gravity Loads: Part I - Design and Properties of a One-Third Scale Model Structure," by J.M. Bracci, A.M. Reinhorn and J.B. Mander, 12/1/92, (PB94-104502, A08, MF-A02).

NCEER-92-0028 "Seismic Resistance of Reinforced Concrete Frame Structures Designed Only for Gravity Loads: Part II - Experimental Performance of Subassemblages," by L.E. Aycardi, J.B. Mander and A.M. Reinhorn, 12/1/92, (PB94-104510, A08, MF-A02).

NCEER-92-0029 "Seismic Resistance of Reinforced Concrete Frame Structures Designed Only for Gravity Loads: Part III - Experimental Performance and Analytical Study of a Structural Model," by J.M. Bracci, A.M. Reinhorn and J.B. Mander, 12/1/92, (PB93-227528, A09, MF-A01).

NCEER-92-0030 "Evaluation of Seismic Retrofit of Reinforced Concrete Frame Structures: Part I - Experimental Performance of Retrofitted Subassemblages," by D. Choudhuri, J.B. Mander and A.M. Reinhorn, 12/8/92, (PB93-198307, A07, MF-A02).

NCEER-92-0031 "Evaluation of Seismic Retrofit of Reinforced Concrete Frame Structures: Part II - Experimental Performance and Analytical Study of a Retrofitted Structural Model," by J.M. Bracci, A.M. Reinhorn and J.B. Mander, 12/8/92, (PB93-198315, A09, MF-A03).

NCEER-92-0032 "Experimental and Analytical Investigation of Seismic Response of Structures with Supplemental Fluid Viscous Dampers," by M.C. Constantinou and M.D. Symans, 12/21/92, (PB93-191435, A10, MF-A03).

NCEER-92-0033 "Reconnaissance Report on the Cairo, Egypt Earthquake of October 12, 1992," by M. Khater, 12/23/92, (PB93-188621, A03, MF-A01).

NCEER-92-0034 "Low-Level Dynamic Characteristics of Four Tall Flat-Plate Buildings in New York City," by H. Gavin, S. Yuan, J. Grossman, E. Pekelis and K. Jacob, 12/28/92, (PB93-188217, A07, MF-A02).

NCEER-93-0001 "An Experimental Study on the Seismic Performance of Brick-Infilled Steel Frames With and Without Retrofit," by J.B. Mander, B. Nair, K. Wojtkowski and J. Ma, 1/29/93, (PB93-227510, A07, MF-A02).

NCEER-93-0002 "Social Accounting for Disaster Preparedness and Recovery Planning," by S. Cole, E. Pantoja and V. Razak, 2/22/93, (PB94-142114, A12, MF-A03).

NCEER-93-0003 "Assessment of 1991 NEHRP Provisions for Nonstructural Components and Recommended Revisions," by T.T. Soong, G. Chen, Z. Wu, R-H. Zhang and M. Grigoriu, 3/1/93, (PB93-188639, A06, MF-A02).

NCEER-93-0004 "Evaluation of Static and Response Spectrum Analysis Procedures of SEAOC/UBC for Seismic Isolated Structures," by C.W. Winters and M.C. Constantinou, 3/23/93, (PB93-198299, A10, MF-A03).

NCEER-93-0005 "Earthquakes in the Northeast - Are We Ignoring the Hazard? A Workshop on Earthquake Science and Safety for Educators," edited by K.E.K. Ross, 4/2/93, (PB94-103066, A09, MF-A02).

NCEER-93-0006 "Inelastic Response of Reinforced Concrete Structures with Viscoelastic Braces," by R.F. Lobo, J.M. Bracci, K.L. Shen, A.M. Reinhorn and T.T. Soong, 4/5/93, (PB93-227486, A05, MF-A02).

NCEER-93-0007 "Seismic Testing of Installation Methods for Computers and Data Processing Equipment," by K. Kosar, T.T. Soong, K.L. Shen, J.A. HoLung and Y.K. Lin, 4/12/93, (PB93-198299, A07, MF-A02).

NCEER-93-0008 "Retrofit of Reinforced Concrete Frames Using Added Dampers," by A. Reinhorn, M. Constantinou and C. Li, to be published.

NCEER-93-0009 "Seismic Behavior and Design Guidelines for Steel Frame Structures with Added Viscoelastic Dampers," by K.C. Chang, M.L. Lai, T.T. Soong, D.S. Hao and Y.C. Yeh, 5/1/93, (PB94-141959, A07, MF-A02).

NCEER-93-0010 "Seismic Performance of Shear-Critical Reinforced Concrete Bridge Piers," by J.B. Mander, S.M. Waheed, M.T.A. Chaudhary and S.S. Chen, 5/12/93, (PB93-227494, A08, MF-A02).

NCEER-93-0011 "3D-BASIS-TABS: Computer Program for Nonlinear Dynamic Analysis of Three Dimensional Base Isolated Structures," by S. Nagarajaiah, C. Li, A.M. Reinhorn and M.C. Constantinou, 8/2/93, (PB94-141819, A09, MF-A02).

NCEER-93-0012 "Effects of Hydrocarbon Spills from an Oil Pipeline Break on Ground Water," by O.J. Helweg and H.H.M. Hwang, 8/3/93, (PB94-141942, A06, MF-A02).

NCEER-93-0013 "Simplified Procedures for Seismic Design of Nonstructural Components and Assessment of Current Code Provisions," by M.P. Singh, L.E. Suarez, E.E. Matheu and G.O. Maldonado, 8/4/93, (PB94-141827, A09, MF-A02).

NCEER-93-0014 "An Energy Approach to Seismic Analysis and Design of Secondary Systems," by G. Chen and T.T. Soong, 8/6/93, (PB94-142767, A11, MF-A03).

NCEER-93-0015 "Proceedings from School Sites: Becoming Prepared for Earthquakes - Commemorating the Third Anniversary of the Loma Prieta Earthquake," Edited by F.E. Winslow and K.E.K. Ross, 8/16/93, (PB94-154275, A16, MF-A02).

NCEER-93-0016 "Reconnaissance Report of Damage to Historic Monuments in Cairo, Egypt Following the October 12, 1992 Dahshur Earthquake," by D. Sykora, D. Look, G. Croci, E. Karaesmen and E. Karaesmen, 8/19/93, (PB94-142221, A08, MF-A02).

NCEER-93-0017 "The Island of Guam Earthquake of August 8, 1993," by S.W. Swan and S.K. Harris, 9/30/93, (PB94-141843, A04, MF-A01).

NCEER-93-0018 "Engineering Aspects of the October 12, 1992 Egyptian Earthquake," by A.W. Elgamal, M. Amer, K. Adalier and A. Abul-Fadl, 10/7/93, (PB94-141983, A05, MF-A01).

NCEER-93-0019 "Development of an Earthquake Motion Simulator and its Application in Dynamic Centrifuge Testing," by I. Krstelj, Supervised by J.H. Prevost, 10/23/93, (PB94-181773, A-10, MF-A03).

NCEER-93-0020 "NCEER-Taisei Corporation Research Program on Sliding Seismic Isolation Systems for Bridges: Experimental and Analytical Study of a Friction Pendulum System (FPS)," by M.C. Constantinou, P. Tsopelas, Y-S. Kim and S. Okamoto, 11/1/93, (PB94-142775, A08, MF-A02).

NCEER-93-0021 "Finite Element Modeling of Elastomeric Seismic Isolation Bearings," by L.J. Billings, Supervised by R. Shepherd, 11/8/93, to be published.

NCEER-93-0022 "Seismic Vulnerability of Equipment in Critical Facilities: Life-Safety and Operational Consequences," by K. Porter, G.S. Johnson, M.M. Zadeh, C. Scawthorn and S. Eder, 11/24/93, (PB94-181765, A16, MF-A03).

NCEER-93-0023 "Hokkaido Nansei-oki, Japan Earthquake of July 12, 1993, by P.I. Yanev and C.R. Scawthorn, 12/23/93, (PB94-181500, A07, MF-A01).

NCEER-94-0001 "An Evaluation of Seismic Serviceability of Water Supply Networks with Application to the San Francisco Auxiliary Water Supply System," by I. Markov, Supervised by M. Grigoriu and T. O'Rourke, 1/21/94, (PB94-204013, A07, MF-A02).

NCEER-94-0002 "NCEER-Taisei Corporation Research Program on Sliding Seismic Isolation Systems for Bridges: Experimental and Analytical Study of Systems Consisting of Sliding Bearings, Rubber Restoring Force Devices and Fluid Dampers," Volumes I and II, by P. Tsopelas, S. Okamoto, M.C. Constantinou, D. Ozaki and S. Fujii, 2/4/94, (PB94-181740, A09, MF-A02 and PB94-181757, A12, MF-A03).

NCEER-94-0003 "A Markov Model for Local and Global Damage Indices in Seismic Analysis," by S. Rahman and M. Grigoriu, 2/18/94, (PB94-206000, A12, MF-A03).

NCEER-94-0004 "Proceedings from the NCEER Workshop on Seismic Response of Masonry Infills," edited by D.P. Abrams, 3/1/94, (PB94-180783, A07, MF-A02).

NCEER-94-0005 "The Northridge, California Earthquake of January 17, 1994: General Reconnaissance Report," edited by J.D. Goltz, 3/11/94, (PB193943, A10, MF-A03).

NCEER-94-0006 "Seismic Energy Based Fatigue Damage Analysis of Bridge Columns: Part I - Evaluation of Seismic Capacity," by G.A. Chang and J.B. Mander, 3/14/94, (PB94-219185, A11, MF-A03).

NCEER-94-0007 "Seismic Isolation of Multi-Story Frame Structures Using Spherical Sliding Isolation Systems," by T.M. Al-Hussaini, V.A. Zayas and M.C. Constantinou, 3/17/94, (PB193745, A09, MF-A02).

NCEER-94-0008 "The Northridge, California Earthquake of January 17, 1994: Performance of Highway Bridges," edited by I.G. Buckle, 3/24/94, (PB94-193851, A06, MF-A02).

NCEER-94-0009 "Proceedings of the Third U.S.-Japan Workshop on Earthquake Protective Systems for Bridges," edited by I.G. Buckle and I. Friedland, 3/31/94, (PB94-195815, A99, MF-A06).

NCEER-94-0010 "3D-BASIS-ME: Computer Program for Nonlinear Dynamic Analysis of Seismically Isolated Single and Multiple Structures and Liquid Storage Tanks," by P.C. Tsopelas, M.C. Constantinou and A.M. Reinhorn, 4/12/94, (PB94-204922, A09, MF-A02).

NCEER-94-0011 "The Northridge, California Earthquake of January 17, 1994: Performance of Gas Transmission Pipelines," by T.D. O'Rourke and M.C. Palmer, 5/16/94, (PB94-204989, A05, MF-A01).

NCEER-94-0012 "Feasibility Study of Replacement Procedures and Earthquake Performance Related to Gas Transmission Pipelines," by T.D. O'Rourke and M.C. Palmer, 5/25/94, (PB94-206638, A09, MF-A02).

NCEER-94-0013 "Seismic Energy Based Fatigue Damage Analysis of Bridge Columns: Part II - Evaluation of Seismic Demand," by G.A. Chang and J.B. Mander, 6/1/94, (PB95-18106, A08, MF-A02).

NCEER-94-0014 "NCEER-Taisei Corporation Research Program on Sliding Seismic Isolation Systems for Bridges: Experimental and Analytical Study of a System Consisting of Sliding Bearings and Fluid Restoring Force/Damping Devices," by P. Tsopelas and M.C. Constantinou, 6/13/94, (PB94-219144, A10, MF-A03).

NCEER-94-0015 "Generation of Hazard-Consistent Fragility Curves for Seismic Loss Estimation Studies," by H. Hwang and J-R. Huo, 6/14/94, (PB95-181996, A09, MF-A02).

NCEER-94-0016 "Seismic Study of Building Frames with Added Energy-Absorbing Devices," by W.S. Pong, C.S. Tsai and G.C. Lee, 6/20/94, (PB94-219136, A10, A03).

NCEER-94-0017 "Sliding Mode Control for Seismic-Excited Linear and Nonlinear Civil Engineering Structures," by J. Yang, J. Wu, A. Agrawal and Z. Li, 6/21/94, (PB95-138483, A06, MF-A02).

NCEER-94-0018 "3D-BASIS-TABS Version 2.0: Computer Program for Nonlinear Dynamic Analysis of Three Dimensional Base Isolated Structures," by A.M. Reinhorn, S. Nagarajaiah, M.C. Constantinou, P. Tsopelas and R. Li, 6/22/94, (PB95-182176, A08, MF-A02).

NCEER-94-0019 "Proceedings of the International Workshop on Civil Infrastructure Systems: Application of Intelligent Systems and Advanced Materials on Bridge Systems," Edited by G.C. Lee and K.C. Chang, 7/18/94, (PB95-252474, A20, MF-A04).

NCEER-94-0020 "Study of Seismic Isolation Systems for Computer Floors," by V. Lambrou and M.C. Constantinou, 7/19/94, (PB95-138533, A10, MF-A03).

NCEER-94-0021 "Proceedings of the U.S.-Italian Workshop on Guidelines for Seismic Evaluation and Rehabilitation of Unreinforced Masonry Buildings," Edited by D.P. Abrams and G.M. Calvi, 7/20/94, (PB95-138749, A13, MF-A03).

NCEER-94-0022 "NCEER-Taisei Corporation Research Program on Sliding Seismic Isolation Systems for Bridges: Experimental and Analytical Study of a System Consisting of Lubricated PTFE Sliding Bearings and Mild Steel Dampers," by P. Tsopelas and M.C. Constantinou, 7/22/94, (PB95-182184, A08, MF-A02).

NCEER-94-0023 "Development of Reliability-Based Design Criteria for Buildings Under Seismic Load," by Y.K. Wen, H. Hwang and M. Shinozuka, 8/1/94, (PB95-211934, A08, MF-A02).

NCEER-94-0024 "Experimental Verification of Acceleration Feedback Control Strategies for an Active Tendon System," by S.J. Dyke, B.F. Spencer, Jr., P. Quast, M.K. Sain, D.C. Kaspari, Jr. and T.T. Soong, 8/29/94, (PB95-212320, A05, MF-A01).

NCEER-94-0025 "Seismic Retrofitting Manual for Highway Bridges," Edited by I.G. Buckle and I.F. Friedland, published by the Federal Highway Administration (PB95-212676, A15, MF-A03).

NCEER-94-0026 "Proceedings from the Fifth U.S.-Japan Workshop on Earthquake Resistant Design of Lifeline Facilities and Countermeasures Against Soil Liquefaction," Edited by T.D. O'Rourke and M. Hamada, 11/7/94, (PB95-220802, A99, MF-E08).

NCEER-95-0001 "Experimental and Analytical Investigation of Seismic Retrofit of Structures with Supplemental Damping: Part 1 - Fluid Viscous Damping Devices," by A.M. Reinhorn, C. Li and M.C. Constantinou, 1/3/95, (PB95-266599, A09, MF-A02).

NCEER-95-0002 "Experimental and Analytical Study of Low-Cycle Fatigue Behavior of Semi-Rigid Top-And-Seat Angle Connections," by G. Pekcan, J.B. Mander and S.S. Chen, 1/5/95, (PB95-220042, A07, MF-A02).

NCEER-95-0003 "NCEER-ATC Joint Study on Fragility of Buildings," by T. Anagnos, C. Rojahn and A.S. Kiremidjian, 1/20/95, (PB95-220026, A06, MF-A02).

NCEER-95-0004 "Nonlinear Control Algorithms for Peak Response Reduction," by Z. Wu, T.T. Soong, V. Gattulli and R.C. Lin, 2/16/95, (PB95-220349, A05, MF-A01).

NCEER-95-0005 "Pipeline Replacement Feasibility Study: A Methodology for Minimizing Seismic and Corrosion Risks to Underground Natural Gas Pipelines," by R.T. Eguchi, H.A. Seligson and D.G. Honegger, 3/2/95, (PB95-252326, A06, MF-A02).

NCEER-95-0006 "Evaluation of Seismic Performance of an 11-Story Frame Building During the 1994 Northridge Earthquake," by F. Naeim, R. DiSulio, K. Benuska, A. Reinhorn and C. Li, to be published.

NCEER-95-0007 "Prioritization of Bridges for Seismic Retrofitting," by N. Basöz and A.S. Kiremidjian, 4/24/95, (PB95-252300, A08, MF-A02).

NCEER-95-0008 "Method for Developing Motion Damage Relationships for Reinforced Concrete Frames," by A. Singhal and A.S. Kiremidjian, 5/11/95, (PB95-266607, A06, MF-A02).

NCEER-95-0009 "Experimental and Analytical Investigation of Seismic Retrofit of Structures with Supplemental Damping: Part II - Friction Devices," by C. Li and A.M. Reinhorn, 7/6/95, (PB96-128087, A11, MF-A03).

NCEER-95-0010 "Experimental Performance and Analytical Study of a Non-Ductile Reinforced Concrete Frame Structure Retrofitted with Elastomeric Spring Dampers," by G. Pekcan, J.B. Mander and S.S. Chen, 7/14/95, (PB96-137161, A08, MF-A02).

NCEER-95-0011 "Development and Experimental Study of Semi-Active Fluid Damping Devices for Seismic Protection of Structures," by M.D. Symans and M.C. Constantinou, 8/3/95, (PB96-136940, A23, MF-A04).

NCEER-95-0012 "Real-Time Structural Parameter Modification (RSPM): Development of Innervated Structures," by Z. Liang, M. Tong and G.C. Lee, 4/11/95, (PB96-137153, A06, MF-A01).

NCEER-95-0013 "Experimental and Analytical Investigation of Seismic Retrofit of Structures with Supplemental Damping: Part III - Viscous Damping Walls," by A.M. Reinhorn and C. Li, 10/1/95, (PB96-176409, A11, MF-A03).

NCEER-95-0014 "Seismic Fragility Analysis of Equipment and Structures in a Memphis Electric Substation," by J-R. Huo and H.H.M. Hwang, (PB96-128087, A09, MF-A02), 8/10/95.

NCEER-95-0015 "The Hanshin-Awaji Earthquake of January 17, 1995: Performance of Lifelines," Edited by M. Shinozuka, 11/3/95, (PB96-176383, A15, MF-A03).

NCEER-95-0016 "Highway Culvert Performance During Earthquakes," by T.L. Youd and C.J. Beckman, available as NCEER-96-0015.

NCEER-95-0017 "The Hanshin-Awaji Earthquake of January 17, 1995: Performance of Highway Bridges," Edited by I.G. Buckle, 12/1/95, to be published.

NCEER-95-0018 "Modeling of Masonry Infill Panels for Structural Analysis," by A.M. Reinhorn, A. Madan, R.E. Valles, Y. Reichmann and J.B. Mander, 12/8/95.

NCEER-95-0019 "Optimal Polynomial Control for Linear and Nonlinear Structures," by A.K. Agrawal and J.N. Yang, 12/11/95, (PB96-168737, A07, MF-A02).

NCEER-95-0020 "Retrofit of Non-Ductile Reinforced Concrete Frames Using Friction Dampers," by R.S. Rao, P. Gergely and R.N. White, 12/22/95, (PB97-133508, A10, MF-A02).

NCEER-95-0021 "Parametric Results for Seismic Response of Pile-Supported Bridge Bents," by G. Mylonakis, A. Nikolaou and G. Gazetas, 12/22/95, (PB97-100242, A12, MF-A03).

NCEER-95-0022 "Kinematic Bending Moments in Seismically Stressed Piles," by A. Nikolaou, G. Mylonakis and G. Gazetas, 12/23/95.

NCEER-96-0001 "Dynamic Response of Unreinforced Masonry Buildings with Flexible Diaphragms," by A.C. Costley and D.P. Abrams," 10/10/96.

NCEER-96-0002 "State of the Art Review: Foundations and Retaining Structures," by I. Po Lam, to be published.

NCEER-96-0003 "Ductility of Rectangular Reinforced Concrete Bridge Columns with Moderate Confinement," by N. Wehbe, M. Saiidi, D. Sanders and B. Douglas, 11/7/96, (PB97-133557, A06, MF-A02).

NCEER-96-0004 "Proceedings of the Long-Span Bridge Seismic Research Workshop," edited by I.G. Buckle and I.M. Friedland, to be published.

NCEER-96-0005 "Establish Representative Pier Types for Comprehensive Study: Eastern United States," by J. Kulicki and Z. Prucz, 5/28/96.

NCEER-96-0006 "Establish Representative Pier Types for Comprehensive Study: Western United States," by R. Imbsen, R.A. Schamber and T.A. Osterkamp, 5/28/96.

NCEER-96-0007 "Nonlinear Control Techniques for Dynamical Systems with Uncertain Parameters," by R.G. Ghanem and M.I. Bujakov, 5/27/96, (PB97-100259, A17, MF-A03).

NCEER-96-0008 "Seismic Evaluation of a 30-Year Old Non-Ductile Highway Bridge Pier and Its Retrofit," by J.B. Mander, B. Mahmoodzadegan, S. Bhadra and S.S. Chen, 5/31/96.

NCEER-96-0009 "Seismic Performance of a Model Reinforced Concrete Bridge Pier Before and After Retrofit," by J.B. Mander, J.H. Kim and C.A. Ligozio, 5/31/96.

NCEER-96-0010 "IDARC2D Version 4.0: A Computer Program for the Inelastic Damage Analysis of Buildings," by R.E. Valles, A.M. Reinhorn, S.K. Kunnath, C. Li and A. Madan, 6/3/96, (PB97-100234, A17, MF-A03).

NCEER-96-0011 "Estimation of the Economic Impact of Multiple Lifeline Disruption: Memphis Light, Gas and Water Division Case Study," by S.E. Chang, H.A. Seligson and R.T. Eguchi, 8/16/96, (PB97-133490, A11, MF-A03).

NCEER-96-0012 "Proceedings from the Sixth Japan-U.S. Workshop on Earthquake Resistant Design of Lifeline Facilities and Countermeasures Against Soil Liquefaction, Edited by M. Hamada and T. O'Rourke, 9/11/96, (PB97-133581, A99, MF-A06).

NCEER-96-0013 "Chemical Hazards, Mitigation and Preparedness in Areas of High Seismic Risk: A Methodology for Estimating the Risk of Post-Earthquake Hazardous Materials Release," by H.A. Seligson, R.T. Eguchi, K.J. Tierney and K. Richmond, 11/7/96.

NCEER-96-0014 "Response of Steel Bridge Bearings to Reversed Cyclic Loading," by J.B. Mander, D-K. Kim, S.S. Chen and G.J. Premus, 11/13/96, (PB97-140735, A12, MF-A03).

NCEER-96-0015 "Highway Culvert Performance During Past Earthquakes," by T.L. Youd and C.J. Beckman, 11/25/96, (PB97-133532, A06, MF-A01).

NCEER-97-0001 "Evaluation, Prevention and Mitigation of Pounding Effects in Building Structures," by R.E. Valles and A.M. Reinhorn, 2/20/97, (PB97-159552, A14, MF-A03).

NCEER-97-0002 "Seismic Design Criteria for Bridges and Other Highway Structures," by C. Rojahn, R. Mayes, D.G. Anderson, J. Clark, J.H. Hom, R.V. Nutt and M.J. O'Rourke, 4/30/97, (PB97-194658, A06, MF-A03).

NCEER-97-0003 "Proceedings of the U.S.-Italian Workshop on Seismic Evaluation and Retrofit," Edited by D.P. Abrams and G.M. Calvi, 3/19/97, (PB97-194666, A13, MF-A03).

NCEER-97-0004 "Investigation of Seismic Response of Buildings with Linear and Nonlinear Fluid Viscous Dampers," by A.A. Seleemah and M.C. Constantinou, 5/21/97, (PB98-109002, A15, MF-A03).

NCEER-97-0005 "Proceedings of the Workshop on Earthquake Engineering Frontiers in Transportation Facilities," edited by G.C. Lee and I.M. Friedland, 8/29/97, (PB98-128911, A25, MR-A04).

NCEER-97-0006 "Cumulative Seismic Damage of Reinforced Concrete Bridge Piers," by S.K. Kunnath, A. El-Bahy, A. Taylor and W. Stone, 9/2/97, (PB98-108814, A11, MF-A03).

NCEER-97-0007 "Structural Details to Accommodate Seismic Movements of Highway Bridges and Retaining Walls," by R.A. Imbsen, R.A. Schamber, E. Thorkildsen, A. Kartoum, B.T. Martin, T.N. Rosser and J.M. Kulicki, 9/3/97.

NCEER-97-0008 "A Method for Earthquake Motion-Damage Relationships with Application to Reinforced Concrete Frames," by A. Singhal and A.S. Kiremidjian, 9/10/97, (PB98-108988, A13, MF-A03).

NCEER-97-0009 "Seismic Analysis and Design of Bridge Abutments Considering Sliding and Rotation," by K. Fishman and R. Richards, Jr., 9/15/97, (PB98-108897, A06, MF-A02).

NCEER-97-0010 "Proceedings of the FHWA/NCEER Workshop on the National Representation of Seismic Ground Motion for New and Existing Highway Facilities," edited by I.M. Friedland, M.S. Power and R.L. Mayes, 9/22/97.

NCEER-97-0011 "Seismic Analysis for Design or Retrofit of Gravity Bridge Abutments," by K.L. Fishman, R. Richards, Jr. and R.C. Divito, 10/2/97, (PB98-128937, A08, MF-A02).

NCEER-97-0012 "Evaluation of Simplified Methods of Analysis for Yielding Structures," by P. Tsopelas, M.C. Constantinou, C.A. Kircher and A.S. Whittaker, 10/31/97, (PB98-128929, A10, MF-A03).

NCEER-97-0013 "Seismic Design of Bridge Columns Based on Control and Repairability of Damage," by C-T. Cheng and J.B. Mander, 12/8/97.

NCEER-97-0014 "Seismic Resistance of Bridge Piers Based on Damage Avoidance Design," by J.B. Mander and C-T. Cheng, 12/10/97.

NCEER-97-0015 "Seismic Response of Nominally Symmetric Systems with Strength Uncertainty," by S. Balopoulou and M. Grigoriu, 12/23/97.

NCEER-97-0016 "Evaluation of Seismic Retrofit Methods for Reinforced Concrete Bridge Columns," by T.J. Wipf, F.W. Klaiber and F.M. Russo, 12/28/97.

NCEER-97-0017 "Seismic Fragility of Existing Conventional Reinforced Concrete Highway Bridges," by C.L. Mullen and A.S. Cakmak, 12/30/97.

NCEER-97-0018 "Loss Asssessment of Memphis Buildings," edited by D.P. Abrams and M. Shinozuka, 12/31/97.

NCEER-97-0019 "Seismic Evaluation of Frames with Infill Walls Using Quasi-static Experiments," by K.M. Mosalam, R.N. White and P. Gergely, 12/31/97.

NCEER-97-0020 "Seismic Evaluation of Frames with Infill Walls Using Pseudo-dynamic Experiments," by K.M. Mosalam, R.N. White and P. Gergely, 12/31/97.

50272-101

REPORT DOCUMENTATION PAGE	1. REPORT NO. NCEER-97-0020	2.	3. Recipient's Accession No.

4. Title and Subtitle
Seismic Evaluation of Frames with Infill Walls Using Pseudo-dynamic Experiments

5. Report Date
December 31, 1997

6.

7. Author(s)
Khalid M. Mosalam, Richard N. White and Peter Gergely

8. Performing Organization Rept. No.

9. Performing Organization Name and Address
Cornell University
School of Civil and Environmental Engineering
Ithaca, NY 14853

10. Project/Task/Work Unit No.
93-3111, 94-3111, 94-3112
95-3111

11. Contract(C) or Grant(G) No.
(C) NSF-BCS 90-25010
(G)

12. Sponsoring Organization Name and Address
National Center for Earthquake Engineering Research
State University of New York at Buffalo
Red Jacket Quadrangle
Buffalo, NY 14261

13. Type of Report & Period Covered
Technical report

14.

15. Supplementary Notes
This research was conducted at Cornell University and was supported in whole or in part by the National Science Foundation under grant number BCS-90-25010 and other sponsors

16. Abstract (Limit: 200 words)

An accurate and practical testing technique to study the seismic performance of multi-story infilled frames is formulated. This technique is based on the pseudo-dynamic method which can provide an acceptable approximation of the dynamic performance of structures under the influence of real earthquake excitation. The pseudo-dynamic experimental technique is outlined and applied for testing a two-bay, two-story gravity load designed steel frame infilled with unreinforced concrete block masonry walls. It was shown that careful implementation of the pseudo-dynamic technique may lead to an excellent control over the experimental error propagation, even for stiff structures such as infilled frames. Based on the obtained results of the pseudo-dynamic experiments, the structural capacity as well as the corresponding seismic demand was assessed. From this study, it is concluded that the imparted energy and the hysteretic energy correlate well with the observed damage state of the infill walls. From the observed crack patterns of the infill walls, a macro-model for the infill panels is suggested.

17. Document Analysis a. Descriptors
Earthquake engineering. Infilled frames. Unreinforced masonry infill walls. Pseudo-dynamic tests. Concrete block masonry. Mortar joints. Finite element analysis.

b. Identifiers/Open-Ended Terms

c. COSATI Field/Group

18. Availability Statement	19. Security Class (This Report)	21. No. of Pages
Release unlimited	Unclassified	98
	20. Security Class (This Page) Unclassified	22. Price